LBL-PUB--433-10-85/205
DE86 004175

μSR NEWSLETTER

Lawrence Berkeley Laboratory, University of California
Meson Science Laboratory, University of Tokyo, Japan

DEFINITION OF μSR

μSR stands for Muon Spin Relaxation, Rotation, Resonance, Research, or what have you. The intention of the mnemonic acronym is to draw attention to the analogy with NMR and ESR, the range of whose applications is well known. Any study of the interactions of the muon spin by virtue of the asymmetric decay is considered μSR, but this definition is not intended to exclude any peripherally related phenomena, especially if relevant to the use of the muon's magnetic moment as a delicate probe of matter.

No. 31 — October 30, 1985

TABLE OF CONTENTS

PUB-433 10-85/205 This work was supported by the U.S. Department of Energy under Contract No. DE-AC03-76SF00098

OBSERVATION OF "DECOUPLED" DIAMAGNETIC MUON STATES IN ALKALI HALIDES BY MUON SPIN RESONANCE

K. NISHIYAMA, Y. MOROZUMI[a)], T. SUZUKI[b)] and K. NAGAMINE

Meson Science Laboratory, Faculty of Science, University of Tokyo, Bunkyo-ku, Tokyo, Japan

The states of positive muons in KCl, NaCl and KI were studied with muon spin resonance method under a 3 KG decoupling longitudinal field, revealing a considerably larger fraction of a diamagnetic muon state than that observed by the conventional spin rotation method. The origin of this fraction which increases with temperatur is attributed to a muonium to muon transition in solids.

a) Permanent address: Accelerator Division, National Laboratory for High Energy Physics, Tsukuba, Ibaraki, Japan

b) Permanent address: Department of Energy Engineering, Hachinohe Institute of Technology, Hachinohe, Aomori, Japan

Little is known about the electronic state of the positive muon in ionic insulators, such as alkali halides. It is known that a small fraction (around 10 %) of muon forms a diamagnetic muon state in alkali halides, which was observed by the conventional spin rotation method in a transverse field [1]. An old decoupling experiment [2] which measured decay e^+ asymmetry as a function of longitudinal magnetic field has indicated that a large fraction of the muons forms a muonium-like paramagnetic state in KCl and that its polarization is mostly lost at magnetic fields below 200 G due to the nuclear hyperfine interaction [3]. The line broadening due to this nuclear hyperfine interaction prevents a direct observation of triplet muonium spin precession in a weak transverse field.

Recently, muonium precession signals in alkali halides have been observed in a high transverse magnetic field where the line brodening due to the nuclear hyperfine interaction is quenched (HTF method) [4]. An apparatus with a high time resolution was necessary to resolve muonium precession signals at high fields. It was found that around 2/3 of the muons are in a muonium state at around room temperature with considerable relaxation rates and that this fraction is reduced to 1/3 at low temperatures below 100 K. In order to obtain a full understanding of the fate of the positive muon in alkali halides, we have developed a new spectroscopic tool for the diamagnetic μ^+ state which arises from a muonium to diamagnetic muon transition.

The intense pulsed muon beam with 50 ns pulse width and 20 Hz repetition rate available at the BOOM (BOOster Meson) Facility of Meson Science Laboratory, University of Tokyo [5,6] located at KEK has permitted a new method of pulsed muon spin resonance with a pulsed rf

field of high peak-power [6,7]. In the present experiment this resonance method was applied to probe hitherto unrevealed diamagnetic muon state in alkali halides. There are two advantages in the muon spin resonance method over the conventional spin rotation method; 1) the muon state can be probed in the presence of a the longitudinal field which decouples the perturbing fields; 2) the diamagnetic muon state after delayed generation can be probed because the phase coherence is not required in the spin resonance method while it is essential in the spin rotation method. The study of diamagnetic muon state which might be formed from a muonium precursor state in alkali halides is a typical example where the resonance method is most effectively applied: the decoupling field is required to preserve muonium polarization against the perturbing nuclear hyperfine interaction; the phase coherence is lost when the diamagnetic muon is formed from muonium.

The experiment was conducted at the superconducting muon channel of of the BOOM Facility [5,6]. In the present experiment, we have used single crystals of NaCl, KCl and KI produced by Horiba Manufacturing Co. Ltd. Each sample has a disk shape of 50 mm diameter with 20 mm thickness (NaCl) or 10 mm thickness (KCl and KI). The sample was held in a cryostat cooled by a flow of liquid He. The temperature of the sample was measured with Au-Fe and copper-constantan thermocouples. The rf coil, composed of several turns of 37 μm Cu foil around the sample, was tuned at the resonance frequency of 40 MHz. The cryostat was placed in the longitudinal coil set-up for standard μSR experiments [6]. A pulsed rf field of about 30 G at the target was achieved using a high power rf source, the detailed description of which is given elsewhere [6,7]. In the present resonance experiment, the

decay e^+ was measured by the digital method of pulsed μSR measurement by using 16 channel scintillation counter telescopes in both forward and backward directions to the beam [6].

The resonance pattern was obtained by measuring the decay e^+ intensity ratio between the forward and backward counters as a function of the longitudinal field (H_L) around the resonance field of 2.95 kG which corresponds to the fixed rf frequency of 40 MHz for the diamagnetic muon state. Once the central position of the resonance curve was obtained, the longitudinal field was fixed. Then the time differential pattern of muon spin resonance, corresponding to the muon spin rotation around the H_1 field, was measured. The decoupling measurement under a longitudinal field was also carried out by measuring forward/backward asymmetry ratio at various values of H_L up to 4 kG. At each temperature, a resonance measurement, a decoupling measurement and a spin rotation measurement were carried out sequentially.

The observed resonance curve for NaCl at room temperature is shown in Fig. 1a. For a comparison, a conventional muon spin rotation spectrum in a transverse field spin rotation is shown in Fig. 1b. A distinct increase of the diamagnetic fraction is clearly seen with $H_L = 2.95$ kG. This is the signal of the "decoupled" diamagnetic muon state which has not been seen in the usual spin rotation experiment. The temperature dependences of the "decoupled" diamagnetic fraction obtained from the depth of the resonance curve (time integrated signal) for NaCl, KCl and KI are summarized in Fig. 2. For comparison, we show in Fig. 2 the fraction of prompt diamagnetic muon formed at time-zero under zero longitudinal field which was obtained from the conventional spin rotation method, as well as typical examples of the decoupling patterns.

The most remarkable features of Fig. 2 are the dramatic increase of the diamagnetic muon fraction seen by the resonance method at higher temperatures compared to that by the spin rotation method. For NaCl and KCl, this increase occurs at around 100 K, while for KI it happens at around 300 K. This observed increase of the diamagnetic fraction at higher temperatures in both NaCl and KCl suggests that a possible chemical reaction may take place from a muonium-like precursor state to a diamagnetic muon final state.

In KCl, where the HTF-method on muonium has been made [4], we can discuss more completely the nature of muonium and diamagnetic muon states than in the other cases. The following facts were readily observed:(1) the fraction of the "decoupled" diamagnetic state has an activation type temperature-dependence; (2) the sum of the muonium fraction at time zero obtained by the HTF-method (seen in Fig. 2) and the diamagnetic fraction obtained by the resonance method is larger than unity at room temperature;(3) as reported elesewhere [8,9], the detailed analysis of the time-differential pattern of the resonance signal provides a measure of the rate of increase of the diamagnetic muon state which was found to be consistent with the disappearance rate of the muonium observed in the HFT method [4]. All of these facts indicate that in KCl above 100 K, the muonium state makes a transition to the diamagnetic muon state Such a transition from muonium to diamagnetic muon state is reasonable if the muonium reacts with other paramagnetic species during a diffusion process [8,9]. Without the present resonance method, the presence of a chemical reaction from muonium to diamagnetic species can only be guessed from the damping of muonium signal. The result of this resonance experiment provides the first direct evidence

for such a reaction process by detecting the final state.

In KCl, the muonium signal obtained from the HTF experiment becomes smaller below 70 K and at the same time the diamagnetic μ^+ fraction observed in the present resonance experiment is also reduced to 10 %. Thus, almost all the signals are missing, while, as seen in Fig. 2, a decoupling pattern shows an existence of muonium-like paramagnetic state. Althcugh there is no clear explanation for this result, one possibility might be that a transition occurs below 70 K from one muonium state to another muonium state with a different hyperfine coupling constant.

As for NaCl, although there has been no detailed report on the experimental data by the HTF measurement, the diamagnetic muon state as well as the muonium state seems to have almost the same character as in the case of KCl. However, the muonium and diamagnetic muon in KI behave quite differently: 1) the decoupled diamagnetic muon state becomes significant only above 300 K; 2) the decoupling curves at all the measured temperatures are substantially suppressed compared to the free muonium. Both of them suggest an existence of the strong spin conversion process in KI at the temperature below 300 K.

In conclusion, a "decoupled" diamagnetic state has been systematically studied for the μ^+ in alkali halides, revealing a muonium chemical reaction in solids. This experiment represents the first observation of the diamagnetic muon state which has been unrevealed due to the strong perturbation at the precursor muonium-like state as well as the muonium to diamagnetic muon transition. Further experimental studies, particularly for the unexplained behaviors in KI as well as in KCl and NaCl below 70 K are now in progress.

We acknowledge Professor T. Yamazaki for valuable comments and encouragements. Helpful informations before publication from Dr. Kiefl and Dr. B. D. Patterson are also appreciated. We also thank Dr. Y. Kuno, Dr. T. Matsuzaki, Dr. J. Imazato and Dr. K. Ishida for their collaborations. We also acknowledge Professor H. Yasuoka, Dr. Y. Kitaoka and Dr. M. Takigawa for their kind kontribution to the rf source preparations. This work is supported by the Grand-in-Aid for Scientific Research of the Japanese Ministry of Education, Culture and Science.

References

[1] J.H. Brewer, K.M. Crowe, F.N. Gygax and A. Schenck, in Muon Physics, edited by V.W. Hughes and C.S. Wu (Academic, New York, 1975) Vol.3, P.3.

[2] I.G. Ivanter, E. V. Minichev, G. G. Myasisheva, Yu. V. Obukhov, V.S. Roganov, G. I. Savel'ev,V. P. Smilga and V. G. Firsov Sov. Phys. JETP 35, 9(1972)

[3] R. Beck, P. F. Meier and A. Schenck, Z. Physik B22, 109(1975)

[4] R. F. Kiefl, E. Holzschuh, H. Keller, W. Kundig, P. F. Meier, B. D. Patterson, J. W. Schneider, K. W. Blazey, S. L. Rudaz and A. B. Denison, Phys. Rev. Lett., 53, 90(1984)

[5] K. Nagamine, Hyperfine Interactions, 8, 787(1981)

[6] UT-MSL NEWSLETTER No. 1-4(1981-4) eds. K. Nagamine and T. Yamazaki, unpublished

[7] Y. Kitaoka, M. Takigawa, H. Yasuoka, M. Itoh, S. Takagi, Y. Kuno, K. Nishiyama, R. S. Hayano, Y. J. Uemura, J. Imazato, H. Nakayama, K. Nagamine and T. Yamazaki Hyperfine Interactions 12, 51(1982)

[8] Y. Morozumi, K. Nishiyama, and K. Nagamine, in preparation

[9] Y. Morozumi, a thesis submitted to University of Tokyo (1985).

Figure Captions

Fig. 1 (a) Muon spin resonance curve obtained for diamagnetic μ^+ in NaCl at room temperature, represented by the decay positron intensity ratio between forward/backward counters, where the *normalization was taken by the ratio with rf off. The ratio* is shown as a function of external magnetic field normalized at the resonance field. (b) Muon spin rotation spectrum obtained in NaCl at room temperature at the transverse field of 100 G.

Fig. 2 Temperature dependences of the "decoupled" diamagnetic fraction obtained from muon spin resonance amplitude for KCl(a), NaCl(b) and KI(c). Also the fraction obtained from the amplitude of the asymmetry with spin rotation method under transverse field of 100 G is shown. The decoupling patterns at typical temperatures are also given for each sample. A normalized decoupling pattern calculated for free muonium with 10 % prompt diamagnetic muon is also shown for comparison. As for KCl, the fraction of muonium observed by the HTF method taken from the reference [4] is also shown.

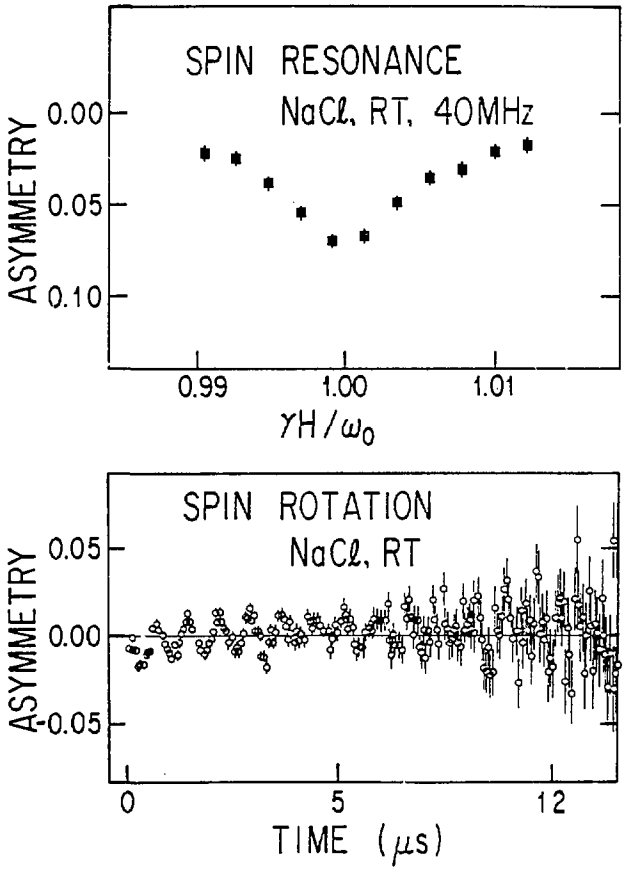
SPIN RESONANCE
NaCl, RT, 40MHz
ASYMMETRY
0.00
0.05
0.10
0.99
1.00
1.01
γH/ω0
SPIN ROTATION
NaCl, RT
ASYMMETRY
0.05
0.00
-0.05
0
5
12
TIME (μs)

Figure 1

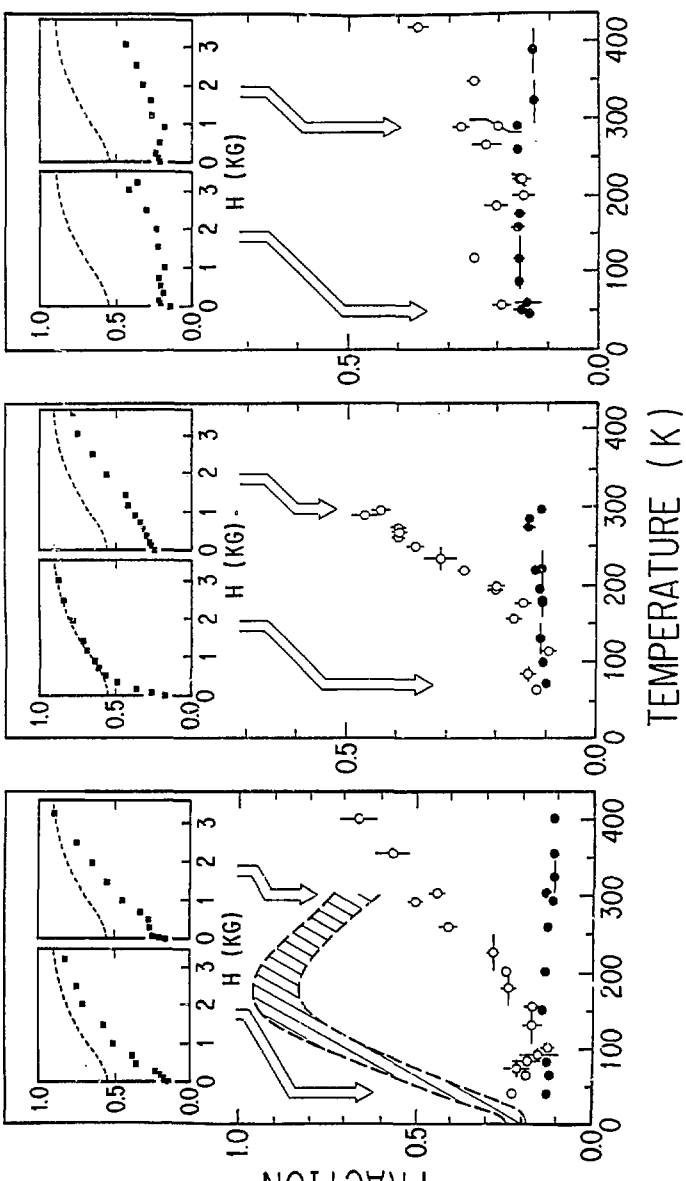
K Cℓ
Na Cℓ
K I
FRACTION
TEMPERATURE (K)
H (KG)
1.0
0.5
0.0
0
100
200
300
400
1
2
3

DIFFUSION PROPERTIES OF THE MUON-PRODUCED SOLITON IN TRANS-POLYACETYLENE

K. Ishida, K. Nagamine, T. Matsuzaki, Y. Kuno and T. Yamazaki
Meson Science Laboratory, University of Tokyo, Bunkyo-ku, Tokyo, Japan

E. Torikai
Doctoral Course in Human Culture, Ochanomizu University,
Bunkyo-ku, Tokyo, Japan

H. Shirakawa
Institute of Materials Science, University of Tsukuba,
Sakura-mura, Ibaraki, Japan

and

J.H. Brewer
Department of Physics and TRIUMF, University of British Columbia,
Vancouver, B.C., Canada

We have measured the longitudinal spin relaxation functions of positive muons injected into trans-$(CH)_x$ at various temperatures and external fields. They showed non-single-exponential functions and were fitted by a model which takes into account both the on-chain diffusion and the disappearance of the muon-produced soliton. It was found that the on-chain diffusion rate $D_{//}$ is almost constant from 29 K to 290 K, while the disappearance rate $D_\perp$ slightly increases with temperature.

Recently, the behaviour of the unpaired electrons in trans-polyacetylene has been extensively studied, both experimentally and theoretically, since it is proposed to be related to the properties of soliton[1]. There seems, however, to remain many unclear aspects to be studied concerning, in particular, on-chain and interchain diffusion properties of the soliton. In the present experiment, we studied this problem by muon spin relaxation method, which is expected to probe the soliton in polyacetylene from a different view-point compared to the conventional ESR or NMR.

In a previous paper[2], we have reported the following observations concerning positive muons in trans-polyacetylene: the positive muon, when it is added to a double bond in trans-polyacetylene, produces an unpaired electron; the unpaired electron exhibits soliton-like one-dimensional diffusion, as demonstrated by the $H^{-1/2}$ dependence of the longitudinal relaxation rate of the muon spin on the longitudinal magnetic field H. The soliton produced and probed by the muon has different properties from the usual soliton probed by NMR, ESR etc. : 1) there is no mechanism similar to nuclear spin diffusion which affects the rate of muon spin relaxation because the muon is an "infinitely" dilute probe; 2) the soliton is created at the time of the muon arrival so that the time evolution of the soliton dynamics can be observed time-sequentially with reference to this "birth" time; 3) the soliton is confined to one side of the chain from the boundary determined by the muon location, because the conjugation is terminated here. In this paper, we describe a further experiment in which a particular attention was paid to deduce the disappearance of the soliton from the chain.

The on-chain spin diffusion rate $D_{//}$ of the unpaired electron and its temperature dependence are interesting, because they reflect the

interaction between soliton and phonons. Theoretically, Wada and Schrieffer[3] have proposed that $D_{//}$ should obey a T^2 temperature dependence, while Maki[4] predicted a $T^{-1/2}$ temperature dependence for $D_{//}$. Experimentally, from the inverse-root type frequency dependence of the proton spin-lattice relaxation rate (T_1^{-1}), it has been concluded that the spin diffusion is highly one-dimensional with $D_{//} \approx 4 \times 10^{13}$ s^{-1} and that the interchain diffusion rate D is less than 10^8 s^{-1} at room temperature[5]. However, it was also pointed out that the nuclear spin diffusion to a fixed paramagnetic spin also reproduces the same frequency dependence[6] so that the above-mentioned interpretation is still unsettled. Recently, the frequency dependence of T_1^{-1} of the unpaired electron was directly observed by ESR[7], where $D_{//}$ and D were found to be 4×10^{13} and 2×10^7 s^{-1}, respectively, at room temperature. This result was almost consistent with that of NMR. However, the temperature dependence of the diffusion rates is not yet clear: the T_1^{-1} of proton NMR obeys a $T^{1/4}$ dependence[5], while that of ESR was proportional to the temperature[8].

The experiment was carried out at the M20 muon channel at TRIUMF, the Tri-University Meson Facility in Vancouver, Canada. There, surface muon beams were stopped in a trans-polyacetylene target composed of a stack of thin films (in total, 2 cm x 2 cm x 80 mg/cm^2). The sample was prepared by the Shirakawa method[9] and sealed into a thin polyethylene bag of 88 μm thickness with an argon atmosphere. The temperature dependence of the longitudinal relaxation above 29 K was measured using a standard muon spin relaxation apparatus on the the M20 channel, where we applied a longitudinal field of up to 4 kG. Samples were cooled by a helium exchange gas contained in a cryostat vessel, where the vessel itself was cooled by

thermal contact with a cold finger cooled by liquid helium flow. The temperature stability was around ±0.5 K.

The measured longitudinal relaxation functions $G_z(t)$ are shown in Fig. 1 for temperatures of both 29 and 281 K, showing the field dependence for 0, 10, 20 and 50 G. A significant temperature dependence can be seen by comparing these two data; the long-lived asymmetry (after 5 μsec) is consistently reduced for the data at 29 K compared to those at 281 K. The relaxation rates decrease as the external field is increased at all the temperatures.

In a previous paper[2], the relaxation functions were fitted by a single exponential relaxation function, where the main relaxation mechanism is considered to be due to the interaction between the muon spin and the one-dimensionally moving unpaired electron (soliton) produced by the μ^+. However, in the present 281 K data, the relaxation seems to cease after about 5 μs, indicating a need of a more complicated relaxation function. Since the nuclear dipolar fields must contribute to the muon spin relaxation ($G_z^n(t)$), we calculated $G_z^n(t)$ by a Monte-Carlo method considering mutual interactions between μ^+ and surrounding protons[10], and took the ratio $G_z^e(t) = G_z(t)/G_z^n(t)$. Then we fitted the data of $G_z^e(t)$ with an exponential relaxation function by changing the analysis time region in a 2 μs step. All the data above 200 K were combined, since there seemed to be almost no temperature dependence above 200 K. The result shown in Fig. 2 exhibited a decrease of the relaxation rate itself with time. This result indicates a model in which the source of the relaxation, namely the soliton, disappears from the chain with time after it is created by the muon arrival.

Before going further along, we have to consider several possible other mechanisms which may cause a change in the muon spin relaxation function

from a single exponential type. Here, let us consider the following three possibilities. 1) As it was shown in the time-domain analysis of ESR[11], for time before the effect of interchain diffusion becomes significant, the relaxation function could become $\exp(-\alpha t^{3/2})$. In our case, however, this time range is estimated to be only before about 20 nsec, which is too short for the change in the relaxation function to be observed. 2) The muon spin relaxation rate will be reduced when the electron spin associated with the soliton is left polarized. The electron spin-lattice relaxation rate measured by ESR, which is 10^7 sec^{-1} at room temperature[7], is much faster than the typical muon spin relaxation times so that this effect is considered to be small. 3) The location of the muon is considered to be randomly distributed on the chain. The relaxation rate is expected to be proportional to the probability of existence of the soliton around the muon; the rate is proportional to the inverse of the distance between the muon location and the end of the chain. This effect was calculated, but the result was found to be not much different from a single exponential relaxation[10].

Since the above-mentioned three effects cannot explain the observed relaxation function, we will now consider the effect of the disappearance of the soliton from the chain. As shown in a previous paper[2], the relaxation rate of the muon spin is proportional to the density of the soliton which remains on the chain. Thus, when the soliton disappears, the relaxation rate may change with time. Now, we introduce the disappearance rate D_3 of the soliton. Then, the time dependent relaxation rate $R(t)$ may be written as

$$R(t) = R_0 \exp(-D_3 t) \qquad (1)$$

where R_0 is the T_1^{-1} at t=0. From the rate equation for the relaxation function of the muon spin $G_z^e(t)$,

$$dG_z^e(t)/dt = -R(t)\, G_z^e(t), \tag{2}$$

we obtain

$$G_z^e(t) = \exp[-R_0/D_3(1-\exp[-D_3 t])]. \tag{3}$$

We fitted D_3 and R_0 simultaneously for the data above 200 K. It was found that D_3 is almost field independent, while R_0 obeys an $H^{-1/2}$ dependence. This indicates that the muon spin relaxation comes mainly from the one-dimensionally diffusing unpaired electron and that the diappearance is due to a dynamical effect independent of the magnetic field. Next, the temperature dependences of R_0 and D_3 were obtained by a fit to the data at all fields, where D_3 was fixed at each temperature. The fitted results are shown in Fig. 3a) and 3b) for R_0 and D_3, respectively. Here, the relaxation rate R_0 was around three times larger than that we obtained using a single exponential function[2]. However, this difference does not change our basic interpretation in the previous paper[2].

The temperature dependence of R_0 reflects mainly the temperature dependence of $D_{//}$. As shown in Fig. 3b), it is almost temperature independent. Above 150 K, this is consistent with the ESR and the NMR results. But, below 150 K, our result does not agree with these results. This is due to the fact that the μSR method observes different aspects of the soliton dynamics from the other methods; e.g., the effect of the soliton trapping may be smaller in the μSR studies.

The soliton disappearance rate D_3 can be related to the interchain diffusion rate D of the soliton. The value of D obtained from the cut-off frequency in the ESR is 2×10^7 s^{-1} at room temperature[7]. Since the mutual spin flip-flop between solitons as well as the interchain hopping of the soliton itself contributes to the relaxation in the ESR experiment, it is not surprising that D is larger than the D_3 obtained in the present experiment. The D_3 slighly increases with temperature, which indicates that hopping between the chains has a small activation energy.

In conclusion, we have measured the temperature dependence of the muon spin relaxation function in trans-polyacetylene. The observed relaxation function was well reproduced by considering both the muon spin relaxation due to the soliton and the disappearance of the soliton from the chain to which the muon is attached. The relaxation rate was almost temperature independent. The disappearance rate D_3 increased only slightly with temperature.

We thank Drs. R. Keitel, S.R. Kreitzman, D.R. Noakes and M. Senba for their helps during the Tokyo Group's stay at TRIUMF. The Tokyo Group is also grateful to E.W. Vogt and staff-members of TRIUMF for their hospitalities. Helpful information from Professor K. Kume is also acknowledged. The present work was supported partly by the Grant in Aid of the Japanese Ministry of Education, Culture, and Science, and partly by the Natural Sciences and Engineering Research Council of Canada.

References

1. W.P. Su, J.R. Schrieffer, and A.J. Heeger, Phys. Rev. Lett. 42, 1698 (1979)
2. K. Nagamine, K. Ishida, T. Matsuzaki, K. Nishiyama, Y. Kuno, T. Yamazaki, and H. Shirakawa, Phys. Rev. Lett. 53, 1763 (1984)
3. Y. Wada, and J.R. Schrieffer, Phys. Rev. B 18, 3897 (1978)
4. K. Maki, Phys. Rev. B 26, 2181 (1982); ibid, 2187 (1982); ibid, 4539 (1982)
5. M. Nechtschein, F. Devreux, F. Genoud, M. Guglielmi, and K. Holczer, Phys. Rev. B 27, 3938 (1983)
6. N.S. Shiren, Y. Tomkievicz, H. Thomann, L. Dalton, and T.C. Clarke, J. de Phys. C3, 223 (1983)
7. K. Mizoguchi, K. Kume, and H. Shirakawa, Solid State Commun. 50, 213 (1984); K. Kume, K. Mizoguchi and H. Shirakawa, Mol. Cryst. and Liq. Cryst. 117, 469 (1985)
8. L.R. Dalton, H. Thomann, A. Morrobel-Sosa, C. Chiu, M.E. Galvin, G.E. Wnek, Y. Tomkiewicz, N.S. Shiren, B.H. Robinson, A.L. Kwiram, J. Appl. Phys. 54, 5583 (1983)
9. H. Shirakawa and S. Ikeda, Polym. J., 2, 231 (1971)
10. K. Ishida, thesis submitted to University of Tokyo (1985)
11. J. Tang, C.P. Lin, M.K. Bowman, J.R. Norris, J. Isoya, and H. Shirakawa, Phys. Rev. Lett. 50, 533 (1983)

Figure Captions

Fig. 1 Longitudinal spin relaxation functions for the μ^+ in trans-$(CH)_x$ (a) at 281 K and (b) at 29 K for longitudinal fields of 0, 10, 20, and 50 G. The curves are best-fitted functions to eq.(3) after correcting for the contribution of nuclear dipolar field to the relaxation function.

Fig. 2 Time dependence of the relaxation rate of μ^+ in trans-$(CH)_x$. The time window for the analysis is 1 μs for the earliest time data, while it is 2μs for the others, as shown in the figure. All the data above 200 K were summed up and used in this analysis. The effect of nuclear dipolar field has been already subtracted before the analysis. The 0 G data after 4 μs are not shown because of the unsatisfactory fit due to a small asymmetry.

Fig. 3 Temperature dependence of (a) soliton diappearance rate D_3 and (b) the muon spin relaxation rate R_0.

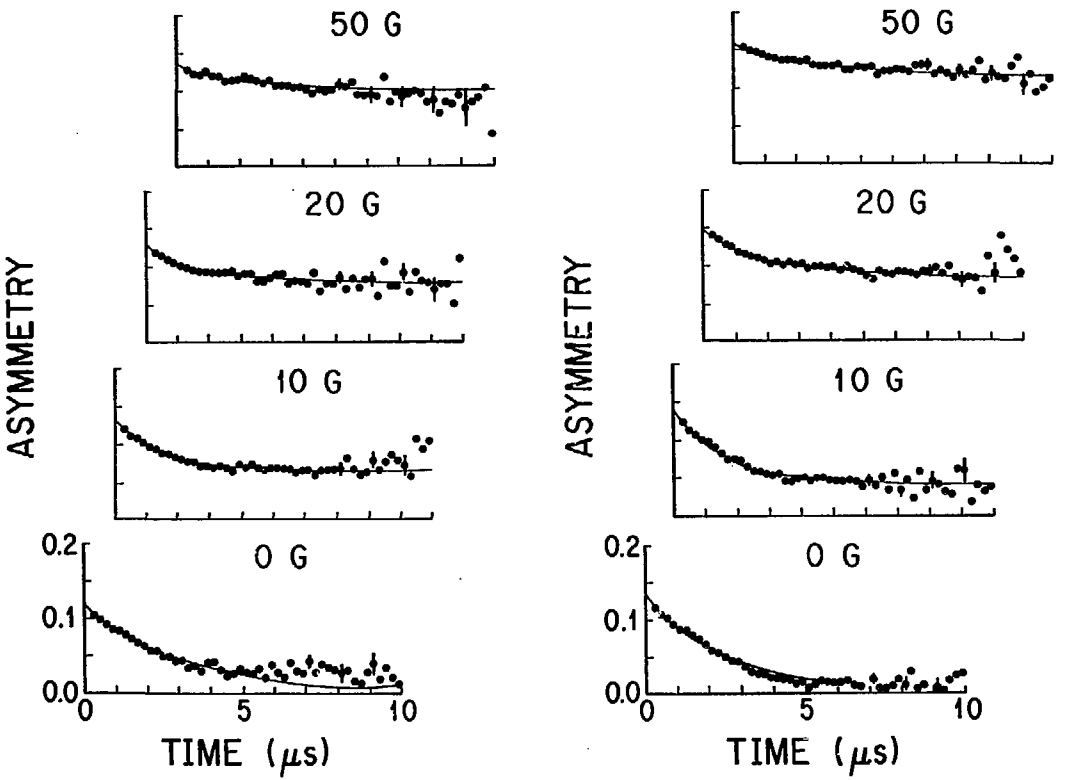
(a) μ^+ in trans-$(CH)_x$ 281 K
(b) μ^+ in trans-$(CH)_x$ 29 K
50 G
20 G
10 G
0 G
ASYMMETRY
0.2
0.1
0.0
0
5
10
TIME (μs)

Figure 1

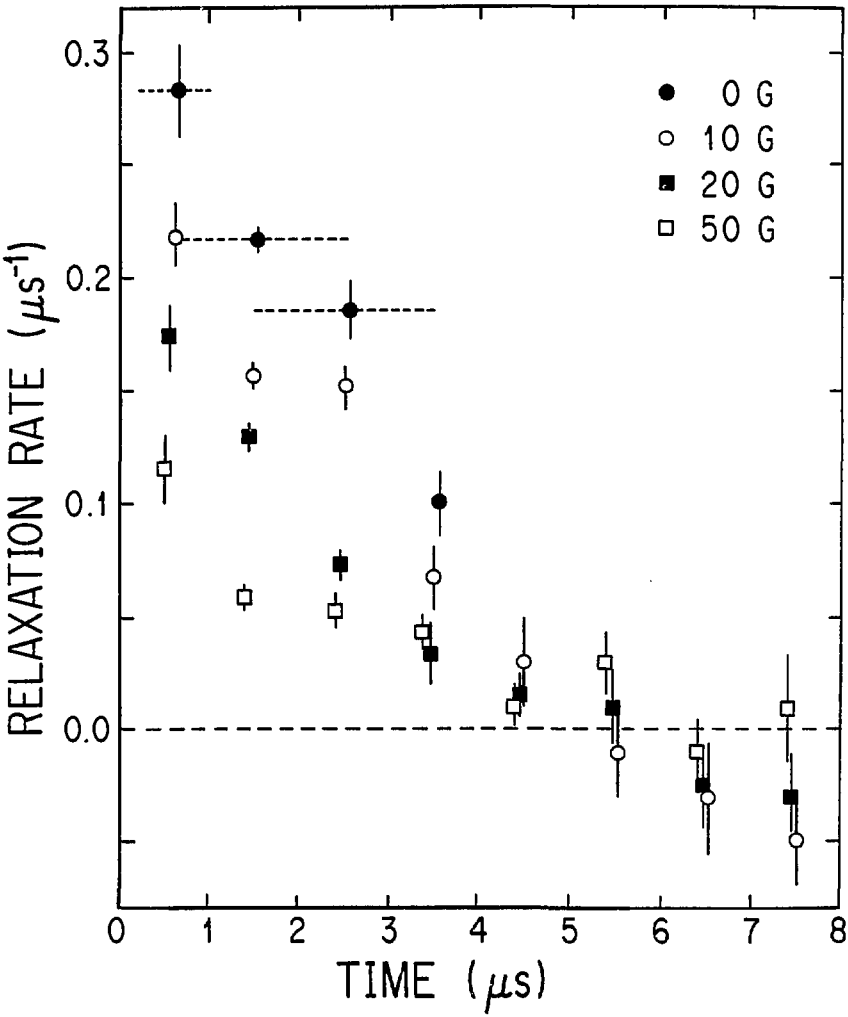
0.3
0.2
0.1
0.0
RELAXATION RATE (μs^{-1})
0 G
10 G
20 G
50 G
0
1
2
3
4
5
6
7
8
TIME (μs)

Figure 2

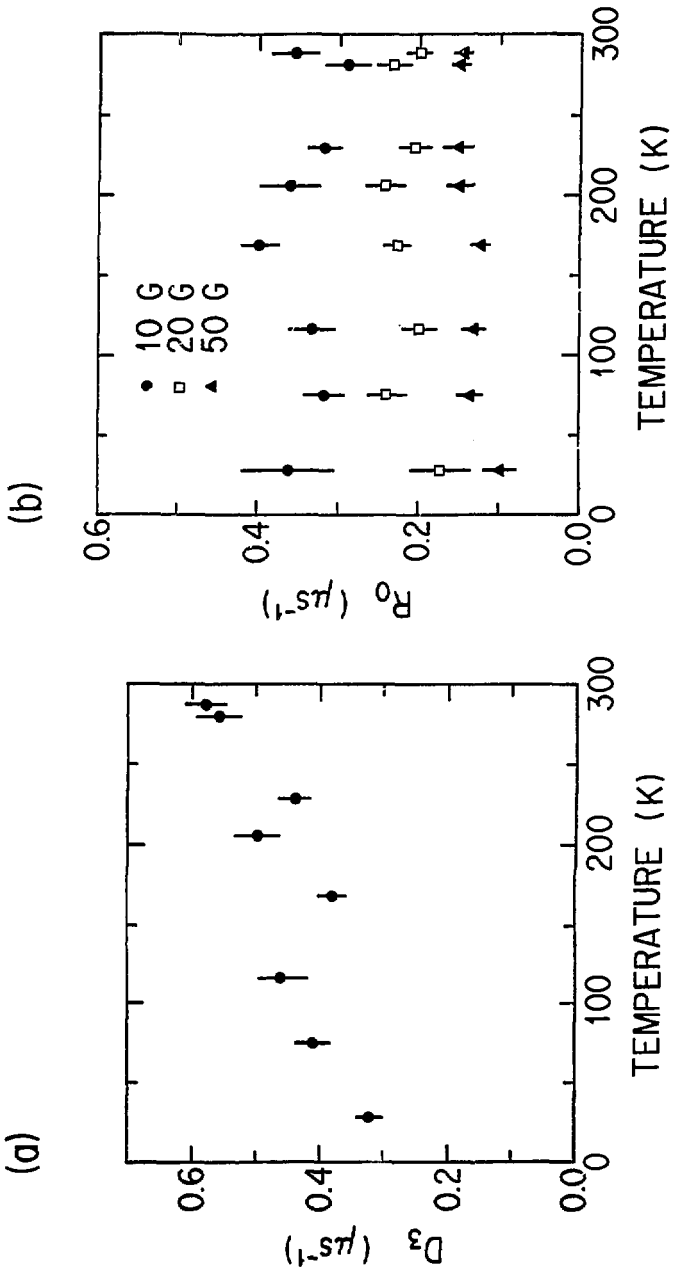
(a)
(b)
D_3 (μs^{-1})
R_0 (μs^{-1})
TEMPERATURE (K)
TEMPERATURE (K)
10 G
20 G
50 G
0.0
0.2
0.4
0.6
0
100
200
300

Figure 3

PULSED μ^-SR MEASUREMENT OF NEGATIVE MUON DEPOLARIZATION IN MUONIC ^{13}C and ^{14}N

K. ISHIDA, J.H. BREWER*), T. MATSUZAKI, Y. KUNO, J. IMAZATO and K. NAGAMINE

Meson Science Laboratory, Faculty of Science,
University of Tokyo, Bunkyo-ku, Tokyo, Japan

Slow depolarization rates of the upper hyperfine (HF) states (F^+) of $\mu^{-13}C$ and $\mu^{-14}N$ were observed by negative muon spin rotation method with a pulsed beam. The result for $\mu^{-13}C$ agrees with the HF transition rates expected by Auger processes, while that for $\mu^{-14}N$ is too high, suggesting HF transition due to intramolecular excitation effect.

---

* Permanent address: Department of Physics and TRIUMF, University of British Columbia, Vancouver, B.C., Canada V6T 2A3.

At the ground state of a muonic atom whose nucleus has spin I, the magnetic g-factor of each hyperfine (HF) state (F^+, F^-) is given by the following formula,

$$g_{\pm} = \left(1 \mp \frac{1}{2I+1}\right) g_I \pm \frac{1}{2I+1} g_\mu \qquad \left(\text{for } F^{\pm} = I \pm \tfrac{1}{2}\right) \qquad (1)$$

where g_I is the g-factor for the nucleus and g_μ is that for the free muon g-factor. Precession of the combined muon-nucleus spin system of low-Z muonic atoms can be observed by using conventional transverse field muon spin rotation (TF-μSR) techniques. Assuming that the nucleus is unpolarized at the time of muon arrival the statistical populations of the F^+ and F^- states can be calculated. The TF-μSR experiments allow a measure of the initial populations of the $F^{\pm}$ states because each initial amplitudes of the precession signals at the corresponding characteristic frequencies $\nu_{\pm}$ can be written as a product of the population and the μ^- polarization at $F^{\pm}$ state. At the same time, the transition rate R from the higher HF state to the lower one is manifested as a depolarization rate λ in the μ^-SR signal. This HF transition rate must be known in order to interpret lifetime measurements in terms of the difference in nuclear muon capture rates λ^+_{nc} and λ^-_{nc} from the F^+ and F^- states, respectively, which in turn inform us of the nature of the weak interaction in nuclei at moderate momentum transfer.

Following the pioneer work on ^{19}F by Winston [1], the μ^-SR experiments of Favart et al. [2] covered the light nuclei ^6Li, ^7Li, ^9Be, ^{10}B and ^{11}B. Recently, a similar experiment extended those measurements to selected nuclei heavier than Z = 9 [3]. All these experiments neglected the two common elements carbon and nitrogen, of

which isotopes with nonzero spin, namely ^{13}C (I = 1/2) and ^{14}N (I = 1), are readily available. These are particularly interesting systems for TF-μ^-SR measurements of R, since they lie in the boundary region of Z between the lightest elements where R is negligible or undetectably small and the heavier elements in which R is usually too fast to be observed directly. Since the HF transitions are governed by Auger processes, the value of R is determined by the HF energy splitting E_{hf} between F^+ and F^- and the energy levels of the surrounding electrons in atomic or even in molecular orbitals. When one wishes to measure a small R manifested as a slow μ^-SR depolarization rate, a pulsed muon beam is advantageous due to its extremely low background at late times (long after the muons arrive in the target).

Recent advances in μ^-SR methods for investigation of condensed matter [4,5] have encouraged us to extend these methods to muonic atoms with nonzero-spin nuclei to allow more flexibility in such applications and to take advantage of the reduced precession frequency and relaxation rate of the $F^\pm$ states (relative to the bare $\mu^\pm$ or a μ^- bound to a spin-zero nucleus) in the huge hyperfine fields often experienced by nuclei in magnetic materials [6].

Experiments were performed with the pulsed backward μ^- beam from the superconducting muon channel at the University of Tokyo, Meson Science Laboratory, Booster Meson facility (UT-MSL BOOM) [7,8] located at the Booster Synchrotron Utilization Facility of KEK (National Laboratory for High Energy Physics) in Tsukuba, Japan. The Polarized μ^- beam has a time structure of one 50 ns pulse every 50 ms, a central momentum of around 75 MeV/c, a beam diameter of 8 cm and a range width of around 2 g/cm^2. It was stopped in targets of ^{13}C (a rectangular box containing 23 g of 99 % enriched powdered

graphite) and ^{14}N (a disc-shaped vessel of 6 cm thickness containing liquid N_2 at atmospheric pressure).

The targets were positioned inside the μSR apparatus where either transverse magnetic fields (TF) or longitudinal magnetic fields (LF) can be applied; 16 scintillation counters telescopes were placed in both forward and backward directions for the digital type of μ^-e decay time interval detection [8]. The solid angle of each 16-channel telescope was 12.% of 4π; the good "e^-" event rates were 80/s for ^{13}C and 200/s for ^{14}N. TF of up to 350 Oe was applied and the resulting precession of the muon spins was detected via their asymmetrically-emitted decay electrons using normal time-differential μSR techniques. A normal graphite (^{12}C) sample was used for several calibration runs. In order to estimate the background depolarization rate λ_s due to inhomogeneous magnetic field over the target, the μ^+ relaxation was measured in an H_2O target of the same dimensions; in H_2O at room temperature the μ^+ is known to experience negligible relaxation. The result was that the λ_s was smaller than 0.007 μs^{-1}.

The observed spin precession signal is shown in Fig. 1a, for μ^- ^{13}C ($F^+=1$ state) and in Fig. 1b, for $\mu^-{}^{14}N$ ($F^+=\frac{3}{2}$ state). Each "signal" is displayed in the form of an asymmetry spectrum by eliminating the exponential decay of muon. The observed time spectra were fitted to the following formula for both cases (as described below, the contribution of F^- state in $\mu^-{}^{14}N$ is negligibly small):

$$N_e(t) = N_0 \exp(-t/\tau_\mu) [1 + A_0 \exp(-\lambda t)\cos(2\pi\nu t + \phi)] + B \quad (2)$$

where τ_μ is the average lifetime of the bound μ^-, A_0 is the initial amplitude of the μSR precession signal, ν is the precession frequency, λ is the depolarization rate and B represents a

time-independent background. The fitted frequencies and asymmetries are expressed relative to the corresponding values for $\mu^{-12}C$ in Table 1 along with the frequencies predicted by formula (1). The experimental data agree well with predictions suggesting the validity of a simple coupling scheme for the muon-nucleus spin system. In the case of ^{14}N, the upper limit for the asymmetry of the $F^- = 1/2$ state was 0.03 times the asymmetry for $\mu^{-12}C$.

In Table 1, the observed asymmetry for the F^+ state of either ^{13}C or ^{14}N is compared with the theoretical prediction, where the hyperfine interaction is assumed to be "switched-on" after the μ^- arrives at the 1s state [9]. The agreement between experiment and prediction is quite good for $\mu^{-13}C$ but not for $\mu^{-14}N$. The latter result is consistent with the previous measurement [10]. But in Ref.10, the asymmetry reduction was attributed to a supposedly fast HF transition; the slow depolarization rate observed here with much longer time range contradicts that explanation. The existing theory, which takes into account HF effects in excited states of muonic atoms, predicts $A(^{14}N)/A(^{12}C) = 0.372$ [11], which again differs from the present result. Possible explanations might be: (1) depolarization mechanisms due to HF interactions other than those considered in the reference [11]; (2) depolarization due to the formation of a paramagnetic precursor state (e.g., paramagnetic ion) before the system reaches its final diamagnetic state. The latter possibility has been suggested as an alternative explanation in the Ref.10.

The most interesting result of the present study is certainly the observation of the slow depolarization (λ) in both $\mu^{-13}C$ and $\mu^{-14}N$ systems. As possible origins of the observed rates λ we have to consider the following three mechanisms : (a) depolarization due to

magnetic interactions with the surrounding environment (solid/liquid effect); (b) the hyperfine transition rate R; and/or (c) apparent depolarization due to the difference in the nuclear capture rate from F^+ and F^- state, which are manifest in the μ^- lifetime.

In the case of $\mu^{-13}C$, the static random local magnetic fields (RLMF) from the nuclear magnetic moments of the surrounding ^{13}C can cause "dipolar broadening" of about 0.006 μs^{-1} to λ (assuming classical nuclear dipole fields); this value will be used as an additive correction to λ in the remaining discussion. Theoretical estimates have been obtained for the nuclear capture rates λ_{nc} from differenc HF states of $\mu^{-13}C$ by Morita's group [12]: $\lambda_{nc}(F=1) = 0.045\ \mu s^{-1}$ and $\lambda_{nc}(F=0) = 0.031\ \mu s^{-1}$ [12]. The difference $d\lambda_{nc} = 0.014\ \mu s^{-1}$ can be converted to an apparent depolarization rate $\lambda_{eff} = -n_- d\lambda_{nc}$, where n_- is the population of F^- state, which is easily obtained solving rate equations [1]. Taking $n_- = \frac{1}{4}$ (assuming a simple statistical average), the result is $\lambda_{eff} = 0.004\ \mu s^{-1}$, which is an order of magnitude smaller than the experimental value of λ. Thus the observed depolarization rate for $\mu^{-13}C$, when corrected for mechanism (a), can be interpreted as a HF transition rate R = 0.020(12) μs^{-1} between F^+ and F^- states.

The HF transitions in ground-state muonic atoms are governed almost completely by Auger processes. The relevant constants required in an estimation of the HF transition rates are summarized in Table 2, where the HF splitting E_{hf} is estimated using the point-nucleus approximation following Winston [1]. As clearly seen in the Table, the HF transition in $\mu^{-13}C$ should be dominated by an L shell Auger process. The point nucleus value of R estimated by the standard model [1] becomes 0.053 μs^{-1} which is not dramatically larger than our own measured value.

In the case of $\mu^{-14}N$, the contribution to λ from dipolar broadening should be negligibly small because of the motional narrowing effect of rapid tumbling and diffusion in the liquid. On the other hand, the HF transition in $\mu^{-14}N$ should be strongly suppressed because the point nucleus value of E_{hf} is smaller than E_{2p} (see Table 2). The nuclear capture rates for each HF states have also been estimated theoretically [12]: $\lambda_{nc}(F=\frac{3}{2}) = 0.109\ \mu s^{-1}$ and $\lambda_{nc}(F=\frac{1}{2}) = 0.060\ \mu s^{-1}$. These rates give us the apparent depolarization $\lambda_{eff} = -n_-[\lambda_{nc}(F=\frac{1}{2}) - \lambda_{nc}(F=\frac{3}{2})] = 0.016\ \mu s^{-1}$ for the $F = \frac{3}{2}$ state. The result is again much smaller than the experimental value, this time by nearly a factor of 6. All these considerations for $\mu^{-14}N$ suggest that there exists an anomalous enhancement in either the Auger transition associated with R or in the HF state dependence of the nuclear muon capture rate. The latter is deemed unlikely, since such a very large discrepancy with theory is hard to believe. In order to understand possible origins of an enhanced R, we need further realistic estimates on E_{hf}, E_{2p}, etc.

The correction of E_{hf} due to finite nuclear size can be estimated using effective Z-values obtained from total muon capture rate measurements. For $\mu^{-14}N$ the corrected E_{hf} becomes 7.5 eV instead of 9.4 eV shown in Table 1. More realistic value of E_{hf} is obtained by estimating Bohr-Weisskopf effect, assuming a realistic nuclear magnetization distribution and solving muon wave function for a finite nuclear charge distribution. The final answer becomes $E_{hf} = 7.9$ eV, which is again much smaller than E_{2p}. The same type of nuclear finite size correction is also required for E_{2p} itself, but it can not be large enough to fill the gap between E_{hf} and E_{2p}.

Other mechanisms are therefore required to explain the observed

enhancement of R for $\mu^{-14}N$. We propose the following model: when the μ^- is captured by one ^{14}N nucleus of an N_2 molecule, the resultant molecule, after stabilization, is the chemical analog of a CN molecule; a CN molecular orbital can be excited from its ground state by a magnetic dipole transition of the μ^-, thereby effecting an $F^+ - F^-$ transition [13]. Further theoretical analysis of this model is in progress.

In conclusion, the slow depolarization rate λ was measured in both $\mu^{-13}C$ and $\mu^{-14}N$ by the pulsed μ^-SR method. In $\mu^{-13}C$ the value of λ is consistent with the expected hyperfine transition rate R due to known L shell Auger processes, while in $\mu^{-14}N$ the λ is too large for an Auger-governed R, and must include an extra HF transition rate due to the M1 excitation of the quasi-CN molecule. The present results suggest interesting future measurements of $\lambda(\mu^{-14}N)$ in other systems, such as metallic NC, gaseous N_2, solid BN, etc., where we might expect different values of R (due to differences in E_{2p}) as well as different λ values due to various relaxation mechanisms acting on the $F^+ = \frac{3}{2}$ system.

The other result of the present experiment is the precise measured value of the muon lifetime τ_μ in $\mu^{-13}C$, giving the total capture rate of μ^- in ^{13}C, which differs from that in ^{12}C: $\tau_\mu^{-1}(^{12}C) - \tau_\mu^{-1}(^{13}C) = 0.00383(45)\ \mu s^{-1}$ and $\tau_\mu^{-1}(^{12}C)/\tau_\mu^{-1}(^{13}C) = 0.898(12)$. This indicates Pauli blocking effects in nuclear muon capture, as suggested by previous theoretical work [14].

We would like to acknowledge the encouragement and valuable comments of Prof. T. Yamazaki throughout the present work. Helpful discussions with Prof. T. Kondow on the molecular excitation effect are also greatly appreciated. One of us (JHB) would like to thank the Japan

Society for the Promotion of Science and the University of Tokyo for generous financial assistance and warm hospitality. The enthusiastic help and cooperation of the UT-MSL group, particularly Dr. K. Nishiyama, are gratefully acknowledged. We are also endebted to Prof.M. Morita, Prof. H. Ohtsubo and Dr. K. Koshigiri for furnishing us with theoretical estimates of the muon capture rates.

REFERENCES

[1] R. Winston, Phy. Rev. 129 (1963) 2766.

[2] D. Favart, F. Brouillard, L. Grenacs, P. Igo-Kemenes, P. Lipnik and P.C. Macq, Phys. Rev. Lett. 25 (1970) 1348.

[3] J.H. Brewer, Hyperfine Interactions 17-19 (1984) 873.

[4] T. Yamazaki, R.S. Hayano, Y. Kuno, J. Imazato, K. Nagamine, S.E. Kohn and C.Y. Huang, Phys. Rev. Lett. 42 (1979) 1241.

[5] J. Imazato, K. Nagamine, T. Yamazaki, B.D. Patterson, E. Holzschuh and R. Kiefl, Phys. Rev. Lett. 53 (1984) 1849

[6] K. Nagamine, Hyperfine Interactions 6 (1976) 347.

[7] K. Nagamine, Hyperfine Interactions 9 (1981) 781.

[8] UT-MSL Newsletter No.1(1981); No.2(1982); No.3(1983), eds. K. Nagamine and T. Yamazaki, unpublished.

[9] H. Uberall, Phys. Rev. 114 (1959) 1640; E. Lubkin, Phys. Rev. 119 (1960) 815.

[10] A.I. Babaev, V.S. Evseev, G.G. Myasishcheva, Yu. V. Obukhov, V.S. Roganov and V.A. Chernogorova, Yad. Fiz. 10 (1969) 964.

[11] A.P. Bukhvostov, Sov. J. Nucl. Phys. 9 (1969) 65.

[12] K. Koshigiri, H. Ohtsubo and M. Morita, to be published.

[13] T. Kondow, private communication.

[14] H. Primakoff, Rev. Mod. Phys. 31 (1959) 802.

Table I Summary of μ^-SR experiments on $\mu^{-13}C$ and $\mu^{-14}N$

Target	HF state	Lifetime τ_μ(μsec)	Relative Frequency ν/ν_C	Relative Asymmetry $A/A(^{12}C)$	Relaxation Rate $\lambda(\mu sec^{-1})$
^{12}C		2.029(3)	1	1	-0.006(9)
^{13}C	F=1	2.045(2)	0.463(2)	0.47(2)	0.026(12)
			[0.4605][a]	[0.50][b]	
^{14}N	$F=\frac{3}{2}$	1.908	0.320(1)	0.29(2)	0.092(33)
				0.270(36)[c]	
			[0.3182][a]	[0.41][b]	

a) Values obtained by formula (1).

b) Values predicted by the theory given in reference [9].

c) Data of Babaev et al [10].

Table 2 Relevant numbers for the estimation of HF transition rates for $\mu^{-13}C$ and $\mu^{-14}N$

Nucleus	Spin	Hyperfine Splitting E_{hf} [a] (eV)	Electron binding energy for Z-1 atom (eV)		
			E_{1s}	E_{2s}	E_{2p}
^{13}C	1/2	11.0	194	14.05	8.30
^{14}N	1	7.5	297	19.39	11.26

a) Values estimated for the point nucleus by the formula given in reference[1].

FIGURE CAPTIONS

Figure 1. Precession pattern obtained by stopping μ^- in enriched ^{13}C targets(a) and for μ^- in ^{14}N of liquid nitrogen(b). The strength of the applied transverse field is indicated. Exponential decay is removed by assuming τ_μ as shown in Table 1. The theoretical curve is obtained from formula (2) using the parameters in Table 1.

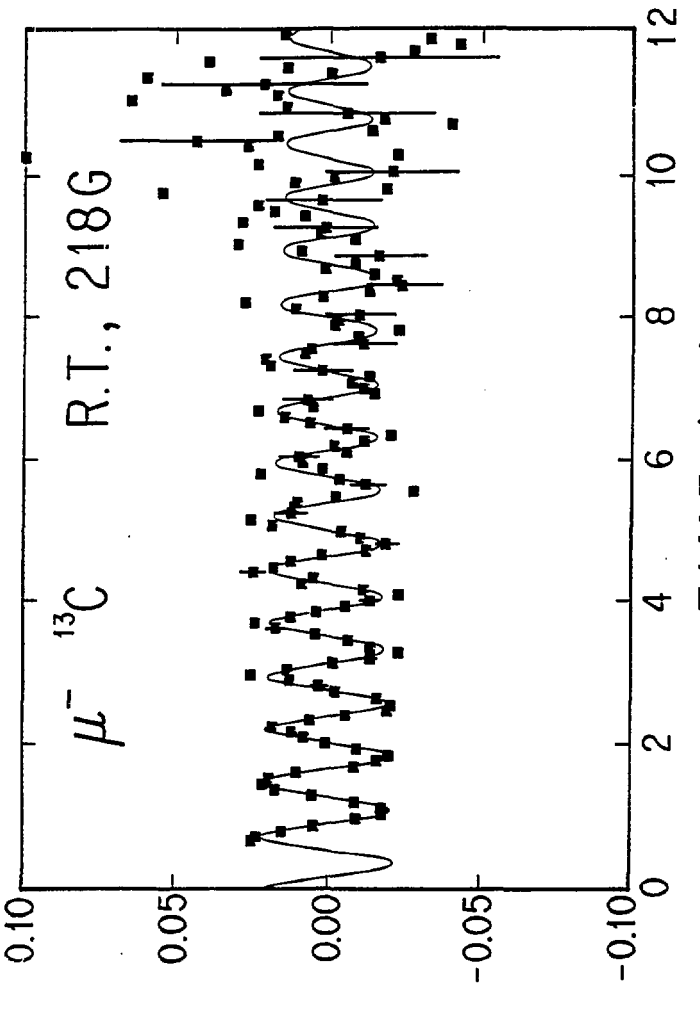
μ^- ^{13}C R.T., 218G
ASYMMETRY
TIME (μs)
0.10
0.05
0.00
-0.05
-0.10
0
2
4
6
8
10
12

Figure 1a

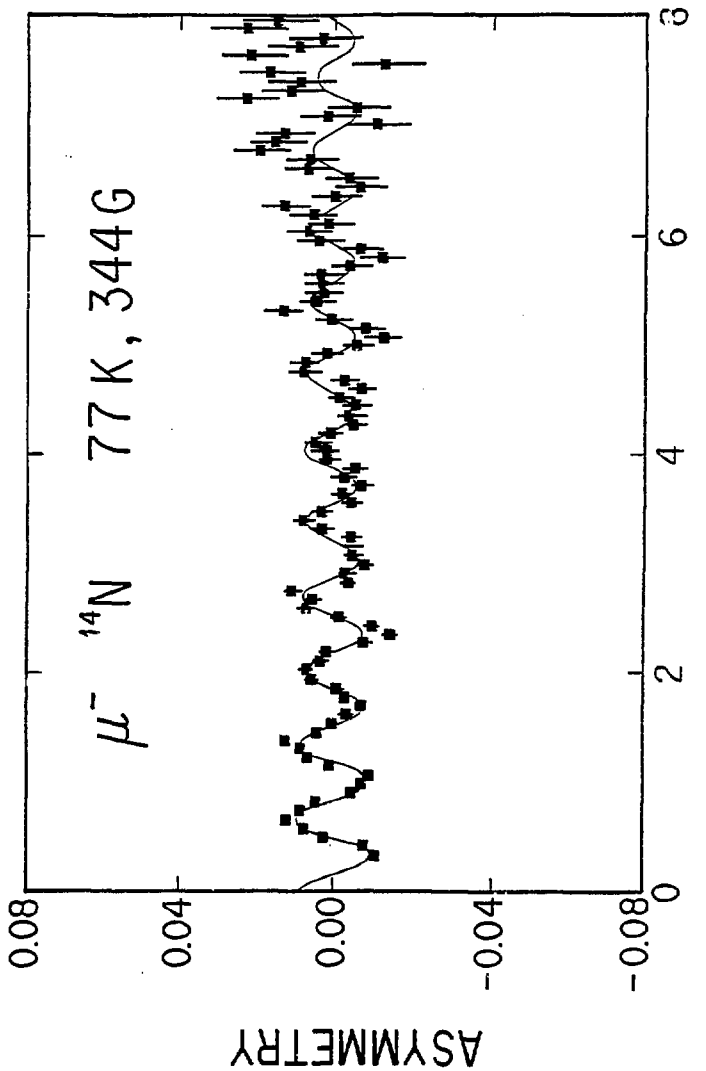

Figure 1b

MUONIUM TO DIAMAGNETIC MUON TRANSITION IN KCl AND NaCl REVEALED BY TIME-DIFFERENTIAL MUON SPIN RESONANCE

Y. Morozumi[a], K. Nishiyama and K. Nagamine

Meson Science Laboratory and Department of Physics, Faculty of Science, University of Tokyo, 7-3-1 Hongo, Bunkyo-ku, Tokyo 113, Japan

The transition of muonium into a diamagnetic muon state in KCl and NaCl was directly observed by detecting a time-delayed diamagnetic muon in a time-differential pattern of the muon spin resonance. The temperature variations of the transition rate $1/\tau$ and the spin flipping rate ν of muonium were simultaneously determined in the temperature range from 100 K to 300 K. The results can be explained by a reaction of a diffusing muonium with the defects created by the muon itself.

a Permanent address: Accelerator Division, National Laboratory for High Energy Physics, Tsukuba, Ibaraki, Japan

In the ionic crystal of alkali halides, positive muons (μ^+) are expected to form various distinct defect centers similar to the hydrogen defect centers. Except for the old experiments in KCl on the μ^+ polarization under longitudinal field[1], there have been limited experimental works on this subject. Recently, muonium (Mu) spin precession has been observed in KCl by decoupling the Mu spin in a high transverse magnetic field, thereby quenching the line broadening due to nuclear hyperfine interaction (NHF)[2]. The experiment has indicated that the observed Mu center is a rapidly moving interstitial and is therefore the muonic analogue of the hydrogen U_2 center observed with EPR and ENDOR techniques. It has been also found that the muonium spin relaxation rate is independent of the strength of the transverse field above 5 kG, indicating that the nuclear hyperfine interaction is totally quenched above 5 kG. There, the field independent relaxation was found to increase with temperature above 200 K.

This transverse relaxation rate of Mu in the high field, where the static depolarization of Mu is quenched may be attributed to dynamic mechanisms such as (a) a transition of Mu into another muon state, probably, a diamagnetic muon state and/or (b) a spin exchange reaction converting Mu spin state from $(S_e,S_\mu) = (1/2,\pm1/2)$ to $(-1/2,\pm1/2)$ and vice versa. So far, there have been no experimental studies which separately determined the transition rate $1/\tau$ and the spin flipping rate ν. Except in special cases, the diamagnetic μ^+ formed through a transition of Mu can not be observed with the ordinary muon spin rotation method because of the loss of phase coherency. This diamagnetic muon state after the Mu transition can only

be detected by the muon spin resonance in a decoupling field: the resonance method demands no phase coherency; at the same time, the applied decoupling field substantially suppresses the effect of the NHF fields and restores the muon spin polarization.

The time evolution of the forward/backward asymmetry $A_D(t)$ of the decay e^+ from this delayed diamagnetic μ^+ can be formulated on the basis of the depolarization model developped by Russian group[3]. When both $1/\tau$ and ν are far smaller than the muonium hyperfine frequency $2\pi\nu_0$ (ν_0 = 4.463 x 10^9 s^{-1} in vacuum), A_D changes with time as

$$A_D(t) = A_{Mu} \frac{(1+2x^2)}{2(1+x^2+\nu\tau)} [1-\exp(-(\frac{1}{\tau} + \frac{\nu}{(1+x^2)})t)], \quad (1)$$

where A_{Mu} is the asymmetry of μ^+ which becomes Mu and x is the applied field normalized by the muonium hyperfine field (1585 G). At the resonance condition, a transition between spin sub-states of diamagnetic muon state is observed time-differentially in a change of forward/backward asymmetry of the decay e^+, exhibiting a spin rotation pattern around the applied rf field H_1. The amplitude A(t) of the diamagnetic muon at the resonance is a sum of the amplitude of the "prompt" μ^+ formed at time-zero and the amplitude of the time-delayed diamagnetic muon produced after the Mu reaction. The time evolution of A(t) is given by

$$A(t) = A_\mu e^{-\alpha t}\cos 2\pi\nu_1 t + \int_0^t \frac{dA_D(t')}{dt'} dt' \, e^{-\alpha(t-t')}\cos 2\pi\nu_1(t-t'), \quad (2)$$

where A_μ is the asymmetry of the prompt diamagnetic μ^+ at time-zero, ν_1 is the spin rotation angular frequency around H_1 and α is the frequency spread mainly due to the inhomogeneity of the H_1 field. In the present experiment, we are able to determine simultaneously both τ and ν by using the above formula of the time-differential resonance signal. The details of this work are described elsewhere[4] and the results of the time-averaged resonance studies on μ^+ in KCl, NaCl and KI and related preliminary discussions are reported separately[5].

The experiment was performed at BOOM (BOOster Meson) Facility of Meson Science Laboratory of the University of Tokyo[6,7], located at KEK. The pulsed backward μ^+ beam (50 nsec width and 50 msec interval) from the superconducting muon channel enabled us to employ a high-power pulsed RF source[7,8] operated in coincidence with beam pulse for the resonance experiment. The measurement covered a wide temperature range from 40 to 300 K by using a specially designed cryostat[4]. The cryostat was installed in the μSR apparatus which was equipped with a longitudinal field Helmholtz coil, a transverse field Helmholtz coil, beam collimators and counters[7]. The time evolution of the decay asymmetry was obtained by detecting decay e^+ at the 16 channel scintillation counter telescopes placed in both forward and backward directions to the beam.

Typical examples of the observed time differential resonance signals are presented in Fig. 1. The rates $1/\tau$ and ν were separately determined by the analysis of the time spectra with the formula (1) and (2) by fixing the values of A_{Mu} to those obtained by the HTF method[2,9] and by using A_μ determined in our separate measurement of muon spin rotation. The results are plotted in Fig. 2. The value of

$1/\tau + \nu$ which corresponds to the transverse relaxation rate of Mu was found to be 2.2(8) μs^{-1} in KCl at 300 K. This is consistent with the experimental results obtained in a high transverse magnetic field[2], 2.1(3) μs^{-1}. Thus, the disappearance rate of Mu polarization is consistent with the appearance rate of the diamagnetic muon state; a clear evidence for the Mu-to-diamagnetic muon transition. The Arrhenius plots of the transition rate $1/\tau$ show a thermal activation characteristic above the specific temperature which is about 100 K for KCl and 80 K for NaCl. The data of the transition rate can be fitted by the function $1/\tau = 1/\tau_0 \exp(-E_A/kT)$ in these temperature regions (Fig. 2). The pre-exponential factor $1/\tau_0$ and the activation energy E_A were determined to be 9.4(27) μs^{-1} and 59(6) meV, respectively, for KCl, and 59(28) μs^{-1} and 90(10) meV, respectively, for NaCl. On the other hand, the spin flip rate ν seems to have a weak temperature dependence within the accuracy of the present experiment.

The observed Mu-to-diamagnetic muon transition is considered to be associated with the defects in the crystal and it should be controlled by the diffusional motions of Mu and/or the reacting defects. Let us consider the nature of the reacting defects which causes Mu to have a transition into diamagnetic muon state. Even in a nominally pure crystal, a variety of defects exist unintentionally and, in addition, the incoming μ^+ beam may also creates defects[10]. First, we consider the possibility that the Mu reacts with the native defects contained in the crystal. There are reactive paramagnetic species such as F centers which are commonly found in any sample of alkali halides and are stable at least up to 400 K[10]. The Mu relaxation rates have been measured by Mu rotation in high fields[9] both in pure KCl and in KCl with F

centers with a concentration of 10^{17}/cc. At 300 K, the measured relaxation rates were consistent with one another[9] indicating that the native F center even in such a highly doped crystal, has no effects on the reaction rate of the Mu.

Another possibility is that there is a reaction with the defects produced by the muon itself. We propose the following picture for a μ^+ implanted in KCl and NaCl. First, the μ^+ loses its energy by ionizing and exciting the surrounding ions creating a considerable amount of intrinsic lattice defects such as F- and H-centers as well as free electrons. With a high probability, the μ^+ comes to rest as a thermal quasi-free Mu at a short distance from the terminal spur. Then the Mu and the paramagnetic defects in the terminal spur begin to migrate by thermally activated diffusion. During this diffusion, the Mu encounters the defects being subject to a spin-flipping or a reaction to form a diamagnetic muon state.

The hopping rate of Mu is estimated to be about 7×10^8 s^{-1} at 300 K by comparing the observed motionally narrowed lines with those expected from the static interaction of Mu with the nearest neighbor Cl nuclei via an isotropic NHF[9], where the NHF coupling strength is taken from the hydrogen U_2 center in KCl. Since the diffusion rate is $a^2/24$ times the hopping rate (a: lattice constant) we estimate that the diffusion rate in KCl at 300 K is about 10^{-7} cm^2/s. This rate gives an average migration distance of 70 A for the Mu after 1 μs at room temperature. The distance between the terminal spur and the Mu rest-point can also be expected to be around 70 A by assuming a slowing down process to be elastic collision[4]. Thus, the reaction time which is of the order of μs at 300 K can be qualitatively explained by the Mu

diffusion to the defects created by the muon itself. Concerning temperature dependence of $1/\tau$, the observed activation energy E_A is considered to reflect potential barriers for both thermal diffusion and chemical reaction. Detailed analysis is in progress.

In conclusion, we have observed a clear evidence for the Mu-to-diamagnetic muon transition above 100 K in both KCl and NaCl using novel technique of muon spin resonance. The origin of the transition may arise from the Mu reaction with the paramagnetic species created by the muon itself during the slowing-down process. Below 100 K, the amplitudes of both delayed diamagnetic muon and Mu become substantially reduced, while the longitudinal decoupling measurements indicate an existence of muonium-like state[5]. We have no clear explanations on the origin of this behavior, except a possible transition from Mu precursor to another Mu. Further experimental studies are now in progress.

We are grateful to Prof. T. Yamazaki for helpful discussions and encouragements. We acknowledge Dr. R. F. Kiefl for his offering of the latest unpublished data and valuable comments after careful reading of the manuscript. We also thank Drs. T. Suzuki, K. Ishida, Y. Kuno, J. Imazato and T. Matsuzaki for their helps in various stages of the experiment. We are indebted to Prof. H. Yasuoka and Drs. Y. Kitaoka and M. Takigawa for their contributions to the RF source development. Helpful discussions with Prof. N. Itoh and Dr. T. Hyodo are also acknowledged. The present work is partly supported by the Grant-in-Aid of the Japanese Ministry of Education, Culture and Science.

REFERENCES

1. I.G. Ivanter, E.V. Minichev, G.G. Myasisheva, Yu. V. Obukhov, V.S. Roganov, G.I. Savel'ev, V.P. Smilga and V.G. Firsov, Sov. Phys. JETP 35 (1972) 9.
2. R.F. Kiefl, E. Holzschuh, H. Keller, W. Kundig, P.F. Meier, B.D. Patterson, J.W. Schneider, K.W. Blazey, S.L. Rudaz, A.B. Denison, Phys. Rev. Lett. 53 (1984) 90.
3. V.G. Nosov and I.V. Jakovleva, Nucl. Phys. 68 (1965) 609; I.G. Ivanter and V.P. Smilga, Sov. Phys. JETP 27 (1968) 301; I.G. Ivanter and V.P. Smilga, ibid 28 (1969) 796.
4. Y. Morozumi, doctor thesis submitted to the University of Tokyo (1984).
5. K. Nishiyama, Y. Morozumi, K. Nagamine and T. Suzuki, to be published.
6. K. Nagamine, Hyperfine Interactions 8 (1981) 787.
7. UT-MSL Newsletter, No.1(1981) - No.4(1984), eds. K. Nagamine and T. Yamazaki, unpublished.
8. Y. Kitaoka, M. Takigawa, H. Yasuoka, M. Itoh, S. Takagi, Y. Kuno, K. Nishiyama, R.S. Hayano, Y.J. Uemura, J. Imazato, H. Nakayama, K. Nagamine and T. Yamazaki, Hyperfine Interactions 12 (1982) 51.
9. R.F. Kiefl private communication.
10. N. Itoh, Adv. Phys. 31 (1982) 491.

FIGURE CAPTIONS

Fig. 1. Typical examples of time differential resonance signals for diamagnetic muon in KCl and NaCl. The chemical reaction rate $1/\tau$ and the spin flip rate ν are shown in each figure; both determined by the analysis of the time spectra of the diamagnetic muon spin resonance by using formula (1) and (2).

Fig. 2. The temperature variations of the chemical reaction rate $1/\tau$ and the spin flip rate ν obtained for Mu in KCl and NaCl, with a best-fit line of the Arrhenius type for the chemical reaction rate $1/\tau$.

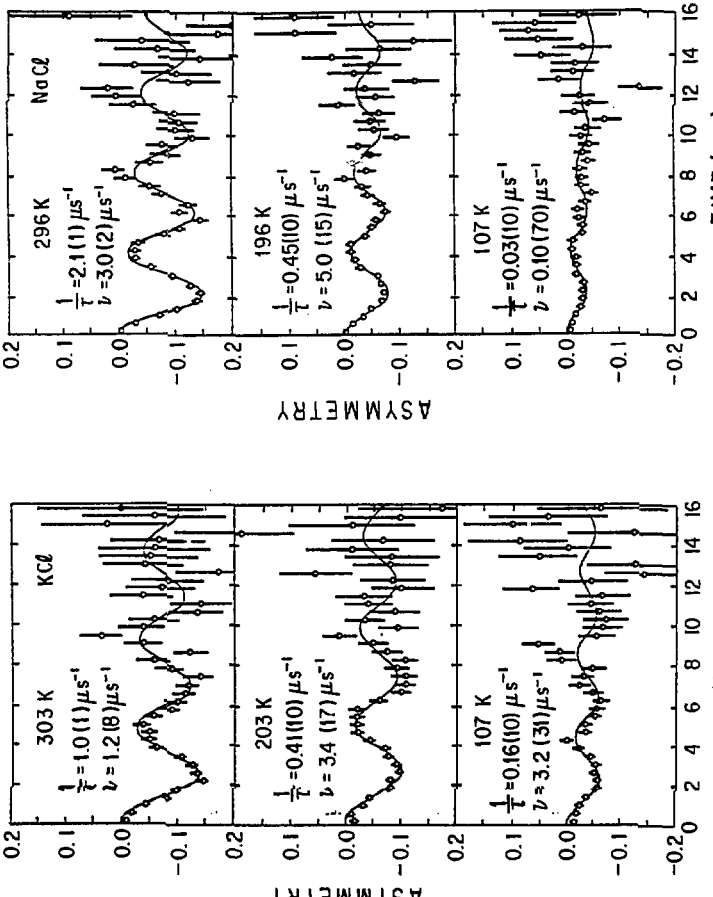
NaCl
296 K
$\frac{1}{\tau}$ =2.1(1) μs^{-1}
ν =3.0(2) μs^{-1}
196 K
$\frac{1}{\tau}$ =0.45(10) μs^{-1}
ν =5.0 (15) μs^{-1}
107 K
$\frac{1}{\tau}$ =0.03(10) μs^{-1}
ν = 0.10(70) μs^{-1}
KCl
303 K
$\frac{1}{\tau}$ =1.0(1) μs^{-1}
ν = 1.2(8) μs^{-1}
203 K
$\frac{1}{\tau}$ =0.41(10) μs^{-1}
ν = 3.4 (17) μs^{-1}
107 K
$\frac{1}{\tau}$ =0.16(10) μs^{-1}
ν = 3.2 (31) μs^{-1}
ASYMMETRY
TIME (μs)

Figure 1

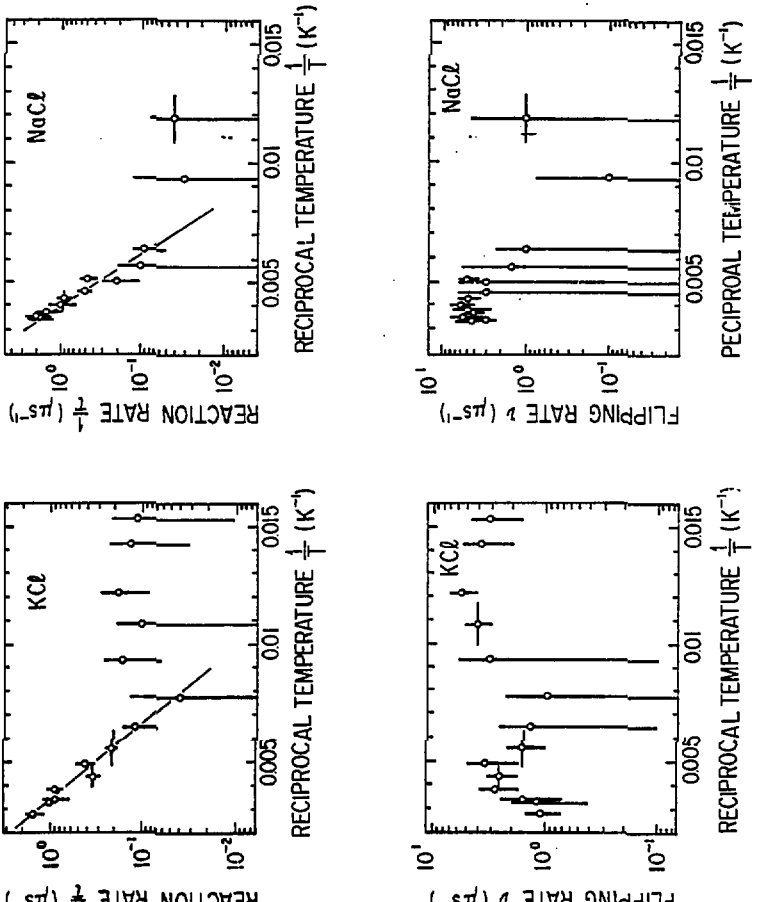
NaCl
KCl
REACTION RATE $\frac{1}{\tau}$ (μs^{-1})
FLIPPING RATE ν (μs^{-1})
RECIPROCAL TEMPERATURE $\frac{1}{T}$ (K^{-1})
10^{0}
10^{-1}
10^{-2}
0.005
0.01
0.015

Figure 2

Recent Topics in Muon Spin Polarization Phenomena and μSR Experiments

K. Nagamine

Meson Science Laboratory, Faculty of Science, University of Tokyo
Bunkyo-ku, Tokyo, Japan

Recent progress in muon polarization phenomena upon which fruitfulness of the applied muon sciences is based is reviewed with the emphasis on the recently realized method of μ^- spin repolarization with polarized nuclear targets as well as the new spectroscopy method of μ^+/Muonium state under decoupling fields, both representing the successful challenge against missing signals at t=0. Then, as a distinguished topics in the recent μSR experiments, soliton in polyacetylene produced and probed by the positive muons is described.

§1. Introduction

Positive and negative muons (μ^+, μ^-) have a decay life time of 2.2 μs in vacuum and masses of around 207 times electron mass or $\frac{1}{9}$ of proton mass. The polarization phenomena originate from the pion decay, where with the help of completely left-handed currents in the weak interaction, 100 % polarized muons are naturally available at relative high energy. When both μ^+ and μ^- are injected inside condensed matter, there are always significant changes in both μ^+ and μ^- polarizations when their energies drop below a few keV after slowing-down process lasting $\pm 10^{-9}$ s or so.

The μ^+, behaving like light protons, stays preferentially at the interstitial site in the atomic crystals during its life-time. In some cases it moves around among several interstitial sites. There, the μ^+ changes degree or direction of its polarization in response to strong local magnetic fields, either static or dynamic, from the surrounding atoms and/or nuclei. The time evolution of the polarization change can be monitored by detecting decay e^+ emitted preferentially along the μ^+ spin. The sensitivity of the μ^+ polarization to the static or fluctuating local field, as summarized in Table 1, is quite unique among the various microscopic magnetic probes like ESR, NMR, etc. When the μ^+ is injected into non-metallic materials, it picks up an electron during its slowing-down process and the muonium (Mu, neutral bound state of μ^+ and e^-) is formed. The triplet spin state of the Mu has 50 % polarization. The magnetic moment of the triplet Mu state is 100 times larger than the μ^+ so that the sensitivity of the μ^+ polarization increases.

The μ^-, when it is injected into materials, forms muonic atom around a nucleus. The μ^- quickly cascades down to the atomic ground state and mostly stays there during most of its life time, determined by the free decay rate and nucleur capture rate.

Table 1 Sensitivity of μ^+ probe

(τ_μ = 2.197 μs)

Rotation frequency under static field	$f = (\gamma_\mu H)/2\pi$
	13.554 kHz for 1 G
Dephasing time constant	$t_d = [\gamma_\mu(dH)]^{-1}$
	11.7 μs for 1 G inhomogeneity
Depolarization rate due to fluctuating fields	$\lambda = (\gamma_\mu H_f)^2 \tau_c$
	0.07-700 (μs^{-1}) for 1 KG of H_f and 10^{-11} - 10^{-7} s of τ_c

Because of strong spin-orbit interactions in the intermediate atomic states, the μ polarization at the ground state becomes down to $\frac{1}{2}$ for zero-spin nuclei and further down for nonzero-spin nuclei, due to the hyperfine interactions between nuclear magnetic moment and the μ^- moment. It should be noted that, although it is small, we can expect polarization of μ^- at the ground state of muonic atoms.

The highly polarized μ^+ or Mu and finitely polarized μ^- have been used for many experiments to probe new aspects of condensed matter: local magnetic structure at interstitial sites for μ^+ and just-beside the nuclei for μ^-; μ^+ diffusion properties in metals; Mu chemical reaction in gas and liquid phase and even in solid phase; etc. These experimental methods have been named μSR, muon spin rotation, relaxation, resonance[1]. Precise measurements of the spin precession frequency, time-dependent change of porization, etc are the basic experimental technique of the μSR studies.

In particle/nuclear physics, polarized μ^+ has been used to test the V-A hypothesis for the weak-interaction by setting the limit of the admixture of the right-handed current[2]. Polarized μ^- has been used for the basic understanding for the nuclear muon capture; high momentum transfer behaviour in nuclear weak current[3].

In the following, recent topics in muon polarization phenomena are summarized, where the discussion is focussed on new techniques of repolarization, restoration methods developed to overcome no or small polarization of the muons at the end of thermalization or at the beginning of time spectrum measurement (t=0).

§2. Negative Muon Spin Polarization Phenomena and Repolarization Experiment

Depolarization mechanism for μ^- in muonic atoms was studied theoretically many years ago[4]. So far, there have been many studies either in nuclear muon capture or in μ^-SR by using the limitedly small polarization. In order to overcome this small μ^- polarization, several ideas have been proposed aiming at precision measurement of the polarization phenomena in muon capture: 1) the selection of muonic transition $2p_{3/2} - 1s_{1/2}$ or $2p_{1/2} - 1s_{1/2}$ by measuring muonic X-ray can enhance the apparent μ^- polarization at the ground state; 2) with the aid of strong hyperfine coupling between nuclear spin I and muon spin J one can expect a highly polarized F-state (F = I + J) by using highly polarized nuclear targets. In the first method, we have to use 4π X-ray detector in order to select the μ^- which pass through either of these two transitions. In the second method, which we call here a repolarization method, we need highly polarized nuclear-targets with a reasonably large size. Recently we have successfully realized this repolarization method for muonic ^{209}Bi, a short summary of which will be given in the followings.

The experiment of the repolarization has been proposed by the present author et al.[5] based upon the concept of polarized muonic atoms[6]. The essential mechanism for the repolarization is schematically shown in Fig. 1. The polarization degree in the hyperfine F state can be given by using the formula developed for the polarized muonic atoms[6]. A more compact form of the statistical tensor of rank k for the F state $B_k(F)$ is given by Kuno et al[7] in terms of the statistical tensors of rank k_1 for the nucleus $B_{k_1}(I)$ and rank k_2 for the muon $B_{k_2}(J)$ as

$$B_k(F) = \frac{(2F+1)^{3/2}(2k+1)^{1/2}}{(2J+1)(2I+1)} \begin{Bmatrix} I & J & F \\ I & J & F \\ k_1 & k_2 & k \end{Bmatrix} B_{k_1}(I) B_{k_2}(J) \qquad (1)$$

where k=1 and k=2 corresponds to the polarization degree and the alignment degree, respectively. In this formula, it is clear that $B_1(F)$ has a non-zero value for the case when $B_1(J)=0$(no muon polarization) with a finite values of $B_1(I)$ (target polarization). Change of the statistical tensors during the transitions between various F-states can be described by using the extended U-cofficients[6,7]. Eventually the hyperfine transition ($F_+ - F_-$) at the ground states of muonic atom gives us the polarization of the lowest muonic hyperfine level where the final μ^- polarization can be obtained by projecting the F_- polarization to the muon spin.

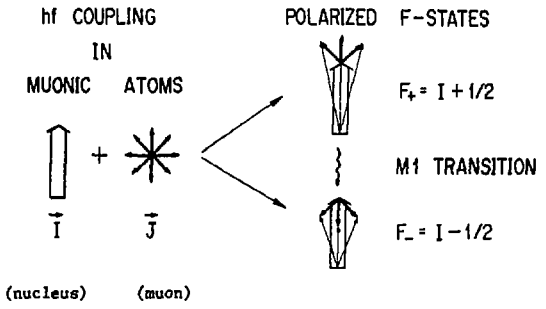

Fig. 1. Basic concept of μ^- repolarization by using highly polarized nuclear targets.

Experiment has been performed at SIN by a Tokyo-Zurich-Lausanne-Louvain collaboration[8] by using the polarized ^{209}Bi target developped by the present author et al.[9]. The highly (59(9) %) polarized ^{209}Bi target (200 gr) was realized in a ferromagnetic compound BiMn with a 7 kG external field to saturate magnetization and at relatively "high" low temperature (0.062 K). The basic experimental arrangement is shown in Fig. 2. As it is clearly seen in Fig. 2, we did not expect any contribution of the original μ^- beam polarization in this experiment ; the axis for repolarization is perpendicular to the beam direction. The repolarization degree was monitored by the asymmetric e^- emission from the polarized μ^-. Specially designed MWPC, plastic scintillation counters plus NaI crystals were used for the measurements of time-spectrum as well as energy spectrum of the decay e^- from the ^{209}Bi target by eliminating the contributing backgrounds from the surrounding materials including Mn in the BiMn compound. The observed e^- asymmetry (energy averaged) was +13.2(38) %. By assuming the energy averaged e^- asymmetry coefficient to be 0.21, taken the from the old calculation[10], we obtain the μ^- repolarization degree as −63(18) %. In these presentations of our results, we have taken the positive sign as the direction of the external field. Since the internal field of BiMn has a positive sign, the negative μ^- polarization (see Fig. 1) as well as the positive e^- asymmetry observed in this experiment is all the correct sign.

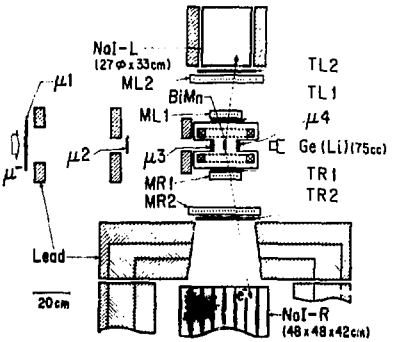

Fig. 2. Schematic view of the essential part of the μ^- repolarization experiment carried out by Tokyo-Zurich-Lausanne-Louvain collaboration at SIN.

The result should be compared to the theoretical prediction of the repolarization degree at full target polarization which becomes -1.0(3). The result is close to the value (-0.8)[7] expected for the case where the hf-interaction is switched-on at the 1s level of muonic atom. Further precise measurement should give us a clear knowledge of the repolarization mechanism; at what level hfs splitting become larger than the natural width.

§3. Positive Muon Spin Polarization Phenomena and New Techniques Using Decoupling Fields

Polarized μ^+ has been used in various types of μSR or MuSR experiments. Spin rotation measurements under traverse field have given us knowledge of the microscopic local magnetic fields for interstitial μ^+ in magnetic materials. On the other hand, spin relaxation measurements under zero or finite longitudinal field have given information on the field distributions around the μ^+ and how these are narrowed by μ^+ diffusion as well as by the spin dynamics of the surrounding magnetic moments[7]. All of these measurements need a phase-coherency; the polarization at t=0 should not be zero. However, in some cases, it has been known that zero or only a very little polarization is left at the time very near to t=0. Typical examples are the μ^+ in alkali halides, μ^+ in some organic liquids, etc. This situation had suppressed further progresses in understanding muonium and/or μ^+ states in these materials. Recently, several types of new methods have been invented in order to overcome this difficulty. All of these new techniques have employed the high magnetic field along the initial polarization direction in order to decouple the static perturbing fields in these materials. In the following, short descriptions are given for these new methods.

a) High transverse Field Rotation Method If a high applied field is applied to the Mu-like paramagnetic state (large compared to the hyperfine field between the bound electron and the μ^+), the precession frequency (ν_{12}, ν_{34}) becomes to be insensitive to the static inhomogeneous field so that the Mu/radical spin rotation can be seen under the presense of the perturbing field, provided that the detection system has adequately high time resolution. The university of Zürich group at SIN has developed this method for radical states[11] and for free Mu-like states in combination with the high time resolution μSR spectrometry[12]. They have successfully observed Mu states in alkali halides, etc. which had been left unobserved due to the strong perturbing fields from nuclear moments.

b) Level Crossing Resonance Method In muonium or muonic radical, the μ^+ is placed under the hyperfine field of the localized electrons with various hyperfine coupling constants according to the orbit sizes of the localized electrons. When the μ^+ Zeeman frequency of the applied longitudinal field becomes equal to one of these hyperfine splittings, there is a strong energy transfer between μ^+ and the electron-bath system causing a substantial depolarization. This method can provide us a precise value of the μ^+ hyperfine field even under the decoupling field. This phenomena called level crossing resonance is proposed recently by Abragam[12] and realized by the μSR group at TRIUMF for μ^+ in Cu and for Mu radicals in tetra-methyl-ethene[14].

c) Decoupling Resonance Method Under a strong longitudinal field applied along the initial muon polarization, the μ^+ polarization can be restored to the full polarization by decoupling either nuclear or electronic fields. Then in order to identify the states of muon e.g. either Mu or diamagnetic μ^+, a powerful method has been developped by the UT-MSL group. By using unique pulsed beam (50 ns width and 20 Hz repetition) available at the UT-MSL BOOM facility[15], one can apply a pulsed rf field whose peak power is strong enough to rotate μ^+ spin around the resonating rf field (H_1) within the muon life-time. For the usual sample size, the peak power amounts to some 10 kW. The principle of this muon spin resonance is schematically shown in Fig. 3. The occurrence of the resonance can be detected by the onset of the spin rotation around the effective field which becomes H_1 at the exact resonance condition. By adjusting the frequency of the rf fields to the Zeeman frequency of either Mu or μ^+, we can identify the states of Mu or μ^+ in the measure of decoupling fields.

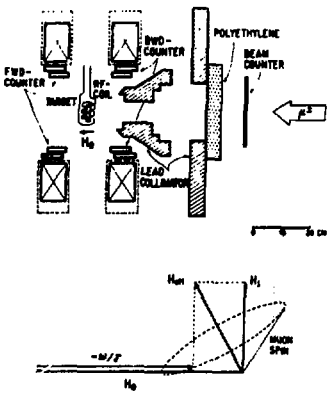

Fig.3. Principle of muon-spin resonance by using rf field under longitudinal fields.

The another advantage of this spin resonance method is the fact that we do not need any phase coherence, while other methods still need the phase memory set at t=0. The resonance signal does appears at the time of the rf-firing. Suppose there is a transition from one muon state to another with a different Zeeman frequency. It is difficult to detect the final state of this transition phenomena in a spin rotation method, but the spin resonance method can easily detect the final state of the transition, such as diamagnetic μ^+ after Mu reaction, etc.

This type of experiment, to see the reaction product of Mu under the decoupling fields has been beautifully carried out for μ^+ in alkali halides at the UT-MSL BOOM facility[16]. The observed strength of diamagnetic μ^+ produced by the Mu chemical reaction is shown in Fig. 4.

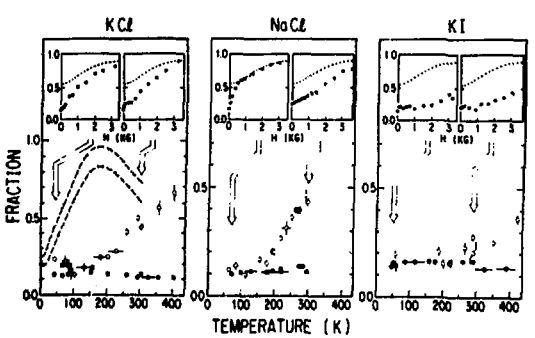

Fig.4. Temperature dependence of the diamagnetic μ^+ fraction produced as reaction products of Mu (open circles) in typical alkali halides, all revealed by muon spin resonance method. For more details, see reference 16.

Recently, significant progress has been marked for the muon spin resonace method at UT-MSL with the completion of a 500 MHz resonance apparatus, shown schematically in Fig. 5. It consists of (1) a 37 kG superconducting Helmholtz pair coil (SHC) with a 25 cm clear bore along the beam direction and a 9 cm clear gap perpendicular to the field direction and (2) a TM_{110} mode cavity made of copper plates with thin stainless sheet windows along the beam path. A typical resonance curve at 500 MHz is also shown in Fig. 5 where one can notice the capability of precise determination of the resonance field. Actually it is not difficult to measure the local field at the level of a ppm or better. Thus, we may observe, e.g., chemical shifts of μ^+ incorporated in a diamagnetic compound. Hopefully, by using this 500 MHz resonace spectrometer, we will study the various chemical reaction dynamics by measuring the chemical shifts as well as the time evolution of the state population for final states.

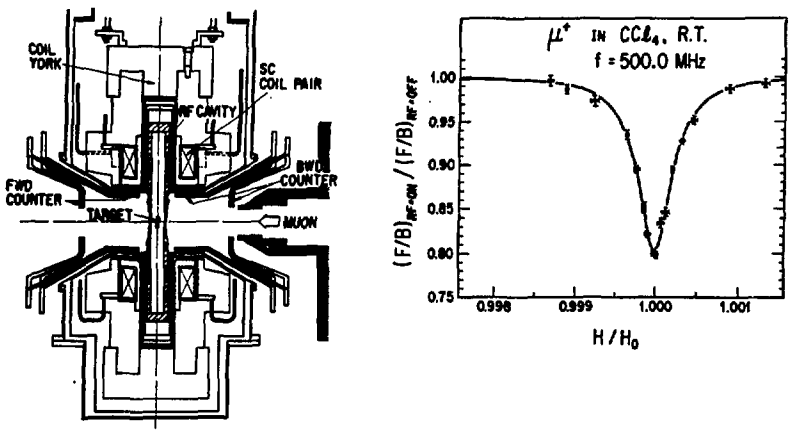

Fig. 5. Schematic view of 500 MHz Muon Spin Resonance spectrometer recently completed at UT-MSL (left) and the first resonance signal observed for the diamagnetic μ^+ in liquid CS_2 (right).

§4. High-light in Recent μSR Experiments: Solitons Produced and Proved by μ^+.

For the last 10 years, the μ^+SR method has been extensively applied to probe microscopic magnetic structure inside matter. There, the μ^+ has been treated as a "gentle" probe and it was considered to see, without significant perturbations, what the material was before the probe was brought-in. Certainly, there are lots of possible processes for the μ^+ to perturb the host material e.g. during slowing down process from a few MeV down to thermal energy. With this respect, the radiation effect of the μ^+ has been considered to explain the mechanism of the muonium formation in chemical substances; a so-called "spur" model[17]. In this picture, the μ^+ is not a "gentle" probe but a "violant" probe which introduces a change in the host system by the probe itself. A recent experiment at UT-MSL has proved that by the perturbation effect of the probe, the μ^+ can produce an interesting new phenomena of "soliton" in the celebrated organic semiconductor material, polyacetylene $(CH)_x$ and $(CD)_x$[18]. Let us explain some details of this new physics in the following.

Polyacetylene is the simplest polymer made of CH- chains with the successive order of double and single bonds, as it is shown in Fig. 6. It has two isomers called trans- and cis-polyacetylene. The ground state trans-polyacetylene can be formed in the thermal isomerzation by heating the cis- isomer above 150 C. In this isomerization process, it is known by the ESR-experiments that the unpaired electron is created in one chain out of some 10 chains. As shown in Fig. 6, the existence of unpaired electron is associated with the change of the bond alternation at the electron location. Theoretical work by Su, Shriefer and Heeger has predicted that one-dimensional motion of this unpaired electron in the trans-isomer followed by the rapid phase change of the bond-alternation is described as a "soliton", such as the non-linear dynamical motion of a chain of coupled pendula as depicted in the Fig. 7. This "soliton" motion exists only in trans-isomer because of the degeneracy of the bond-alternated states. Many experiments using ESR, NMR, etc. have uncovered this soliton behavior of the unpaired electron in polyacetylene. Almost all of these results are consistent with the soliton picture. However, the details of these results contain unclear discrepancies mainly due to the effect of paramagnetic impurities in the sample.

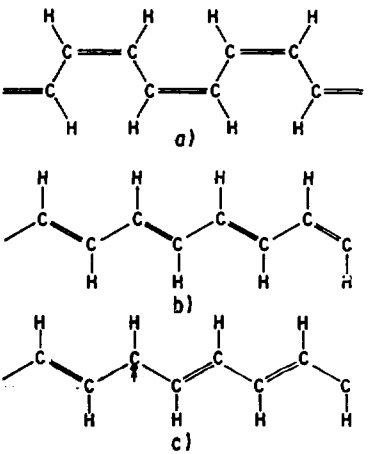

Fig. 6. Chemical structures of cis- and trans- polyacetylene with the trans-polyacetylene with unpaired electrons.

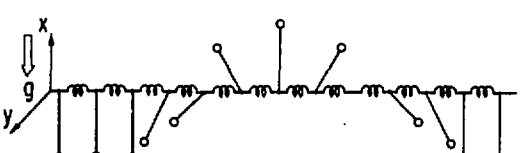

Fig. 7. Concept of "soliton" represented by the classical dynamics of chain of coupled pendula.

The μ^+ has been injected into these cis- and trans- $(CH)_x$ and $(CD)_x$ and time-evolution measurements of positron asymmetry have been done under various fields and temperatures. The data in Fig. 8 represent the counter geometry and the time-dependent change of the e^+ asymmetry or equivalently μ^+ polarization in polyacetylene at room temperature under various external fields applied along the initial μ^+ polarization direction. A clear contrast can be seen in the μ^+ polarization phenomena between cis- and trans- isomers: in cis-$(CH)_x$, the μ^+ polarization at t=0 increases drastically with the increase of the applied field with no significant relaxations at any fields; on the other hand, in trans-$(CH)_x$, the initial polarization stays almost constant at its maximum value with significant field-dependent changes in relaxation.

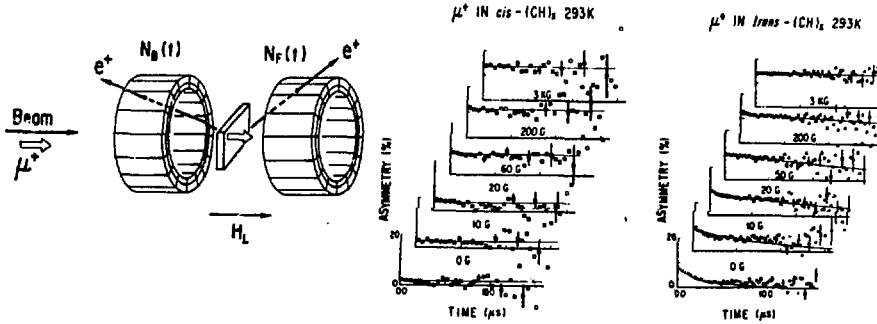

Fig.8. Counter geometry and observed time-dependence of e^+ asymmetry from polarized μ^+ stopped in (a) cis-$(CH)_x$ and (b) trans-$(CH)_x$.

The observed spin polarization behaviour in cis-$(CH)_x$ reminds us of the decoupling or quenching pattern of the μ^+ polarization when the muonium-like paramagnetic state is formed. In chemistry, it is called the muon-radical state. The formation of the radical state in cis-polyacetylene has been further confirmed by the muon spin resonance method[19] at UT-MSL and very recently by the high transverse field rotation method by the UT-MSL group at TRIUMF. The latter result is shown in Fig. 9. Thus, we have learned that the radical state formed by the μ^+ in cis-polyacetylene has a hyperfine coupling constant of 96.3(3) MHz corresponding to the electron localization at 3 times larger radius compared to free muonium. What is the mechanism of this radical state formation? According to the present understanding of the muonic radical formation in various chemical substances, the following picture seems to be adequate: the μ^+ picks up one electron to form epithermal muonium during its slowing-down process and the muonium is preferably added to the double bond of polyacetylene, where one left-out electron is localized at a nearby carbon site forming a radical electron.

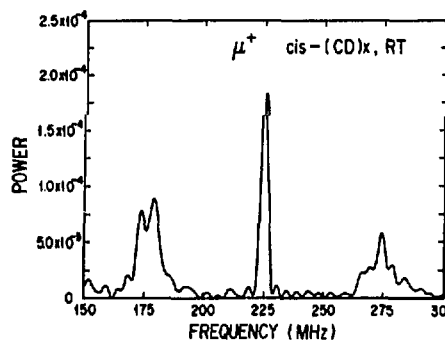

Fig.9. The μ^+ rotation frequency spectrum exhibiting the radical state rotation seen in the splitted peaks around diamagnetic μ^+.

On the contrary, the μ^- polarization phenomena in trans-$(CH)_x$ reminds us of the picture wherein the diamagnetic μ^+ is subject to a spin relaxation due to a dynamical perturbing field. Now, we have to answer why the localized electron seen in cis-$(CH)_x$ is missing in trans-$(CH)_x$. It is quite strange by considering similarities of the various physical constants between these two isomers. As a natural explanation based upon "soliton" picture, we propose the following picture: a similar process as in cis-$(CH)_x$ occurs in trans-$(CH)_x$ until one unpaired electron is formed. Then, because of degeneracy of the conjugated states, an unpaired electron takes a one-dimensional soliton-like motion followed by a rapid, change of the bond alternation. The proposed picture is seen in Fig. 10. Thus, the μ^+ sees a "soliton" and becomes subject to spin relaxation due to a rapidly fluctuating magnetic field from the moving electron. The picture is supported by the fact that the μ^+ relaxation does follow an inverse-root dependence on the applied field[18]. The absolute relaxation rate, when it is compared to the H relaxation in trans$(CH)_x$, is almost one order of magnitude enhanced. This fact is also supporting the proposed picture; the μ^+ probes soliton at the chain where the soliton is produced by the μ^+ itself, while NMR does probe the soliton with the density of 1/10 chains[18].

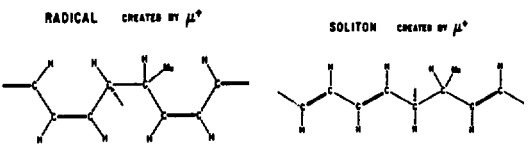

Fig. 10. Pictures of the Mu radical state in cis-polyacetylene (left) and the unpaired electron whose motion can be taken as μ^+ produced soliton in trans-polyacetylene (right).

Precise measurements of the μ^+ relaxation in trans.$(CH)_x$ have been carried out at various temperatures providing the diffusion properties of the muon-produced soliton[20]; the on-chain diffusion rate has no temperature dependence, while off-chain 3-dimensional diffusion starts to be significant above 150 K. The μ^+ produced "soliton" might be less sensitive to the effect of the paramagnetic impurities and the μ^+ probe does not show any spin diffusion phenomena because of the perfect dilute character. All of these features are quite important for further understanding of the "soliton" in condensed matter. An extensive experimental program is now in progress at UT-MSL.

§5. Conclusion and Perspectives

New ideas have been applied successfully to overcome the limited initial polarization for the μ^- in odd-nucli as well as for μ^+ and Mu in condensed matter under perturbing fields. With these techniques, these research fields will be drastically expanded in the nearest future. Soon or later, by using these methods we may have new experimental results on, e.g., photon asymmetry after radiative μ^- capture to ^{209}Bi, Mu reactions and chemical shifts of the reaction product in condensed matter, etc. etc.

As for the muon condensed matter studies, the systematic and potential use of the "Probe-effect" will become much interesting and more applicable. The "soliton" problem described here might be a tip of iceberg. More dramatic new worlds might be awaiting us!

Acknowledgement

The author would like to acknowledge Prof. T. Yamazaki for stimulating daily discussions and encouragements. He also acknowledge the strong collaborations of the UT-MSL group, particularly Drs. J. Imazato, K. Nishiyama, Y. Kuno, T. Matsuzaki, K. Ishida (now at RIKEN), Y. Morozumi (now at KEK) and Y. Yamazaki (KEK), Mr. T. Ishikawa (Dept. of Physics), Mr. R. Kadono and Mr. T. Azuma (Dept. of Atomic Engineering). The works described here are partly done at the laboratories abroad and the author would like to appreciate Prof. Truöl, Prof. Deutsch and their collaborators for repolarization experiment at SIN and Prof. Brewer and his collaborators for μSR experiment at TRIUMF. The work was partly supported by the grant-in-aid of the Ministry of Education, Science and Culture of Japan.

References

1) For general review of recent studies, see Proceedings of the Yamada Conference VII on Muon Spin Rotation and Associated Problems. eds. T. Yamazaki and K. Nagamine(J.C. Baltzer AG, Basel, Switzerland, 1984).
2) J. Carr, G. Gidal, B. Gobbi, A. Jodidio, C.J. Oram, K.A. Shinsky, H.M. Steiner, D. Stoker, M. Strovink and R.D. Tripp, Phys. Rev. Lett. 51(1983)627.
3) For most recent experiment, see Y. Kuno, J. Imazato, K. Nishiyama, K. Nagamine, T. Yamazaki and T. Minamisono, Phys. Lett. 148B (1984) 270.
4) R.A. Mann and M.E. Rose, Phys. Rev. 114(1959) 1640; K. Nagamine, Hyperfine Interactions 6 (1979)347 and references there in.
5) K. Nagamine and T. Yamazaki, TRIUMF Research Proposal E73 (1975); T. Yamazaki, Nucl-Phys. A335(1980)537.
6) K. Nagamine and T. Yamazaki, Nucl Phys. A219(1974)104.
7) Y. Kuno, K. Nagamine and T. Yamazaki, contribution to this conference
8) R. Kadono, J. Imazato, T. Ishikawa, K. Nishiyama, K. Nagamine, T. Yamazaki, A. Basshard, M. Döbeli, L. Van. E. Schand, P. Truöl, A. Bay. T.P. Perroud, J. Deutach and B. Tasiaux, contribution to this conference.
9) K. Nagamine, N. Nishida and H. Ishimoto, Nucl Instr. 105(1972)265; H. Koyama, K. Nagamine, N. Nishida, K. Tanaka, and T. Yamazaki, Hyperfine Interactions 5(1977)27.
10) V. Gilinsky and J. Mathews, Phys. Rev. 120(1960) 1450
11) For recent review. E. Roduner, Hyp. Interactions 8(1981)561.
12) R. Kiefl, E. Holzschuh, H. Keller, W. Kündig, P. F. Meier, B.D. Patterson, J. W. Schneider, K. W. Blazey, S. L. Rudaz and A. B. Denison,Phys. Rev. Lett. 53(1984)90.
13) A. Abragam, C. R. Acad. Sc. Paris, t. 299, 3(1984) 95.
14) C. Kreitzaman, private communication; R. Kiefl, private communication
15) K. Nagamine, Hyperfine Interactions 8(1981)787 ; UT-MSL Newsletter No.1-4(1981-84), eds K. Nagamine and T. Yamazami.
16) Y. Morozumi, K. Nishiyama and K. Nagamine, submitted to Phys. Rev. Lett.; K. Nishiyama, Y. Morozumi, K. Nagamine and T. Suzuki, Phys. Lett. in press.
17) for example,P. Percival, hyperfine Interaction 8(1981)315.
18) K. Nagamine, K. Ishida, T. Matsuzaki, K. Nishiyama, Y. Kuno, T. Yamazaki and H. Shirakawa, Phys. Rev. Lett. 53(1984)1763.
19) K. Ishida, T. Matsuzaki, K. Nishiyama, K. Nagamine and H. Shirakawa, to be published.
20) K. Ishida, K. Nagamine, T. Matsuzaki, Y. Kuno, T. Yamazaki, E. Torikai, H. Shirakawa and J.H. Brewer, submitted to Phys. Rev. Lett.

OBSERVATION OF MUON-FLUORINE "HYDROGEN BONDING" IN IONIC CRYSTALS

J.H. Brewer, S.R. Kreitzman,* D.R. Noakes,**
*E.J. Ansaldo,** D.R. Harshman and R. Keitel*
TRIUMF, 4004 Wesbrook Mall, Vancouver, B.C., Canada V6T 2A3

ABSTRACT

The simple spin system $^{19}F:\mu^+:^{19}F$ coupled by dipole-dipole interactions between the muon and the fluorine nuclei has been observed in transverse-field muon spin rotation (TF-μSR) and zero field muon spin relaxation (ZF-μSR) studies of single crystals of LiF, NaF, CaF_2 and BaF_2. In TF the μ^+ precession frequency splits into three or more frequencies depending upon the crystal orientation; in ZF the dipolar spin hamiltonian generates coherent oscillations of the muon polarization. With increasing temperature this coherence is progressively disrupted by μ^+ hopping. We conclude that dilute H^+ ions may form very similar hydrogen bonds between adjacent F^- ions in all metal fluoride crystals.

μ^+–FLUORINE HYDROGEN BONDING

INTRODUCTION

The behaviour of the positive muon (μ^+) implanted in alkali halide crystals has been studied for more than a decade, both theoretically[1-3] and experimentally[4-6] by means of μSR (muon spin rotation/relaxation/resonance) techniques. Most previous work has been devoted to an understanding of the electronic structure and chemical properties of the paramagnetic muonium (μ^+e^- or Mu) centre, which is formed by a fraction f_{Mu} of the muons. Recent high field, high time resolution experiments[5] have revealed that Mu forms the equivalent of the hydrogenic U_2 centre (i.e., a neutral atom in an interstitial location at the centre of the unit cube) in virtually all the alkali halides; muon resonance experiments[6] have shown that the Mu centre undergoes a thermal transition to a diamagnetic state (which could be a μ^+, a Mu^- ion or a covalently-bonded Mu atom) in NaCl, KCl and KI.

In all these experiments it was recognized that a separate fraction f_d of the muons thermalize initially in a diamagnetic state, but this fraction has not been subjected to much scrutiny until now. In this communication we report the first detailed μ^+SR investigation of this "prompt" diamagnetic fraction in fluoride crystals. Our results show that these muons form the equivalent of a double hydrogen bond, with the μ^+ located midway between two F^- ions along the line of shortest F–F separation. The dynamics of the diamagnetic configuration ^{19}F:μ^+:^{19}F observed in this work (henceforth denoted "$F\mu F$") provide a useful test

case for theories of the time evolution of the spin polarization of an implanted μ^+ in interaction with host nuclear moments.[3] These theories are of considerable interest because a great deal of μSR research is devoted to investigation of the location, diffusion and trapping of μ^+ and Mu as light counterparts of the proton and hydrogen atom impurities in solids.[7-9]

EXPERIMENT

In this typical time-differential μ^+SR experiment[7] the separated beam of 4.1 MeV "surface muons"[10] from the M15 channel at TRIUMF was stopped in single crystals of LiF or NaF (rock salt structure) or CaF_2 or BaF_2 (fluorite structure) situated in a He gas flow cryostat with thin windows. The <100> axes of the crystals were aligned parallel to the incident beam direction. As the orientation of the other axes was known only for the NaF sample, additional orientations were studied in that case, as described below.

The μ^+ spin ensemble is initially 100% polarized in the direction opposite to the muon beam. Subsequently the μ^+ polarization $\vec{P}^{\mu}$ precesses in and/or is relaxed by interaction with magnetic fields, either applied externally or due to (e.g.) the dipole moments of the host nuclei. This time dependence is manifest in the anisotropy of the positrons emitted from $\mu^+ \longrightarrow e^+ \nu \bar{\nu}$ decay,[7] which are detected as a function of time in "backward" (B), "forward" (F), "left" (L) and "right" (R) scintillation counters, where the directions described are

relative to the muon beam momentum. The time distributions $F(t)$, $B(t)$, $L(t)$ and $R(t)$ of such events (relative to the muon's entry into the target at t=0) were collected in a computer and later combined to form the "raw" asymmetry spectra

$$A'_{BF}(t) = [B(t)-F(t)]/[B(t)+F(t)] \qquad [1a]$$

$$A'_{LR}(t) = [L(t)-R(t)]/[L(t)+R(t)] \qquad [1b]$$

following subtraction of time-independent background. Each of these "raw" spectra includes a systematic "baseline shift" due to the ratio of F to B or R to L counting efficiencies, N_F^o/N_B^o or N_R^o/N_L^o; this factor, a fitted parameter in the analysis, relates the "raw" asymmetry spectra to the "corrected" asymmetry spectra via the algorithm

$$A(t) = [(1+\alpha)A'(t) - (1-\alpha)]/[(1+\alpha) - (1-\alpha)A'(t)] \qquad [2]$$

with $\alpha = N_F^o/N_B^o$ or N_R^o/N_L^o, respectively, for $A(t) = A_{BF}(t)$ or $A_{LR}(t)$. Each component of the initial asymmetry $A_i(0)$ {i = BF,LR} reflects the fraction $f_d = A_i(0)/A_0^i$ of muons thermalizing in a diamagnetic state at t = 0. The "full asymmetry" values A_0^{BF} = 0.322(2) and A_0^{LR} = 0.352(2) were determined from a control experiment on a high purity Al foil target, in which there is negligible polarization loss.[7-9]

It is conventional to have $\hat{z}$ represent the direction of the external applied field, $\vec{H}_0 = H_0\hat{z}$. In zero applied field (ZF) or longitudinal field (LF), $\hat{z}$ is also the direction of $\vec{P}^\mu(0)$, and one is mainly concerned with $G_{zz}(t)$, the longitudinal relaxation

function, obtained by simply monitoring the time dependence of P_z^μ via $A_{BF}(t)$: $G_{zz}(t) = A_{BF}(t)/A_{BF}(0)$. In transverse field (TF), $\bar{P}^\mu(0)$ defines the $\hat{x}$ direction, and the resulting precession of the muon polarization in the xy plane decays with a transverse relaxation function $G_{xx}(t)$: $A_{BF}(t) = A_{BF}(0)\ G_{xx}(t)\cos(\omega_\mu t + \phi)$, where $\omega_\mu = \gamma_\mu H_0$ and $\gamma_\mu = 8.5137\ 10^4\ s^{-1}\ Oe^{-1}$; similarly, $A_{LR}(t) = A_{LR}(0)\ G_{yy}(t)\sin(\omega_\mu t + \phi)$. When several precession frequencies ω_i are present, this TF "signal" is modified to $A_{BF}(t) = \sum_i A_{BF}^i(0)\ G_{xx}^i(t)\cos(\omega_i t + \phi_i)$ and similarly for $A_{LR}(t)$. In this work a TF magnitude $H_0 \simeq 220$ Oe was chosen so that H_0 would be high compared to typical dipolar fields and yet not high enough to appreciably deflect the μ^+ beam in the apparatus.

RESULTS: TRANSVERSE FIELD

The $F\mu F$ configuration for the diamagnetic muon fraction f_d was deduced mainly from the orientation dependence of the TF μSR spectra, as shown in Figs. 1 and 2 for the case of NaF at 100 K. Two features are readily apparent in the data of Fig. 1: a reduced initial asymmetry [relative to the value 0.322(2) measured in Al] and a clear beat pattern in the precession signal $A_{BF}(t)$. The reduction of the asymmetry (amplitude of the precession signal) is due to the fraction f_{Mu} of the muons that initially thermalize as paramagnetic Mu atoms, which have a low-field gyromagnetic ratio $\gamma_{Mu} \simeq 103\ \gamma_\mu$ and are depolarized by their interactions with nuclear spins on a nanosecond time scale.[2,5] In the present experiment they are conspicuous only in the absence of their polarization component:

$f_d = 1 - f_{Mu}$. The second phenomenon is of primary interest here and is revealed more clearly in the Fourier transform (FT) frequency spectra of Fig. 2. When the μ^+ spin $\bar{S}$ interacts with the spins $\bar{I}^i$ of lattice nuclei in the presence of a comparatively high external field $\bar{H}_0$, only "secular" terms (proportional to $S_z I_z^i$) need to be considered in the spin hamiltonian.[11] Theoretical FT spectra were calculated in this limit for the μ^+ located in a tetrahedral interstitial position and for the μ^+ bonded to anion nuclei along the <110>, <111> and <100> directions. The $F\mu F$ assumption (i.e., bonding along the <110> directions to two anions) was the only case in qualitative agreement with the observed frequency spectra; the line spectra predicted for a dipolar interaction frequency $\nu_3 = 0.220$ MHz are shown with the data in Fig. 2. For the case of $\bar{H}_0 \parallel$ <111>, where the splitting is both predicted and observed to be the largest, a three-frequency χ^2 minimization fit was made to the $A_{BF}(t)$ and $A_{LR}(t)$ spectra simultaneously. This fit yielded a central frequency of 2.9980(7) MHz, a lower sideband splitting of $\Delta\nu_- = 0.1983(15)$ MHz and an upper sideband splitting of $\Delta\nu_+ = 0.2204(15)$ MHz. Theory predicts both sidebands split equally by the dipolar interaction frequency $\nu_3 = \omega_3/2\pi$, where

$$\hbar\omega_3 = \gamma_\mu \gamma_F / r^3 \qquad [3]$$

and r is the μ^+–^{19}F distance, which is thus determined to have a value $r = 1.17(6)$ Å if we use the average of the two splittings. The 10% asymmetry in the splitting, $\Delta\nu_+ - \Delta\nu_- = 0.022(2)$ MHz, could be due to next-nearest neighbour dipolar interactions

and/or to an asymmetric distortion of the $F\mu F$ configuration.

RESULTS: ZERO FIELD

Representative ZF-μSR relaxation functions are displayed in Fig. 3. The prominent oscillations evident in these data are completely atypical of ZF-μSR spectra previously obtained in media exhibiting nuclear dipolar relaxation, which have always qualitatively resembled the stochastic ZF relaxation function $g_{zz}^{KT}(t)$ first calculated by Kubo and Toyabe (KT)[12] long before the advent of the ZF-μSR technique by which it was first observed.[13] In the KT approach the effect of the nuclear dipoles is modelled by a static random local field at the μ^+ with an isotropic Gaussian distribution of width Δ given by the second moment: $2\Delta^2 = M_2 = \frac{1}{3}I(I+1)\sum_i \hbar\gamma_\mu\gamma_I\,[5 - 3\cos^2\theta_i]/r_i^3$. The resultant relaxation function, $g_{zz}^{KT}(t)$, consists of an initial gaussian relaxation followed by a recovery to $\frac{1}{3}$ at late times; this function, and its generalization to cases in which the local field at the muon fluctuates due to muon "hopping", has provided a good empirical description of muon relaxation in metals with $I > \frac{1}{2}$, where its is used extensively to characterize μ^+ diffusion mechanisms.[9,14] However, the increasing precision and resolution of ZF-μ^+SR techniques has forced the realization that the KT formulation, though elegant, is only an approximation. Recently, $G_{zz}(t)$ has been calculated in a fully quantum mechanical formulation for several simple configurations of nearest neighbor (nn) nuclei around the μ^+ impurity.[15] Even the simplest case considered, with the μ^+ in a tetrahedral site

with 4 *nn* spin-$\frac{1}{2}$ nuclei, had to be solved numerically. For this and more complex situations the $G_{zz}(t)$ obtained deviate from $g_{zz}^{KT}(t)$, displaying extra oscillations at long times (i.e., for $t \gtrsim 2/\Delta$), which can be understood qualitatively as due to the combination of two effects: first, the actual field distribution produced by a small number of dipoles in a simple regular array is not quite Gaussian, but includes sharper features in the spectral density which manifest themselves as oscillations in the time domain; second, quantum mechanics allows "flip-flop" transitions involving the muon and individual nuclei, which if isolated from other interactions would be manifest as coherent oscillations of the two-spin-$\frac{1}{2}$ density matrix -- just as seen in Fig. 3. Unfortunately the cases of current interest that have been well studied experimentally before this experiment (e.g., the octahedral μ^+ site and enhanced low-T diffusion in Cu crystals) are very complicated (calculations have to include the $I = \frac{3}{2}$ nuclear quadrupole terms in the EFG induced by the muon)[16,17] and result in a more complex pattern of reduced-amplitude oscillations, barely detectable in the usual experiments in metals,[18] that qualitatively resemble the KT function. The far simpler case treated here illustrates the power of quantum mechanical calculations based on at least partial lattice sums to reveal details of the μ^+ site through precise measurements of the ZF relaxation function.

Another striking feature of the oscillations in Fig. 3 is the similarity of their frequencies for different crystals and even different crystal structures; this is in accord with the

proposed $F\mu F$ configuration, since both the local structure around the F–F axis and the shortest F–F distance -- 2.85 Å for LiF, 3.27 Å for NaF, 2.73 Å for CaF_2 and 3.10 Å for BaF_2 -- are quite similar in the rock salt and fluorite structures.

As a first approximation, $G_{zz}(t)$ was calculated from first principles in a static 3-spin model assuming the $F\mu F$ colinear geometry with the μ^+ at the centre of the line joining the ^{19}F nuclei (quantization axis for the ZF problem) and considering only the μ^+–^{19}F dipolar interaction. Averaging over equivalent directions in the cubic lattice, one obtains

$$G_{F\mu F}(t) = \tfrac{1}{6} \exp[-\Lambda(t)] \left[3 + \cos(\sqrt{3}\,\omega_3 t) + (1 - \tfrac{1}{\sqrt{3}}) \cos\{(\tfrac{3 - \sqrt{3}}{2})\,\omega_3 t\} + (1 + \tfrac{1}{\sqrt{3}}) \cos\{(\tfrac{3 + \sqrt{3}}{2})\,\omega_3 t\}\right] \quad [4]$$

The solid lines in Fig. 3 are best fits to the sum of two relaxation functions,

$$G_{zz}(t) = f_{F\mu F}\, G_{F\mu F}(t) + f_?\, G_?(t), \quad [5]$$

where the extra term represents a small fraction $f_?$ of the μ^+ ensemble with a nondescript relaxation function $G_?(t)$, apparently unrelated to the $F\mu F$ system, which was always required for an acceptable fit. Both $G_?(t)$ and the $F\mu F$ relaxation envelope were allowed to have the form of a generalized exponential, $\exp[-\Lambda(t)]$, with

$$\Lambda(t) = [\lambda t]^{\beta} \qquad [6]$$

The parameters extracted from these fits are presented in Table I.

Values β=1 and β=2 of the phenomenological "shape parameter" β correspond, respectively, to the usual exponential and gaussian limits. For LiF and NaF a value of $\beta \simeq 1.5$ gave the best fits. For CaF_2 and BaF_2, $\beta \simeq 0.5$; values of $\beta < 1$ may indicate the presence of fast-relaxing components in the μSR signal. One may speculate that such components are due to the products of a heretofore undetected reaction pathway for muonium.

"HOPPING" AT HIGH TEMPERATURE

ZF-μ^+SR measurements were also made in NaF at elevated temperatures, where the μ^+ shows an increasing tendancy to "hop" from one $F\mu F$ site to another. This causes an averaging effect on the $G_{zz}(t)$ function. As shown by Kehr,[19] such effects can be modelled by a convolution of random processes, fits to which yield a hop rate ν_{hop} as a function of temperature. Using these methods we find that $\nu_{hop}(T)$ in NaF obeys a simple Arrhenius activation behaviour with an activation temperature of $T_a \simeq 1700$ K and a preexponential factor of $\nu_0 \simeq 10^6\ \mu s^{-1}$. The small "extra" component $f_?$ was only weakly temperature dependent. Since this fraction does not show up in the TF diamagnetic precession signal, it can probably be associated with at least part of that fraction f_{Mu} of muons which initially thermalize as Mu atoms. In view of the extremely rapid depolarization of

static Mu by nuclear hyperfine fields,[2,5] this component must be diffusing rapidly to be visible in this experiment. Other experiments[4] have shown that Mu atoms in alkali halides undergo subsequent reactions leaving them in diamagnetic states; possibly the products are Mu^- ions in vacancies, which would then experience only weak relaxation. In any case the weak T-dependence is somewhat surprising.

BOND LENGTHS

The muon-fluorine bond lengths deduced from Eq. [3] using the ZF data are as follows: LiF: $2r$ = 2.36(2) Å [compare 2.85 Å rigid-lattice F–F separation]. NaF: $2r$ = 2.38(1) Å [compare 3.27 Å rigid-lattice F–F separation]. NaF: $2r$ = 2.38(1) Å [compare 3.27 Å rigid-lattice F–F separation]. CaF_2: $2r$ = 2.34(2) Å [compare 2.73 Å rigid-lattice F–F separation]. BaF_2: $2r$ = 2.37(2) Å [compare 3.10 Å rigid-lattice F–F separation]. For NaF the ZF result is consistent with the TF value of r obtained earlier. In each case, the F^- ions have been "pulled in" by the μ^+ to a separation slightly less than their rigid-lattice distance; the constancy of the r values so obtained, and their similarity to the length of about 1.14 Å for the H^+–F^- bond in $NaHF_2$,[20] suggest that "hydrogen bonding" is the most apt description of the formation of the $F\mu F$ complex, and that it is likely to be a ubiquitous feature of μ^+ (or H^+) behaviour in ionic crystals.

SUMMARY: "HYDROGEN" BONDING OF MUONS IN FLUORIDES

In summary, this work has revealed the existence of a remarkably stable diamagnetic state of the positive muon in ionic insulators, largely independent of crystal structure or temperature, in which the μ^+ is bonded to two anions with an average bond length of about 1.2 A. This state is vividly evident for the case of F^- anions because of the large ^{19}F moment and the lack of complications due to quadrupole moments. The bond lengths found are consistent with that of the H^+—F^- bond in $NaHF_2$, one of the "most hydrogen-bonded" materials known. We therefore surmise that similar bonds may be formed whenever hydrogen atoms are implanted into alkali halides.

The $F\mu F$ model of Eqs. [4-6] describes the main features of the data well, but as can be seen from Figs. 2 and 3, there are additional effects to be considered. Corrections due to cation nuclear moments, for instance, should be largest in LiF; this is borne out in Fig. 3 by the poor agreement between Eq. [5] and the ZF LiF data for $t > 5$ μs. Similarly, the TF frequency spectra are not symmetric as predicted; considering the local lattice distortion implied by the reduction of the μ—F bond length, one must expect large electric field gradients, muon zero-point motion, and the opportunity for Jahn-Teller effects. These subtle effects can be investigated experimentally through the deviations from the simple $F\mu F$ model.

ACKNOWLEDGEMENTS

We would like to thank Dr. K. Nagamine and Dr. A. Mills for the loan of their samples; we are also indebted to them and to Dr. R. Kiefl for enlightening discussions of their work on muonium and positronium in alkali halides. This research was supported by NSERC of Canada and, through TRIUMF, by the Canadian NRC.

REFERENCES

* Department of Physics, University of British Columbia, Vancouver, B.C., Canada V6T 2A3

** Department of Physics, University of Saskatchewan, Saskatoon, Sask., Canada S7N 0W0.

1. V.G. Nosov and I.V. Yakovleva, JETP 16, 1236 (1962); I.G. Ivanter and V.P. Smilga, JETP 27, 301 (1968); I.G. Ivanter and V.P. Smilga, JETP 28, 796 (1969); I.G. Ivanter, JETP 29, 761 (1969); I.G. Ivanter and V.P. Smilga, JETP 33, 1070 (1971); I.G. Ivanter and V.P. Smilga, JETP 34, 1167 (1972).

2. P.F. Meier and A. Schenck, Phys. Lett. **50A**, 107 (1974); R. Beck, P.F. Meier and A. Schenck, Z. Physik B22, 109 (1975).

3. M. Celio and P.F. Meier, Phys. Rev. **B28**, 39 (1983).

4. I.G. Ivanter, E.V. Minaichev, G.G. Myasishcheva, Yu.V. Obukhov, V.S. Roganov, G.I.Savel'ev, V.. Smilga and V.G. Firsov, JETP 35, 9 (1972).

5. R.F. Kiefl, E. Holzschuh, H. Kellar, W. Kundig, P.F. Meier, B.D. Patterson, J.W. Schneider, K.W. Blazey, S.L. Rudaz and A.B. Denison, Phys. Rev. Lett. 53, 90 (1984).

6. Y. Morozumi, K. Nishiyama and K. Nagamine, private communication (submitted to Phys. Lett.); K. Nishiyama, Y. Morozumi, K. Nagamine and T. Suzuki, *ibid.*

7. A. Schenck, in *Nuclear and Particle Physics at Intermediate Energies, ed.* J.B. Warren (Plenum, New York, 1976) p. 159; J.H. Brewer and K.M. Crowe, Ann. Revs. Nucl. Part. Sci. 28, 239 (1978).

8. D. Richter, in Springer Tracts in Modern Physics 101 (Springer-Verlag, New York, 1983).

9. Proceedings of the First International Topical Meeting on Muon Spin Rotation, Hyperfine Int. 6 (1979); Proceedings of the Second International Topical Meeting on Muon Spin Rotation Hyperfine Int. 8 (1981); Proceedings of the Yamada Conference on Muon Spin Rotation and related problems, Hyperfine Int. 17-19 (1984).

10. T. Bowen, Physics Today **38**, No.7, P. 22 (1984).

11. C.P. Slichter, *Principles of Magnetic Resonance*, Second Edition, Ch. VI (Springer-Verlag, New York, 1978).

12. R. Kubo and T. Toyabe, in *Magnetic Resonance and Relaxation*, ed. by R. Blinc (North-Holland, Amsterdam, 1966).

13. R.S. Hayano, Y.J. Uemura, J. Imazato, N. Nishida, T. Yamazaki and R. Kubo, Phys. Rev. B20, 850 (1979).

14. C.W. Clawson, Ph.D. Thesis, UC Berkeley, 1982. LBL-14489.

15. M. Celio and P.F. Meier, Phys. Rev. B27, 1908 (1984);

E. Holzschuh and P.F. Meier, Phys. Rev. B29, 1129 (1984).

16. O. Hartmann, Phys. Rev. Lett. 39, 832 (1977); M. Camani, F.N. Gygax, W. Ruegg, A. Schenk and H. Schilling, Phys. Rev. Lett. 39, 836 (1977).

17. S.R. Kreitzman, J.H. Brewer, D.R. Harshman, R. Keitel, D.Ll. Williams, K.M. Crowe and E.J. Ansaldo, submitted to Phys. Rev. Lett. (1985).

18. R. Kadono, J. Imazato, K. Nishiyama, K. Nagamine, T. Yamazaki, D. Richter and J.-M. Welter, Phys. Lett. 107A, 279 (1985).

19. K.W. Kehr, Phys. Rev. B 26, 567 (1982).

20. S.N. Vinograd and R.H. Linnell, *Hydrogen Bonding* (Van Nostrand, New York, 1971).

Table I.

Summary of parameters of Eqs. [3-5] extracted from ZF-μ^+SR time spectra by χ^2-minimization fits.

Crystal	T(K)	$f_?$	$f_{F\mu F}$	$\nu_3(\mu s^{-1})$	$2r$ (Å)	Lattice F–F (Å)
NaF	15.0(2)	0.03(2)	0.223(9)	0.214(3)	2.38(1)	3.27
NaF	210(1)	0.05(2)	0.227(9)	0.217(2)	2.38(1)	3.27
LiF	89(2)	0.10(1)	0.163(5)	0.222(2)	2.36(2)	2.85
CaF_2	80(1)	0.10(2)	0.174(3)	0.226(2)	2.34(2)	2.73
BaF_2	211(2)	0.29(3)	0.382(7)	0.214(2)	2.37(2)	3.10

FIGURE CAPTIONS

1. TF-μ^+SR precession signals $A_{BF}(t)$ in NaF at 100 K with $H_o \simeq$ 220 Oe along the crystalline <111> axis.

2. Fourier transform frequency spectra of the TF-μ^+SR signals in NaF at 100 K with the indicated crystal axes aligned parallel to an applied magnetic field $H_o \simeq 220$ Oe. The bar diagrams are predicted line spectra for the colinear $F\mu F$ configuration along the $\langle 110 \rangle$ direction, using a dipolar interaction frequency of $\nu_3 = 0.220$ MHz.

3. ZF-μ^+SR asymmetry spectra $A_{BF}(t) = f_d A_o^{BF} G_{zz}(t)$ for several metal fluoride crystals at the indicated temperatures, with the crystalline $\langle 100 \rangle$ axis parallel to the initial muon polarization. The solid line in each case is a fit to Eq. [5]; the parameters extracted from the fits are listed in Table I.

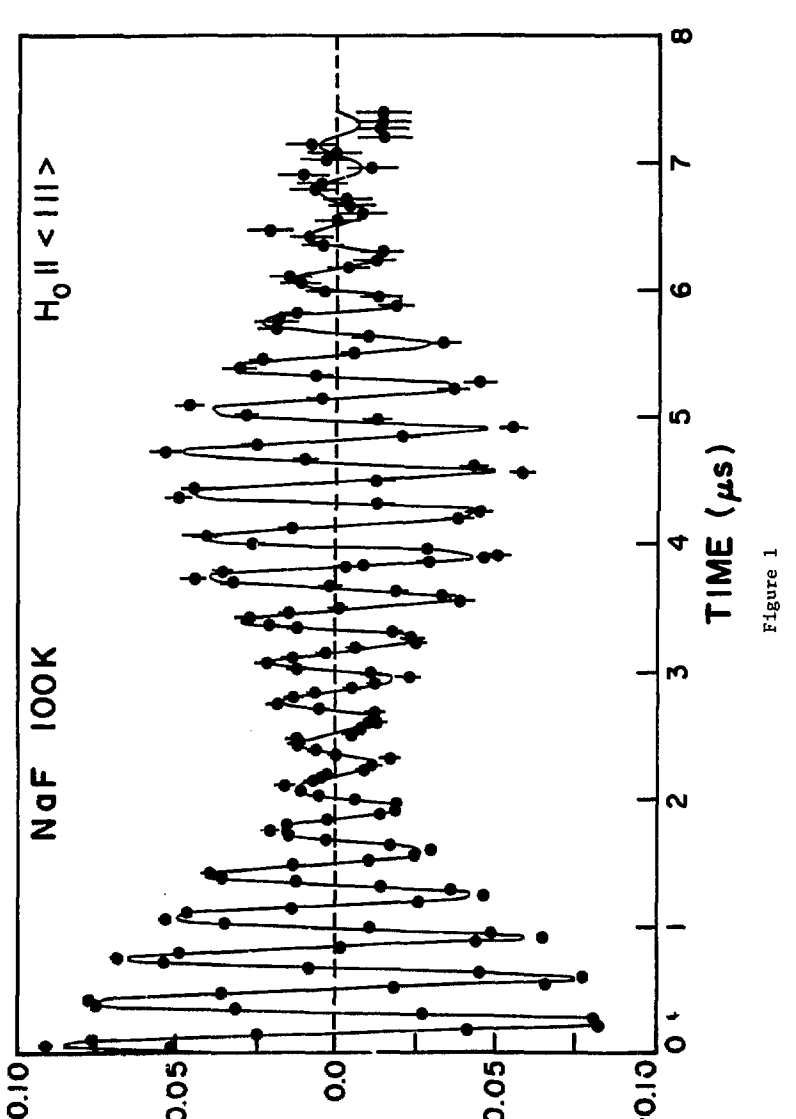
NaF 100K
$H_0 \parallel <111>$
ASYMMETRY
0.10
0.05
0.0
-0.05
-0.10
0
1
2
3
4
5
6
7
8
TIME (μs)

Figure 1

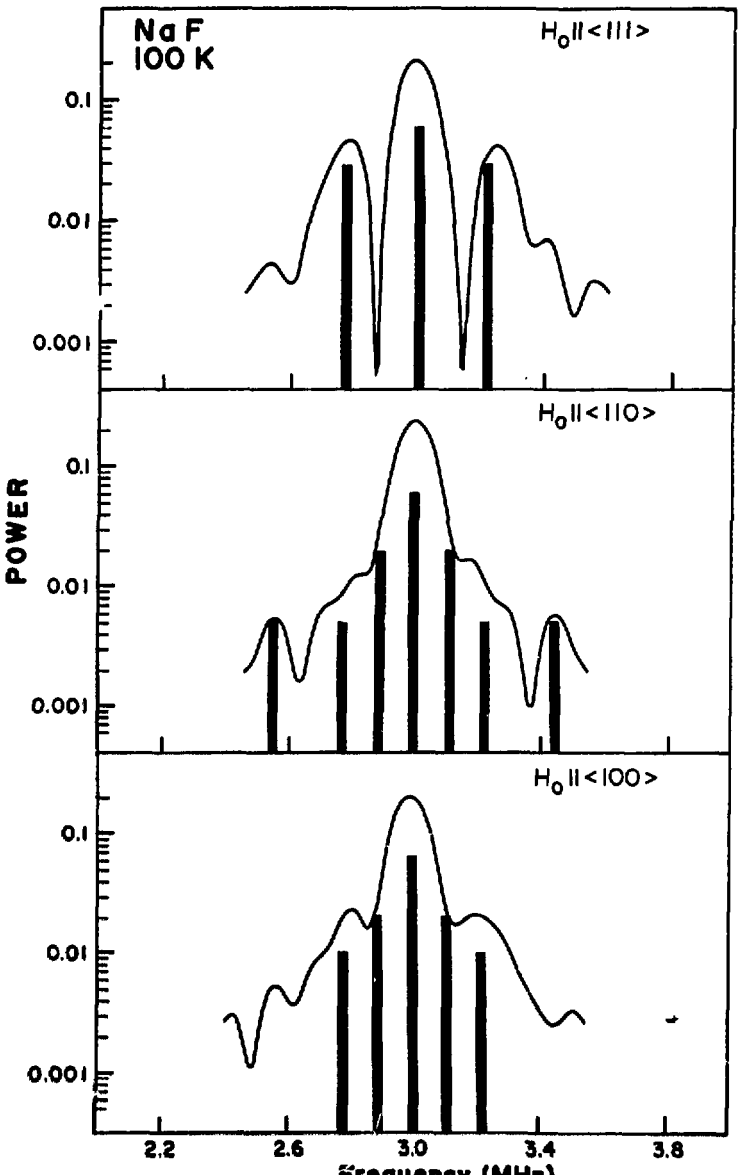
Na F
100 K
$H_0 \| <111>$
$H_0 \| <110>$
$H_0 \| <100>$
POWER
0.1
0.01
0.001
2.2
2.6
3.0
3.4
3.8
Frequency (MHz)

Figure 2

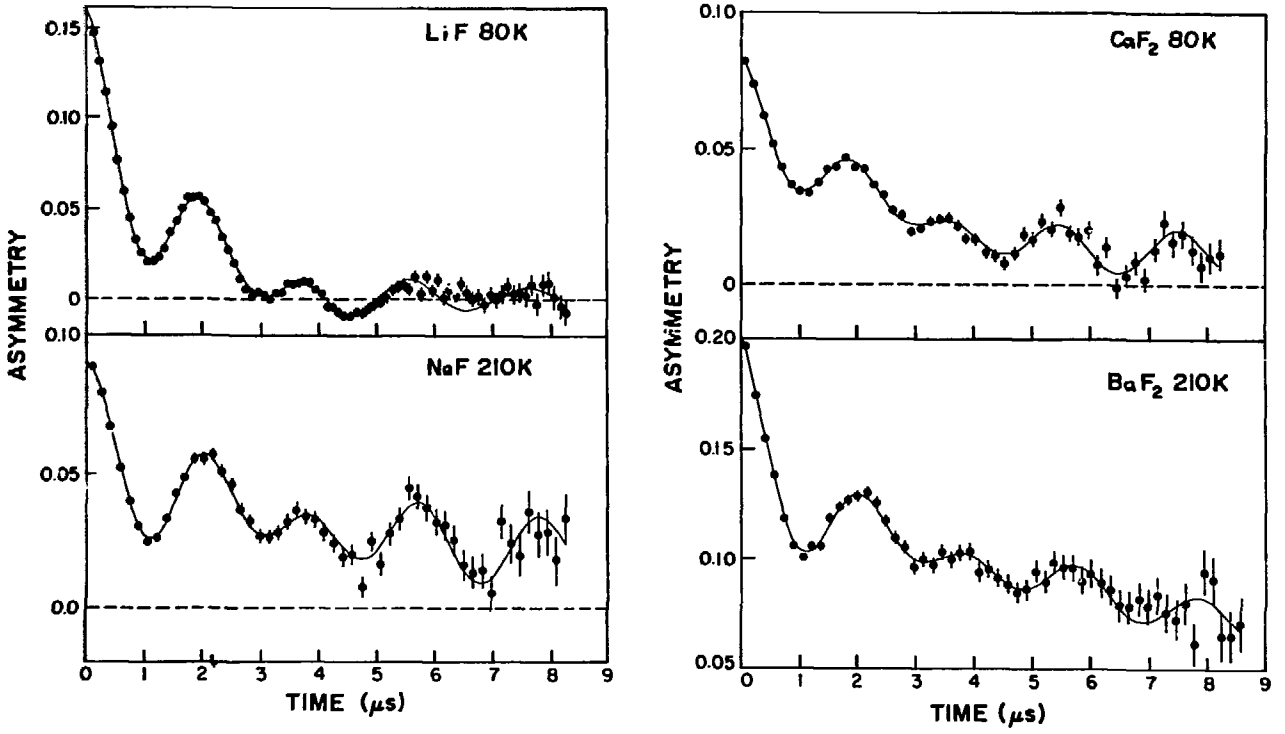

Figure 3

A Spin Rotator for Surface μ^+ Beams on the New M20 Muon Channel at TRIUMF(*)

John L. Beveridge, Jacob Doornbos, David M. Garner,
TRIUMF, 4004 Wesbrook Mall, Vancouver, B.C., Canada, V6T 2A3.

and

Donald J. Arseneau, Ivan D. Reid and Masayoshi Senba,
Department of Chemistry, University of British Columbia,
Vancouver, B.C., Canada, V6T 1Y6.

Abstract

The TRIUMF low energy muon channel, M20, was completely rebuilt in 1983. Amongst the features incorporated into the new channel is a 3-metre long Wien filter or D.C. separator. For surface and sub-surface μ^+ beams, the magnetic field of this device is sufficient to rotate the muon spin from its natural orientation, antiparallel to the beam momentum, by 90° into a transverse orientation. The performance of this muon "spin rotator" is described.

(*) Meson Facility of the University of Alberta, University of Victoria, Simon Fraser University and the University of British Columbia.

I. Introduction

The term "surface muon" refers to the μ^+ formed from pions decaying at rest within a few microns of the surface of a meson production target [1,2]. Since the construction of the prototype surface μ^+ beamline by Pifer et al. [3] at the 184" cyclotron at the Lawrence Berkeley Laboratory in the late 1960s, surface μ^+ channels have been commissioned at many accelerator laboratories. Surface muons have a maximum momentum of 29.8 MeV/c and a momentum spectrum which falls off as $p'^{/2}$ below this maximum. In recent years the phrase "sub-surface muon" has been used to denote lower energy (e.g. 400 keV or 9.2 MeV/c) muons which are derived from pions decaying at rest deep inside the meson production target [4,5]. For the purposes of this paper "surface" μ^+ will be used to encompass all muons arising from pion decay within the production target.

The primary advantages associated with surface muon beams are: (1) the high beam flux available due to the high pion stopping densities at the production target surface [2]; (2) the high luminosity and good optics of the beam [6] due to the direct imaging of the meson production target; (3) the short range (<150 mg/cm^2) and low range straggling (< 30 mg/cm^2) [6], allowing the use of very thin targets such as low pressure gases [7], or thin foils [4,5]; (4) the high (~100%) longitudinal spin polarization [8].

However, two attributes of such beams may be disadvantageous [6]: (1) surface μ^+ beams are normally contaminated by ~30 MeV/c e^+. Depending upon the meson production target material and shape, take-off angle of the surface μ^+ channel, etc., the e^+/μ^+ ratio may vary from 1:1 [2] to ~5:1 [9]. Unfortunately, the beam e^+ energy of ~30 MeV is almost that of the

average e^+ emitted in μ^+ decay within the experimental target, making it difficult to reject this background from the muon decay signal; (2) the radius of curvature of surface μ^+ in a magnetic field is <1 m/kG which may make it difficult to inject surface μ^+ into a strong magnetic field oriented transversely to the muon beam momentum.

Several means have been used to circumvent these problems such as the use of a thin degrader at the intermediate focus of the channel [6] or the injection of surface μ^+ into a specially designed, small, field-clamped transverse magnetic field apparatus [10]. A more elegant approach was demonstrated by Brewer in 1980 [6]. It was shown with the M9 channel at TRIUMF that a D.C. separator (Wien filter) can be used both to remove the positron contamination in the surface μ^+ beam and to rotate the muon spin so that it is transverse to the momentum. Such a beam is easily injected into a strong magnetic field oriented longitudinally to the momentum but transversely to the (rotated) muon spin. Besides demonstrating the application of a D.C. separator as a surface muon spin rotator, Brewer noted many of the advantages that would result from the use of such a device [6], especially the possibility of a single experimental apparatus for both longitudinal field (muon spin parallel to the magnetic field) and transverse field (muon spin perpendicular to the magnetic field) μSR (muon spin rotation) experiments.

The complete upgrade of the M20 muon channel at TRIUMF in 1983 presented the opportunity to incorporate the D.C. separator formerly located in M9 into a design which restores the surface μ^+ spin rotator capability which, to our knowledge, is presently unique in the world.

II. The M20 Spin Rotator

Figure 1 gives a plan view of the TRIUMF M20 channel showing the

spin rotator in the 37.5° M20B leg. The M20 channel is extremely versatile, capable of delivering a wide variety of cloud and decay $\mu^{\pm}$ beams as well as surface μ^{+} beams to both experimental areas (M20A and M20B). The detailed performance of these various operational modes will be presented in a subsequent publication [9]; the present paper will focus on the performance of the spin rotator as used with surface μ^{+} on M20B.

The spin rotator is 3 metres long and consists of a vertically oriented electric field and horizontally oriented magnetic field. The high-voltage gap is 10 cm and it can support an electric field in excess of 60 kV/cm. The rotator vacuum is isolated from the rest of the beamline by thin (0.0008 cm) Kapton windows, since for high voltage operation (>20 kV/cm), a low pressure (~0.001 torr) of Ar gas is maintained in the electrode gap to suppress high voltage discharges [11]. Between the rotator and final quadrupole triplet (QB11-QB13) are a set of independently movable horizontal and vertical 7.5 cm thick copper jaws to intercept positrons deflected from the beam by the rotator. The rotator is housed in a 2 cm thick enclosure of lead to shield personnel from X-rays produced by high voltage discharges from the electrodes.

To operate the rotator, the electric field is manually set to the desired value and then the magnetic field is swept, via computer control, to optimize the transmission of the appropriate particles. The vertical jaws may be adjusted to define a horizontal slit to eliminate beam halos or, as shown below, narrow the momentum bite.

III. Theory of Operation.

The underlying principles of a muon spin rotator are quite simple and have been well treated elsewhere, e.g. Frosch [12]. The magnetic elements of the beamline select particles according to their momenta but,

because of the disparity in mass between positrons and muons, these two beam components have greatly different velocities and can be easily separated. In operation, the crossed magnetic and electric fields of the rotator are adjusted so that they produce equal and opposite forces on the particles of interest. Only particles with nominal velocity given by

$$\beta_0 = A\, E_0/B_0 \tag{1}$$

where E_0 and B_0 are the electric and magnetic fields respectively, and A=3.33 Gauss $(kV/cm)^{-1}$, will traverse the spin rotator without deflection [12]. Selecting an appropriate electric field and then adjusting the magnetic field to maximise the flux of transmitted surface muons quite effectively removes the positron contamination.

The muons, in traversing the rotator, experience a magnetic field of B_0/γ_0 in their rest frame, where $\gamma_0 = (1-\beta_0^2)^{-1/2}$, and will undergo gyromagnetic precession in this field. The angle of precession is [12]

$$\phi = eB_0L/p_0\gamma_0 \tag{2}$$

where L is the effective magnet length, p_0 is the muon beam central momentum, and e is the electronic unit charge. The magnetic field required to rotate the muon's spin by 90° into a direction transverse to its momentum is, in the present case (L=2.94 m, p_0=27 MeV/c, β_0=0.247, γ_0=1.032)

$$B_0 = 496 \text{ Gauss} \tag{3}$$

with a corresponding electric field of

$$E_0 = 36.8 \text{ kV/cm} \tag{4}$$

The spin rotator causes particles which have momenta different from p_0 to be dispersed. Frosch [12] presents a transport matrix for particles passing through a spin rotator, giving, in the case of 90° rotation:

$$x(L) = 2L\theta(0)/\pi - 2L\,\delta(0)/\pi\gamma_0 \tag{5a}$$

$$\theta(L) = -\pi x(0)/2L - \delta(0)/\gamma_0 \qquad (5b)$$

$$\delta(L) = \delta(0) \qquad (5c)$$

where $x(z)$ and $\theta(z)$ are the distance and angle respectively from the rotator centreline, and $\delta(z) = p(z)/p_0 - 1$, z being measured from the entrance to the rotator. A slit of width S centred on the z axis at a distance D from the separator exit intercepts dispersed particles and thus restricts the momentum band transmitted further along the beamline. For the particular case of particles entering the rotator midway between the electrodes and travelling along the z-axis (i.e. $x(0) = 0$, $\theta(0) = 0$), only those particles with

$$| x(L) + D \sin(\theta(L)) | < S/2 \qquad (6a)$$

will pass through the slit. Substituting from Eq. 5, and making the approximation $\sin(\delta(0)/\gamma_0) = \delta(0)/\gamma_0$ yields

$$| \delta(0) | < S\,\gamma_0/2(2L/\pi + D) \qquad (6b)$$

In the present study, the horizontal slit was 15 cm wide and positioned 1.75 m from the end of the rotator, giving

$$| \delta(0) | < 0.021 \qquad (6c)$$

This is, of course, the best possible momentum selection capability of this slit in our experiments, since, in fact, the muons enter the rotator with a distribution of values in x and θ.

IV. *Experimental Technique*

Measurements of the spin rotator characteristics were primarily conducted using the transverse field muon spin rotation (TF-μSR) technique which is now a well-established experimental tool of materials science, atomic physics and chemistry [13,14]. TF-μSR involves the observation of the coherent spin precession of muons at the Larmor frequency of 8.52×10^4 B rad/s, where B is a magnetic field oriented

transversely to the muon spin polarization. The anisotropic decay of the muon via the reaction:

$$\mu^+ \rightarrow e^+ + \nu_e + \bar{\nu}_\mu \qquad (6)$$

with a mean lifetime of 2.2 μs results in positron emission preferentially along the muon spin. Thus, μSR histograms, such as those shown in Figures 3 and 5, are simply radioactive decay curves of the muon upon which are superimposed the modulations due to muon spin precession.

The apparatus used for the present experiments was built for studies of the exotic atom muonium (μ^+e^-) in the gas phase [7], which accounts for the large physical size of this μSR spectrometer. The 1.5 metre diameter Helmholtz coils provide a uniform magnetic field of up to 350 Gauss and they may be readily moved to a transverse (Figure 2b) or longitudinal (Figure 2a) orientation, relative to the muon beam momentum. The incoming muon beam was detected with a thin (0.018 cm) NE110 scintillator, and stopped in an aluminium plate located inside an evacuated vessel 20 cm in diameter. Positrons from muon decay were detected by top and bottom scintillator telescopes each consisting of three large 0.6 cm thick scintillators.

Complete sets of experiments were conducted with the Helmholtz coils in both field orientations: longitudinal and transverse to the beam momentum. The target, detector, and collimator geometry as well as beamline settings (except for the spin rotator) were held unchanged for all measurements. The M20 channel was tuned to transport μ^+ with a central momentum of 27 MeV/c and a momentum spread, $\Delta p/p_0$ (FWHM) ~ 7%.

V. Results

(a) Magnetic Field Parallel to the Muon Beam Momentum (Figure 2a).

When the magnetic field is parallel to the muon spin, as it is with

the spin rotator off, there can be no coherent spin precession of the muon and thus no oscillations appear in a μSR histogram [13] as shown in Figure 3a. As the muon spin is rotated into the upwards direction with the spin rotator, coherent spin precession is observed (Figure 3b). The amplitude of the μSR signal is proportional to the sine of the spin rotation angle, reaching a maximum when the spin is rotated by 90°, exactly transverse to the magnetic field. Figure 4 shows the data (diamonds) fitted to a sine function which gives a maximum amplitude of 35.9 ± 0.3% at 33.2 ± 1.2 kV/cm, in reasonable agreement with the electric field calculated in (4).

(b) Magnetic Field Perpendicular to the Muon Beam Momentum (Figure 2b).

With this geometry the muon spin is always completely transverse to the magnetic field and thus the μSR signal will always show the maximum ampltitude regardless of the spin rotator voltage (Figure 5). This spin rotator-independent amplitude was 35.4 ± 1.2% which compares well with the maximum amplitude obtained in part (a) above. This indicates that there is no loss of muon spin polarization due to a 90° spin rotation, as expected. The effect of the spin rotator on the transverse field μSR spectra of Figure 5 can be seen in the initial phases of the precession signals: with the spin rotator off (Figure 5a) the initial spins of the incoming muons point about 90° away from the top positron telescope; with the spin rotator set to 35 kV/cm (Figure 5b) the initial spins point upwards towards this detector. The complete data are given in Figure 4 (squares), showing the μSR precession phase as a function of the spin rotator electric field. The straight line is a fit to the data with a slope of -2.52 ± 0.2 deg$(kV/cm)^{-1}$; a 90° spin rotation is achieved with 35.7 ± 0.3 kV/cm spin rotator field, in fair agreement with the value

obtained in part (a). It will be noted that there is a slight phase offset apparent in Figure 4 - the spin rotator off phase is 100° rather than 90°. This offset arises from precession of the muon spin in the 210 Gauss field of the μSR spectrometer before the muons reach the Al target.

Of considerable practical importance is the effect of the spin rotator on muon flux. This is illustrated in two ways in Figure 6. The "% background" data (squares) represents the time independent background in the μSR histograms taken in transverse field in part (b). The apparent exponential drop in background with increasing spin rotator field is a measure of the separator function of the spin rotator in removing positrons from the muon beam. Although the background scale has no general absolute meaning (since it depends on the actual experimental apparatus employed) the shape of this curve will apply to most μSR experiments conducted on M20B.

Similarly, the "muon flux" data of Figure 6 (diamonds) reflect the average muon flux incident on the 5 cm^2 collimator per microampere of primary beam protons incident upon the 10 cm Be pion production target. Again, this figure is only valid for the exact experimental conditions under which the data were taken (horizontal and vertical slit widths, positions, etc.). However, the Figure does show a loss in muon flux by about a factor of 3 as the spin rotator is set to the 90° rotation mode, given a beam with a central momentum of 27 MeV/c and a momentum spread $\Delta p/p_0 \sim 7\%$. It will be noted that the rotator-off flux datum of Figure 6 does not fall on the line of best fit because the thin muon beam detector has some small efficiency for detecting beam positrons which are transmitted to the target when the rotator is off (see Figure 7a).

(c) Time of Flight Measurements.

In order to investigate the loss of muon flux in the spin rotator, time of flight (TOF) measurements were made (Figure 7) by starting a time digitizer with a pulse from the muon beam detector and stopping it with a capacitive pickup of the primary proton beam; thus the sense of time illustrated in the raw data of the Figure is reversed from the actual order of events. The 43 ns TRIUMF cyclotron period is evident in these TOF spectra. Figure 7c is a "text-book" example of a surface muon TOF: a sharp build-up of the peak followed by an exponential decay with the 26 ns lifetime of the pion. In Figure 7b, with the spin rotator operating at low fields, the TOF spectrum is so smeared out that no exponential shape is obvious. In Figure 7a, a sharp positron peak is evident, superimposed upon the smeared out muon peak.

Since the ~30 MeV beam positrons are relativistic, the width of the positron peak of Figure 7a is a measure of the experimental time resolution including the time width of the proton beam burst. The sharp rise in the TOF peak of Figure 7c is a convolution of the experimental time resolution and the time spread in muon transit through M20B, which is 20.4 metres long. Given the muon beam central momentum of 27 MeV/c, it is possible to obtain an estimate of the beam momentum bite from the TOF rise-time. For the spin rotator off this calculation gives $\Delta p/p_0 \sim 7.4\%$; for the spin rotator on at 35 kV/cm, $\Delta p/p_0 \sim 4.6\%$. This result reflects the velocity spectrometer aspect of the spin rotator discussed earlier. The narrowed momentum band of surface μ^+ transmitted through the spin rotator operating at high field accounts for about one half of the loss of muon flux observed in part (b) above. Re-tuning the channel with the

spin rotator on at 35 kV/cm while leaving the central momentum at 27 MeV/c did not result in an appreciable muon flux enhancement.

V. Conclusions.

The M20 spin rotator is a remarkably simple device which simultaneously removes positron contamination from the surface μ^+ beam and makes it easy to inject the muons into a strong magnetic field transverse to the muon spin but longitudinal to the momentum. The primary disadvantages of the spin rotator are: (1) it reduces the muon flux, partially by momentum selection; and (2) it produces X-rays which may cause a serious background in certain types of detectors.

At TRIUMF, the spin rotator has so far been used for transverse field μSR studies of Knight shifts in antimony alloys at 3.8 kGauss, and studies of muonium molecular ion formation in low pressure gases. In the latter studies, the surface muons travel about 30 cm in the low pressure moderator gas before stopping. With such an extended stopping distance, the orientation of the magnetic field longitudinal to the muon momentum results in some solenoidal focussing of the beam [15] and eliminates the large bending of the beam seen in the transverse field orientation. A new μSR spectrometer is being built at TRIUMF to realize the benefits foreseen by Brewer in 1981 [6] for condensed matter μSR, namely to make it possible to do transverse field and longitudinal field μSR with the same spectrometer simply by rotating the spin of the surface muon beam. Recently, Turner [16] has proposed that "skewed field μSR," in which the muon spin is neither parallel nor perpendicular to the magnetic field, may result in the elimination of certain systematic errors for a class of solid state μSR experiments. The muon spin rotator will readily accommodate this new technique.

Acknowledgements

We are indebted to many people at TRIUMF who built and maintain the facilities described above, particularly to G.S. Clark, J. van Gool, and J. McIlroy.

References

[1] J.H. Brewer and K.M. Crowe, Ann. Rev. Nucl. Sci. 28 (1978) 239.

[2] C.J. Oram, J.B. Warren, G.M. Marshall and J. Doornbos, Nucl. Instrum. Methods 179 (1981) 95.

[3] A.E. Pifer, T. Bowen and K.R. Kendall, Nucl. Instrum. Methods 135 (1976) 39.

[4] C.J. Oram, J.M. Bailey, P.W. Schmor, C.A. Fry, R.F. Kiefl, J.B. Warren, G.M. Marshall and A. Olin, Phy. Rev. Lett. 52 (1984) 910.

[5] A. Badertscher, S. Dhawan, P.O. Egan, V.W. Hughes, D.C. Lu, M.W. Ritter, K.A. Woodle, M. Gladisch, H. Orth, G. zu Putlitz, M. Eckhause, J. Kane, F.G. Martin and J. Reidy, Phys. Rev. Lett. 52 (1984) 914.

[6] J.H. Brewer, Hyperfine Interactions 8 (1981) 831.

[7] D.G. Fleming, R.J. Mikula, M. Senba, D.M. Garner and E.J. Arseneau, Chem. Phys. 82 (1983) 75.

[8] J. Carr, G. Gidal, A. Jodidio, K.A. Shinsky, H.M. Steiner, D.P. Stoker, M. Strovink, R.D. Tripp, B. Gobbi and C.J. Oram, Phys. Rev. Lett. 51 (1983) 627.

[9] J.L. Beveridge and J. Doornbos, to be submitted to Nucl. Instrum. Methods.

[10] R.F. Kiefl, E. Holzschuh, H. Keller, W. Kundig, P.F. Meier, B.D. Patterson, J.W. Schneider, K.W. Blazey, S.L. Rudaz and A.B. Denison, Phys. Rev. Lett. 53 (1984) 90.

[11] A. Yamamoto, A. Maki, Y. Maniwa and A. Kusumegi, Jpn. J. Appl. Phys. 16 (1977) 343.

[12] R. Frosch, "First Order Beam Transport Matrices for a Muon Spin Rotator", Schweizerisches Institut fur Nuklearforschung Study No. TM-37-14 (1980).

[13] Proceedings of the Yamada Conference VII, Muon Spin Rotation, Shimoda, 1983, Hyperfine Interactions, Vol 17-19 (1983).

[14] V.W. Hughes and C.S. Wu, eds, Muon Physics, Vol 1-3 (Academic Press, New York, 1975); D.G. Fleming, D.M. Garner, L.C. Vaz, D.C. Walker, J.H. Brewer and K.M. Crowe, Adv. Chem. Series 175 (1979) 279.

[15] R.M. Pearce, Nucl. Instrum. Methods 164 (1979) 11.

[16] R.E. Turner, Phys. Rev. B 31 (1985) 112.

Figure Captions

1. A plan view of the M20 channel at TRIUMF. The spin rotator (denoted 1720BSEP in the Figure) is located in the M20B leg.
2. Orientation of the muon spin rotation apparatus: (a) magnetic field longitudinal to the muon beam momentum; (b) magnetic field transverse to the muon beam momentum.
3. Muon spin rotation histogrammes in the longitudinal field orientation: (a) with the spin rotator off; (b) with the spin rotator operating at 35 kV/cm.
4. Effect of the spin rotator field on the measured precession amplitude (denoted "asymmetry") from the longitudinal field orientation (diamonds) and initial precession phase from the transverse field orientation (squares).
5. Muon spin rotation histogrammes in the transverse field orientation: (a) with the spin rotator off; (b) with the spin rotator operating at 35 kV/cm.
6. Effect of the spin rotator field on the time-independent background of the μSR spectra and on the muon flux incident on the experimental target.
7. Effect of the spin rotator field on the time-of-flight (TOF) spectrum: (a) with the spin rotator off; (b) with the spin rotator operating at 6 kV/cm; (c) with the spin rotator operating at 35 kV/cm.

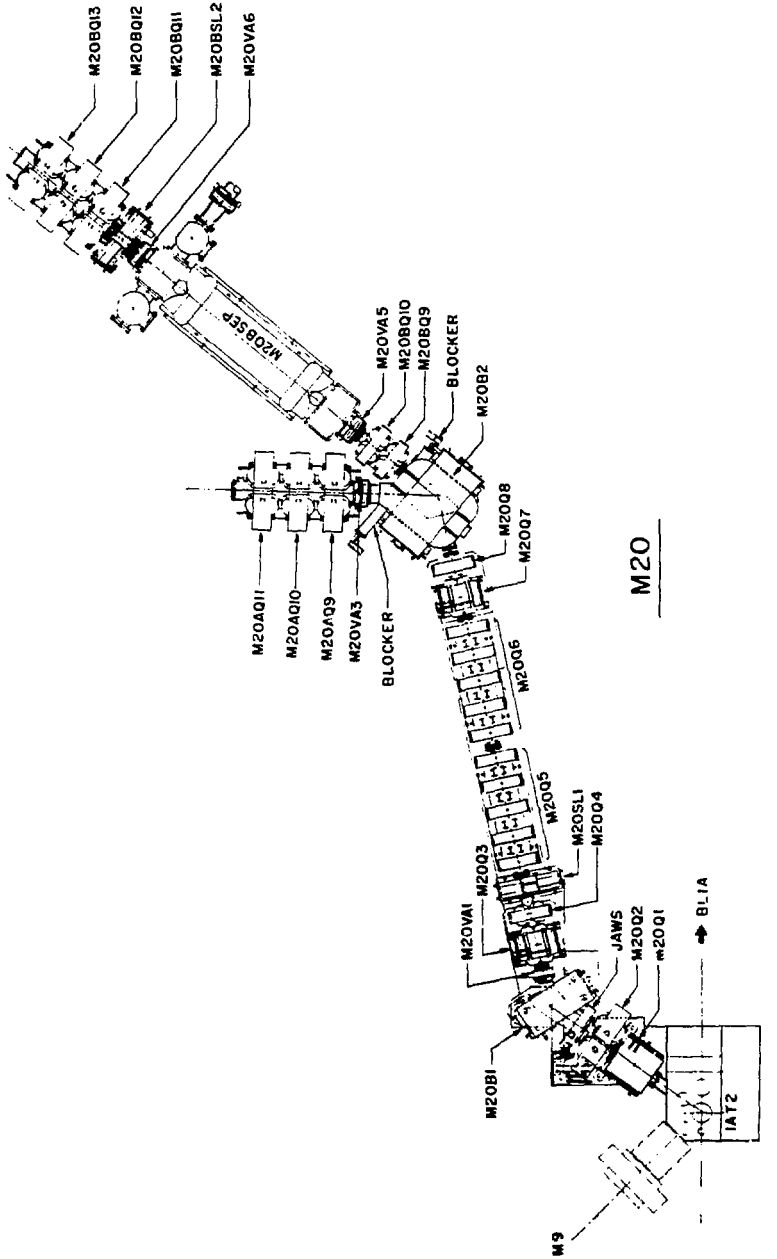
M20BQ13
M20BQ12
M20BQ11
M20BSL2
M20VA6
M20BSEP
M20VA5
M20BQ10
M20BQ9
BLOCKER
M20B2
M20Q8
M20Q7
M20AQ11
M20AQ10
M20AQ9
M20VA3
BLOCKER
M20Q6
M20Q5
M20SL1
M20Q4
M20VA1
M20Q3
JAWS
M20Q2
M20Q1
BL1A
M20B1
IAT2
M9
M20

Figure 1

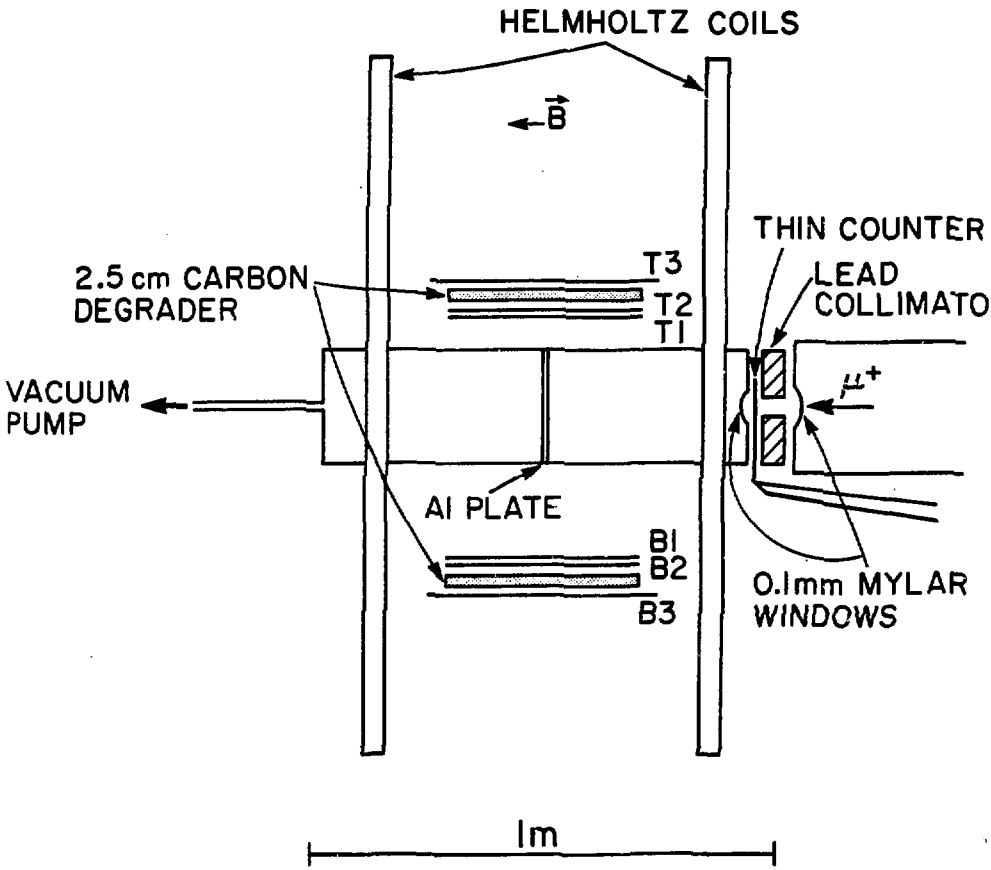
HELMHOLTZ COILS
$\vec{B}$
THIN COUNTER
LEAD COLLIMATO
2.5 cm CARBON DEGRADER
T3
T2
T1
VACUUM PUMP
μ^+
Al PLATE
B1
B2
B3
0.1mm MYLAR WINDOWS
1m

Figure 2a

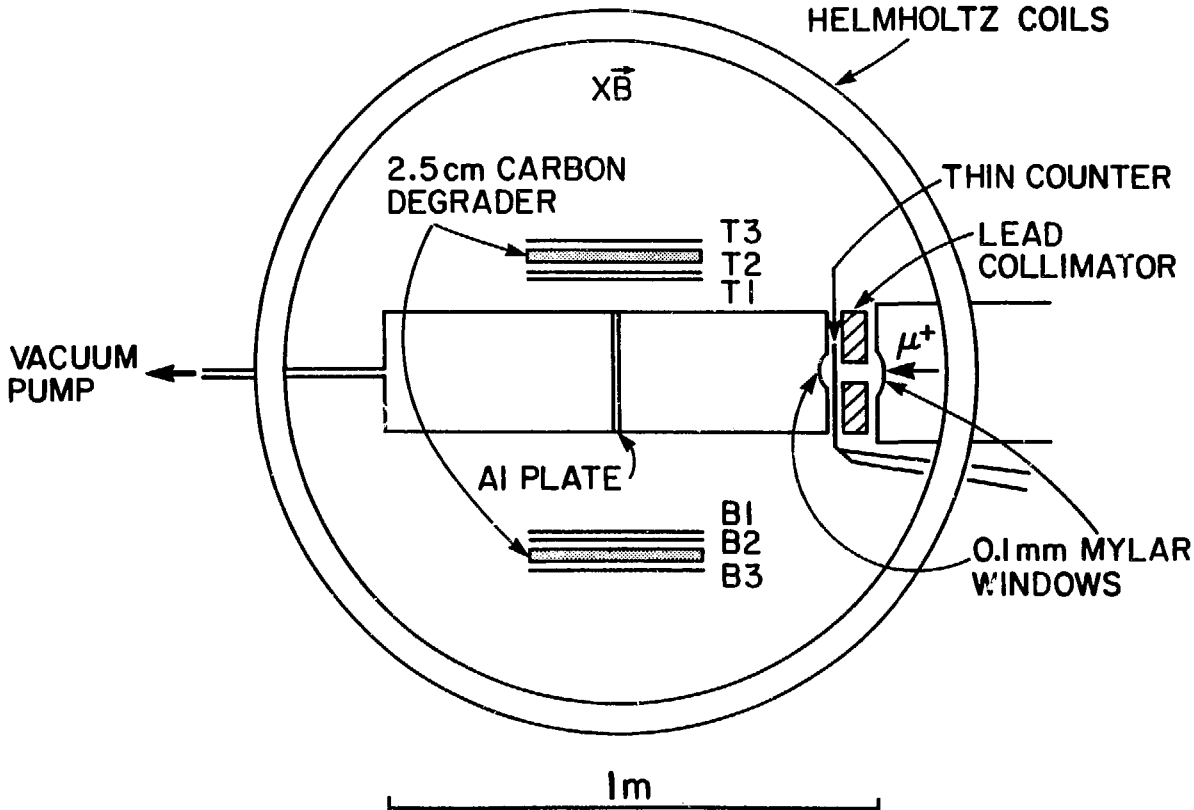
HELMHOLTZ COILS
$\vec{XB}$
2.5cm CARBON DEGRADER
THIN COUNTER
LEAD COLLIMATOR
T3
T2
T1
VACUUM PUMP
μ^+
Al PLATE
B1
B2
B3
0.1mm MYLAR WINDOWS
1m

Figure 2b

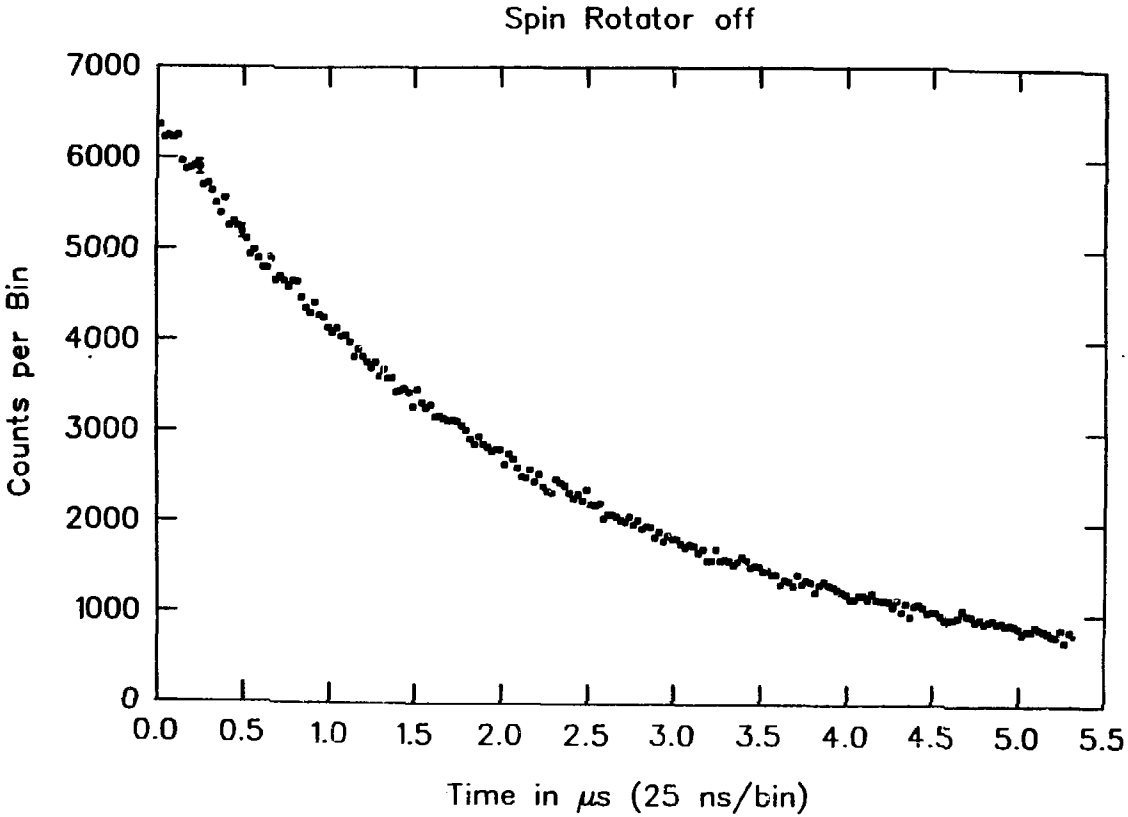
Spin Rotator off
Counts per Bin
7000
6000
5000
4000
3000
2000
1000
0
0.0
0.5
1.0
1.5
2.0
2.5
3.0
3.5
4.0
4.5
5.0
5.5
Time in μs (25 ns/bin)

Figure 3a

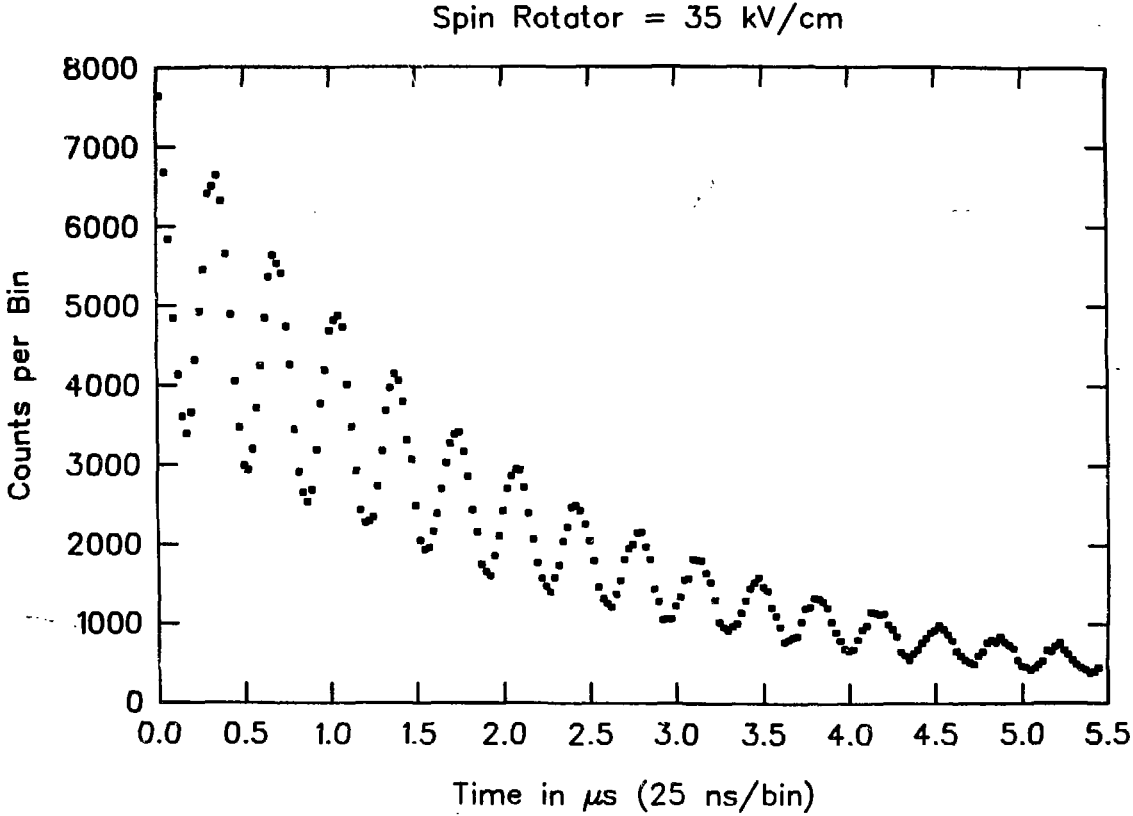

Figure 3b

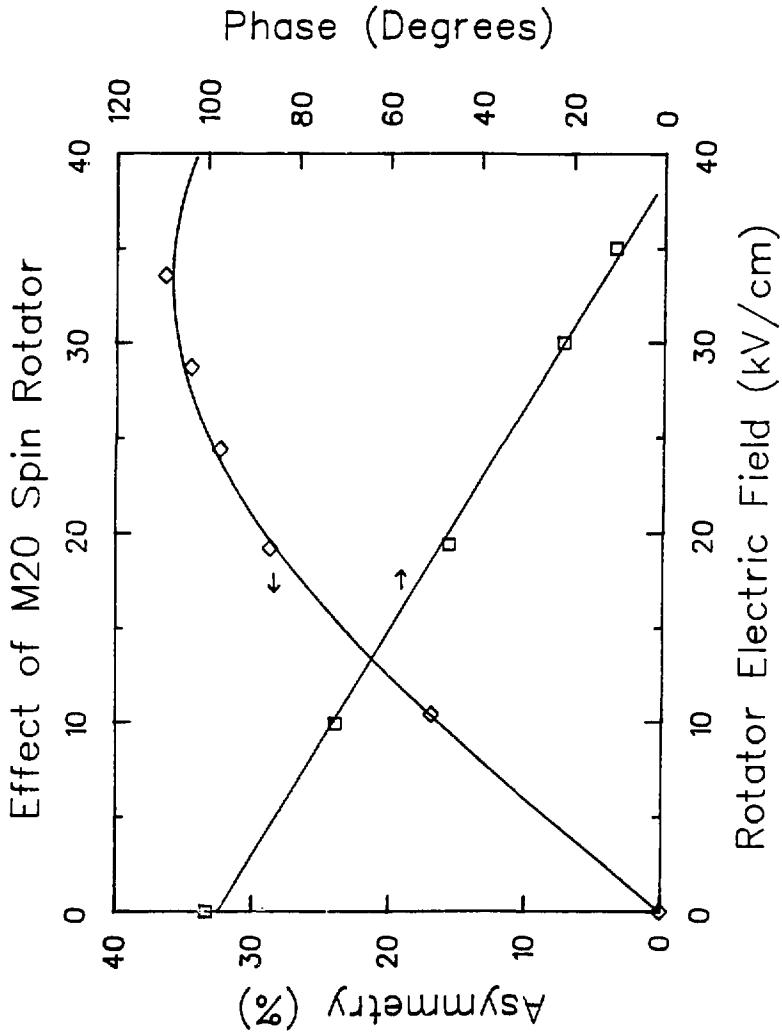
Effect of M20 Spin Rotator
Asymmetry (%)
Phase (Degrees)
Rotator Electric Field (kV/cm)
0
10
20
30
40
0
20
40
60
80
100
120
↓
↑

Figure 4

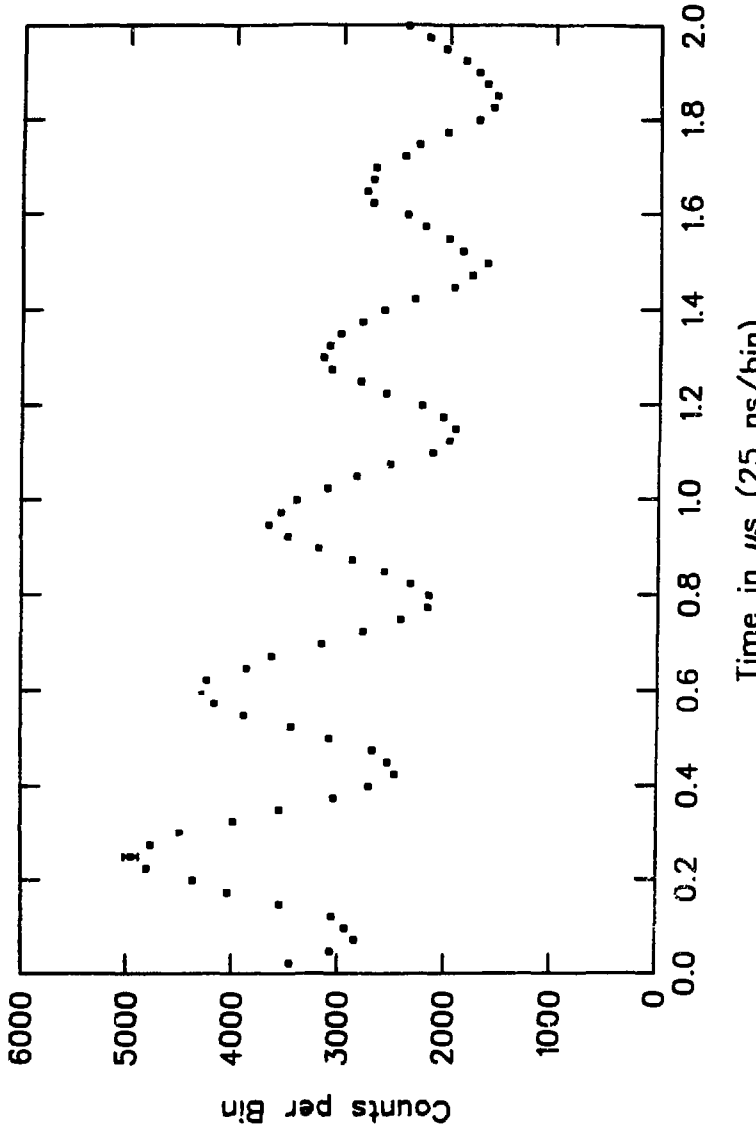
Spin Rotator off
Counts per Bin
6000
5000
4000
3000
2000
1000
0
0.0
0.2
0.4
0.6
0.8
1.0
1.2
1.4
1.6
1.8
2.0
Time in μs (25 ns/bin)

Figure 5a

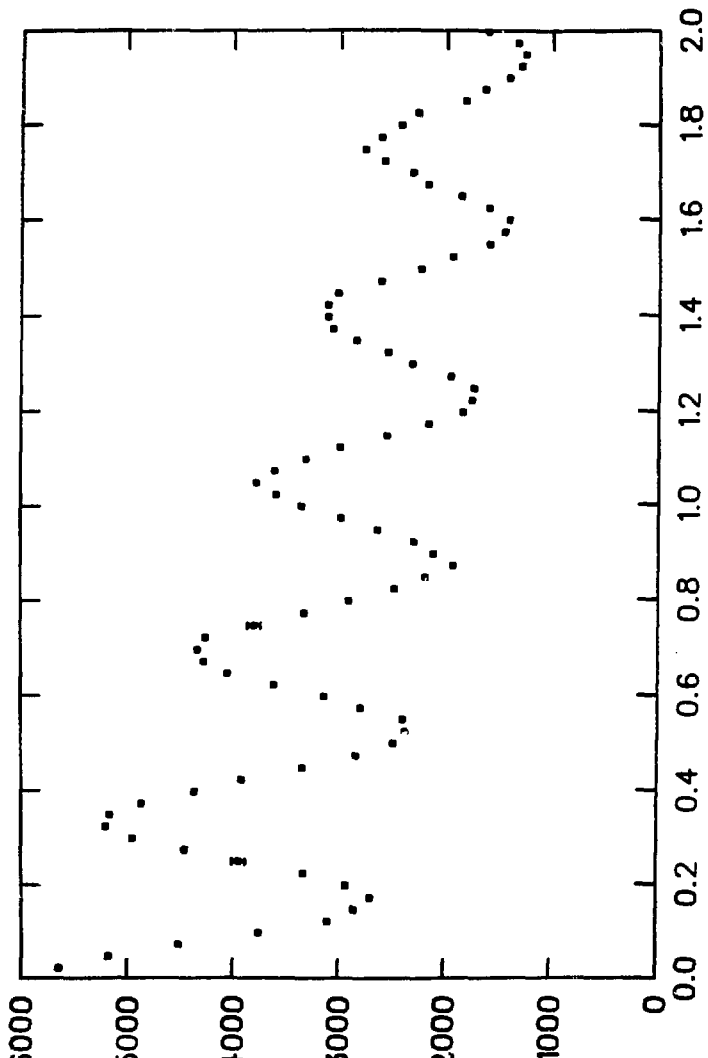
Spin Rotator = 35 kV/cm
Counts per Bin
6000
5000
4000
3000
2000
1000
0
0.0
0.2
0.4
0.6
0.8
1.0
1.2
1.4
1.6
1.8
2.0
Time in μs (25 ns/bin)

Figure 5b

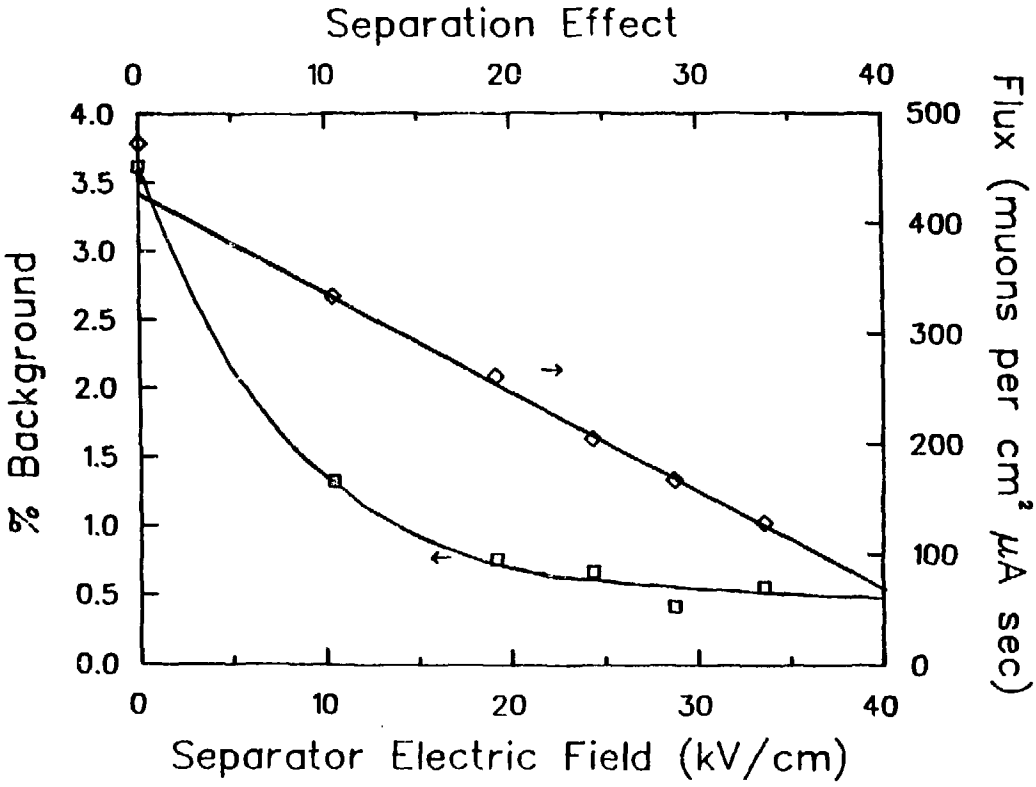
Separation Effect
0
10
20
30
40
4.0
3.5
3.0
2.5
2.0
1.5
1.0
0.5
0.0
% Background
500
400
300
200
100
0
Flux (muons per cm² μA sec)
Separator Electric Field (kV/cm)

Figure 6

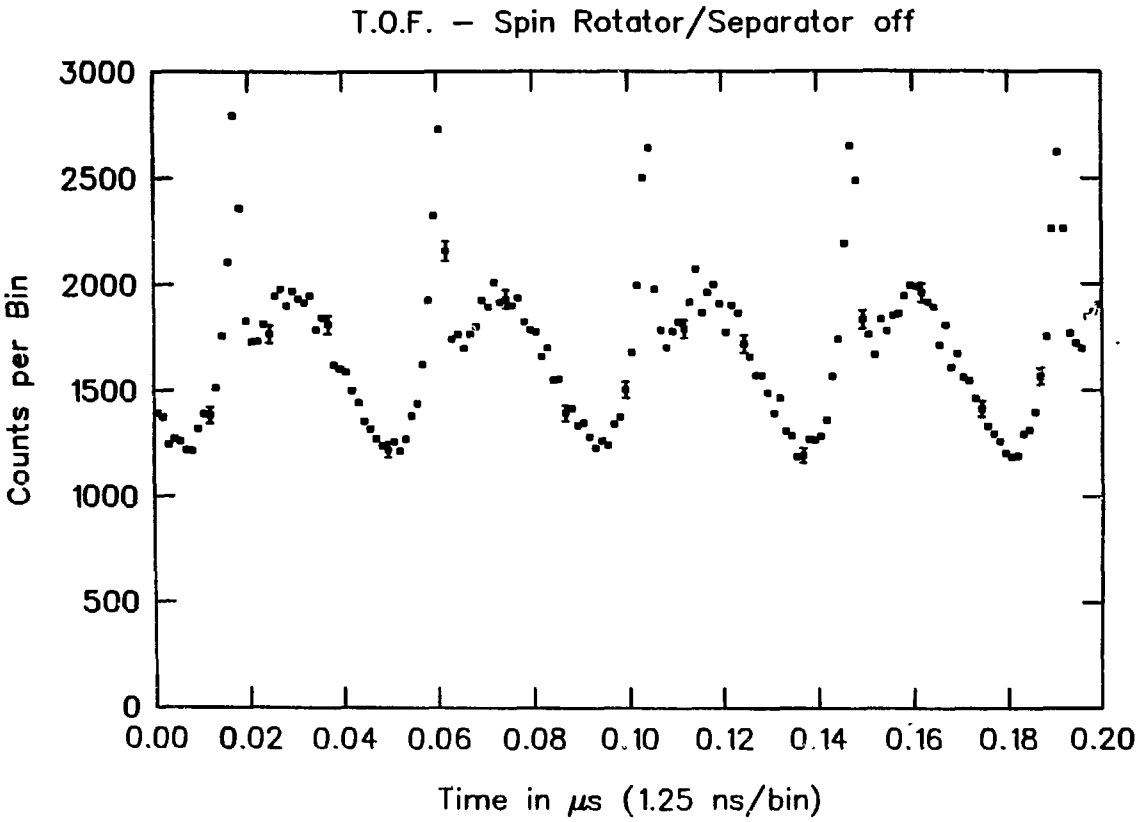
T.O.F. – Spin Rotator/Separator off
Counts per Bin
3000
2500
2000
1500
1000
500
0
0.00
0.02
0.04
0.06
0.08
0.10
0.12
0.14
0.16
0.18
0.20
Time in μs (1.25 ns/bin)

Figure 7a

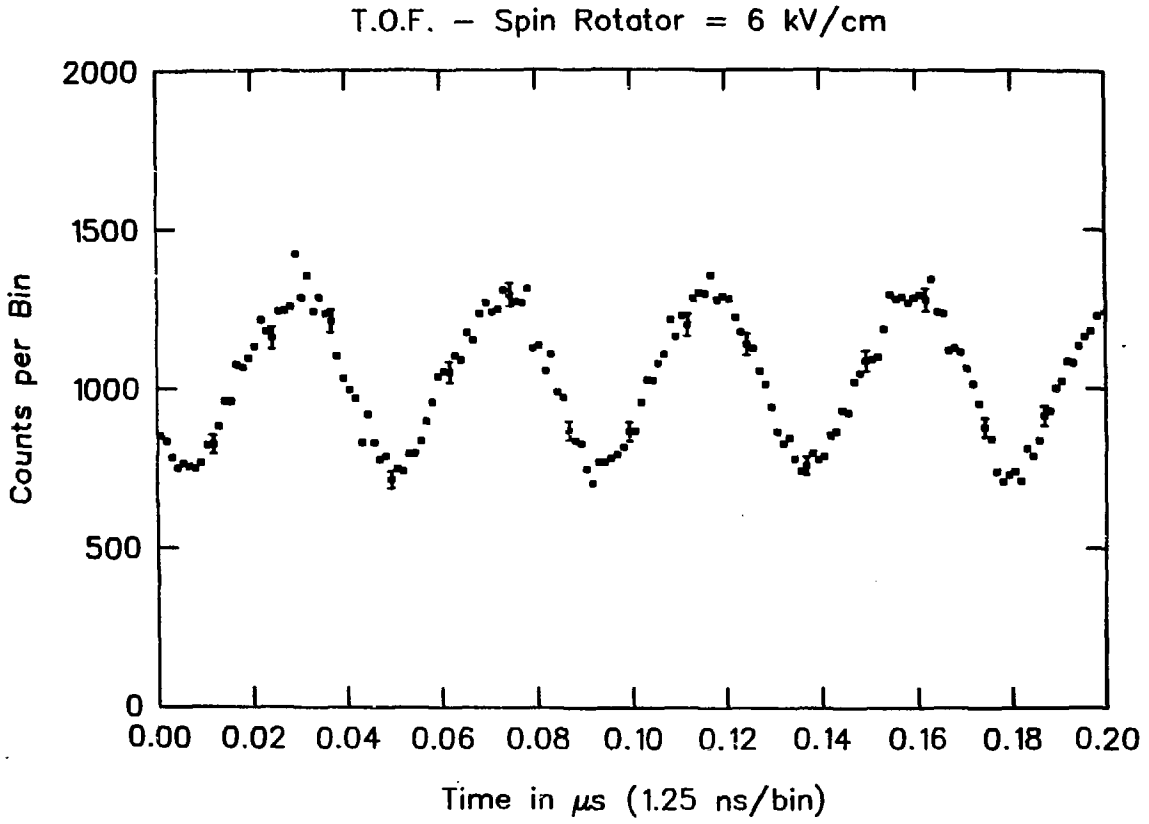
T.O.F. – Spin Rotator = 6 kV/cm
Counts per Bin
2000
1500
1000
500
0
0.00
0.02
0.04
0.06
0.08
0.10
0.12
0.14
0.16
0.18
0.20
Time in μs (1.25 ns/bin)

Figure 7b

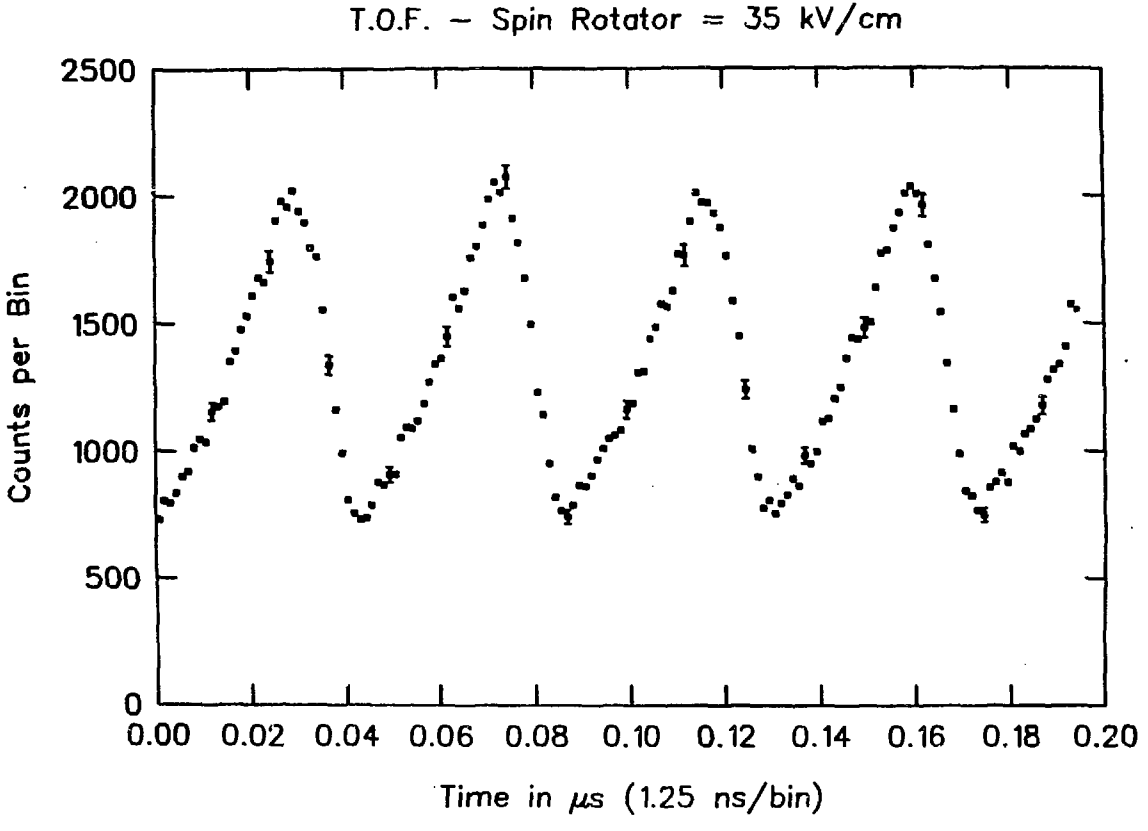
T.O.F. – Spin Rotator = 35 kV/cm
Counts per Bin
2500
2000
1500
1000
500
0
0.00
0.02
0.04
0.06
0.08
0.10
0.12
0.14
0.16
0.18
0.20
Time in μs (1.25 ns/bin)

Figure 7c

Resolved nuclear hyperfine structure of muonated free radicals using level crossing spectroscopy

R.F. Kiefl and R. Keitel

TRIUMF, 4004 Wesbrook Mall, Vancouver, B.C., Canada V6T 2A3

S. Kreitzman, G. Luke, J.H. Brewer and D.R. Noakes

Department of Physics,

University of British Columbia, Vancouver, B.C., Canada V6T 1W5

P.W. Percival

Department of Chemistry

Simon Fraser University, Burnaby, B.C., Canada V5A 1S6

T. Matsuzaki and K. Nishiyama

Meson Science Laboratory, University of Tokyo, Tokyo 113, Japan

ABSTRACT

The nuclear hyperfine parameters of the muonated free radical $\cdot C_6F_6Mu$ have been measured using a novel level crossing resonance technique. Slow oscillations of the muon spin in a large longitudinal magnetic field or frequency splittings in transverse field occur at particular field values where there is a zeroth order degeneracy in the muon-nuclear-electron hyperfine levels. A resonant-like effect on the μSR spectrum as a function of magnetic field is observed. The positions of level crossing resonances allow an accurate determination of the magnitude and sign of the nuclear hyperfine parameters relative to the muon hyperfine parameter.

A large part of μSR research is based on the physics and chemistry of muonium-like systems such as muonated free radicals and muonium defect centers in solids. Most often the spin Hamiltonian for these systems contains terms describing the nuclear hyperfine (NHF) interaction between the unpaired electron and the surrounding nuclear spins. This leads to a complicated multi-component frequency spectrum in low transverse magnetic fields (TF) which cannot be resolved. However, in the high field limit, where the electron, muon and nuclear spins are decoupled, a relatively simple two-component frequency spectrum is observed, from which the muon-electron hyperfine parameter can be determined with high precision. Roduner et al. [1] were the first to apply this high TF technique in the case of muonated free radicals, where the decoupling occurs in moderate fields of 0.2-0.3 T, and where the precession frequencies, in the range 100-300 MHz, are just resolvable with standard techniques. Following this breakthrough an extensive amount of information on the muon hyperfine parameters and reaction dynamics of muonated radicals has been obtained. A non-trivial extension of this technique has lead to a wealth of new information on the hyperfine structure of muonium defect centers in solids where the decoupling fields, and precession frequencies are an order of magnitude larger [2,3].

Despite its successes the TF decoupling technique is limited in the sense that it provides little information on the NHF structure, except in a few ideal situations [1]. The ability to resolve the NHF interaction would have considerable impact on almost every aspect of this field since the NHF parameters provide details on the spin density distribution away from the muon and also on the spin and number of

nearest neighbour nuclei. This information would be useful in determining the site of the muon and testing calculations on the electronic structure of the system under study.

The possibility of using level crossing resonance (LCR) spectroscopy in μSR was first pointed out by Abragam [4]. The first successful LCR experiment was carried out by Kreitzman et al. [5] who resolved the nuclear quadrupolar interaction of the nearest neighbour nuclei of muons in Cu. In this letter we report the first LCR results in a muonium-like system. The results show that LCR spectroscopy is a powerful technique which can be used to determine the NHF parameters with high precision.

Figure 1 shows the LCR spectrum for the muonated free radical $\cdot C_6F_6Mu$. The signal in Fig. 1 is the integrated forward-backward muon decay asymmetry, modulated by a small field (±5 mT), and thus is approximately equal to the derivative of the asymmetry with respect to applied field. The modulation field is necessary to remove systematic errors inherent in the integral technique. The four resonances are attributed to the level crossings in the muonated free radical $\cdot C_6F_6Mu$, whose muon hyperfine parameter has been reported previously to be 200.9 MHz at room temperature [6].

The resonances in Fig. 1 occur at field values where a muon transition frequency ($\nu_\mu^\pm$) matches a corresponding nuclear transition frequency ($\nu_N^\pm$), where ± signs refer to the z component of electron spin ($S_z = \pm 1/2$). On resonance there is a near degeneracy or level crossing between two muon-nuclear-electron spin levels. This results in flip-flop oscillations between the muon and the nucleus which are otherwise suppressed. In the high field limit $\nu_\mu^\pm$ and $\nu_N^\pm$ are approximately given by:

$$\nu_{\mu}^{\pm} = 1/2\ \nu_{o}^{\mu} \mp \gamma_{\mu} B \qquad (1a)$$

$$\nu_{N}^{\pm} = 1/2\ \nu_{o}^{N} \mp \gamma_{N} B \qquad (1b)$$

where ν_{o}^{μ} and ν_{o}^{N} are isotropic muon and nuclear hyperfine parameters respectively and B is the magnetic field. If the NHF parameter is substantially less than the muon hyperfine parameter, as is the case for the F_4, $F_{2,6}$ and $F_{3,5}$ nuclei in Fig. 1 [7], then the level crossing occurs when $\nu_{\mu}^{+} = \nu_{N}^{+}$, which corresponds to a field value:

$$B_{R}^{+} = (\nu_{o}^{\mu}-\nu_{o}^{N})/2(\gamma_{\mu}-\gamma_{N}) \quad . \qquad (2)$$

Note that the position of the resonance depends on the magnitude and sign of the NHF parameter relative to the muon hyperfine parameter. Alternatively if the NHF parameter is substantially larger than the muon hyperfine parameter, as in the case of the F_1 nucleus [7], there is no level crossing for $S_z = 1/2$. However, under these conditions there is a level crossing for $S_z = -1/2$, when $\nu_{\mu}^{-} = \nu_{N}^{-}$. This occurs at a field:

$$B_{R}^{-} = (\nu_{o}^{N}-\nu_{o}^{\mu})/2(\gamma_{\mu}-\gamma_{N}) \quad . \qquad (3)$$

In some cases where ν_{o}^{μ} happens to be very close to ν_{o}^{N}, there are no level crossings in high field. Although there may be LCR's in low field these are difficult to observe since then the system is not decoupled.

Non degenerate perturbation theory predicts that if a large magnetic field is applied along the muon spin direction there will be no observable time dependence in the muon polarization. However, when there is a level crossing, such as described above, this will no longer be true. This situation must be treated with degenerate perturbation theory. This amounts to diagonalizing a relatively small part of the Hamiltonian, the size of which depends on the number of equivalent nuclei and their spin. The end result is that on or near a level crossing the muon spin polarization exhibits slow oscillations in

longitudinal field. In transverse fields the level crossing manifests itself as a small splitting in either ν_μ^- or ν_μ^+. For the resonances in $\cdot C_6F_6Mu$ the oscillations or splittings are of order 0.5 MHz and are easily detectable. As can be seen in Fig. 1 the slow oscillations on resonance in a longitudinal field result in a change in the integrated muon decay asymmetry. It is important to note that the position, width and amplitude of the level crossing resonances do not depend on the number of nuclei off resonance. This is a key point since it implies that the resonances do not become more difficult to observe as the number of nuclei increases. This is in contradistinction to normal μSR in low transverse magnetic fields which cannot be used to determine NHF parameters, except in trivial situations.

The LCR's are predicted to occur in a wide range of magnetic fields, 0.5-3.0 T for radicals and 0.5-16.0 T for muonium defect centers in solids. Considering the possible difficulty in finding resonances, one should appreciate the usefulness of the integral technique which allows a 100 fold increase in the data rate compared to the standard time differential technique. The data rate in the present experiment was an impressive $5 \times 10^5/s$. However, in order to determine the spin Hamiltonian unambiguously one must also do standard time differential μSR measurements on resonance in both longitudinal and transverse field. The measurements in longitudinal field are necessary to determine the number of equivalent nuclei involved in the resonance, whereas those in transverse field are necessary to determine which muon transition frequency (ν_μ^+ or ν_μ^-) of which radical is involved in the resonance.

Some possible applications of the technique are (1) to test calculations on electronic structure of muonium-like systems; (2) to aid in making site assignments for the muon since the LCR spectrum is far more distinctive than the muon hyperfine parameter alone; and (3) to determine reaction channels in solid state or radical chemistry. This last point arises because LCR can be used to study muonium defect centers or radicals which form several μs after the muon enters the target.

Level crossing resonances were also detected for the $(CH_3)_2MuC\text{-}\dot{C}(CH_3)_2$ radical and for the anomalous muonium center in GaAs. More details on the experiment and the results will be presented in a forthcoming publication.

REFERENCES

1. E. Roduner and H. Fischer, Chem. Phys. 54, 261 (1981) and references therein.
2. R.F. Kiefl, E. Holzschuh, H. Keller, W. Kündig, P.F. Meier, B.D. Patterson, J.W. Schneider, K.W. Blazey, S.L. Rudaz and A.B. Dennison, Phys. Rev. Lett. 53, 90 (1984).
3. R.F. Kiefl, J.W. Schneider, H. Keller, W. Kündig, W. Odermatt, B.D. Patterson. K.W. Blazey, T.L. Estle and S.L. Rudaz, Phys. Rev. B32, 530 (1985).
4. C.R. Abragam, Acad. Sc. Paris, t. 299, Serie II, 3, 95 (1985).
5. S.R. Kreitzman, J.H. Brewer, D.R. Harshman, R. Keitel, D.Ll. Williams, K.M. Crowe and E.J. Ansaldo, submitted to Phys. Rev. Lett. (1985).
6. E. Roduner, G.A. Brinkman and P.W.F. Louwrier, Chem. Phys. 73, 117 (1981).
7. M.J. Yim and D.E. Wood, J. Amer. Chem. Soc. 97, 1004 (1975).

FIGURE

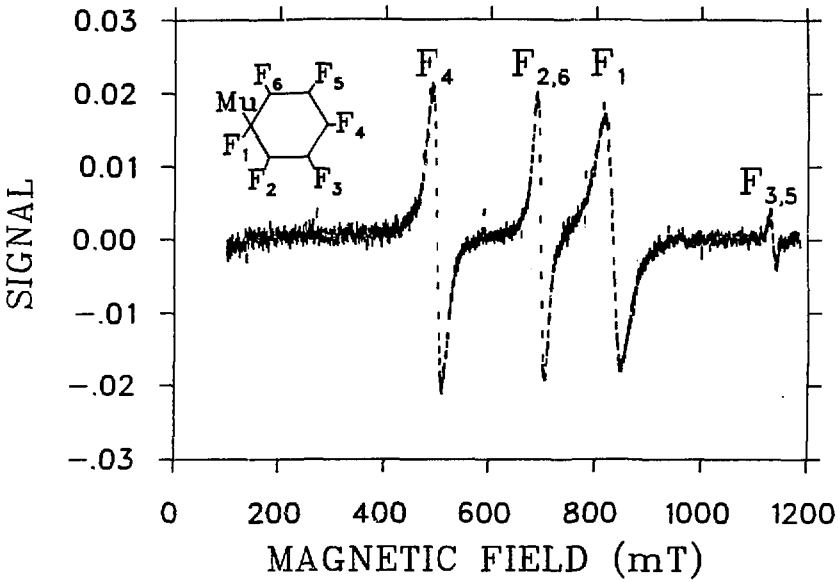

Level crossing spectrum in the $\cdot C_6F_6Mu$ radical. The four resonances correspond to the four inequivalent fluorine nuclei. The magnetic field is applied along the muon spin direction.